Ultracold Bose gases - from the Gross-Pitaevskii to the fractional quantum Hall regime

by

Satyan Gopal Bhongale

B.Tech., Indian Institute of Technology, Bombay, 1996

A thesis submitted to the

Faculty of the Graduate School of the

University of Colorado in partial fulfillment

of the requirements for the degree of

Doctor of Philosophy

Department of Physics

2004

This thesis entitled:
Ultracold Bose gases - from the Gross-Pitaevskii to the fractional quantum Hall regime
written by Satyan Gopal Bhongale
has been approved for the Department of Physics

Murray Holland

Prof. John Bohn

Date

The final copy of this thesis has been examined by the signatories, and we find that both the content and the form meet acceptable presentation standards of scholarly work in the above mentioned discipline.

Satyan Gopal Bhongale, (Ph.D., Physics)

Ultracold Bose gases - from the Gross-Pitaevskii to the fractional quantum Hall regime

Thesis directed by Prof. Murray Holland

Ultra-cold Bose gases present an ideal environment for the study of many-body physics. These systems can be prepared under various experimental conditions with precise control. Techniques like Feshbach resonances allow us to dynamically tune the inter atomic interaction, from strongly attractive to a strongly repulsive one.

In the first part of the thesis, we study the weakly interacting Bose gas in connection with the dynamics of an atom laser. Here we propose a possible optical pumping model for loading the reservoir of a continuous wave atom laser. The finite temperature effects like phase diffusion require a thorough understanding of the kinetic regime of the dilute Bose gas. In this respect, we develop a non-Markovian quantum kinetic theory and thereby show the emergence of different time scales for correlation and subsequent relaxation to an equilibrium states. Using numerical simulations, we also predict the damping rates and frequencies of collective modes.

In the second part, we study the strongly correlated regime where the interaction energy is greater than any other (single particle) energy scale of the problem. Here, in the presence of a Feshbach interaction we predict the generation of novel strongly correlated paired states. Such states while similar to the one observed in a 5/2 fractional quantum hall effect, are unique in symmetry to the Bose gas system.

Dedication

To my parents

Acknowledgements

I would first like to thank my advisor Prof. Murray Holland for his guidance and encouragement through out the course of this thesis. He has provided me with a research atmosphere that enhanced my ability towards becoming an independent researcher. His informal attitude, not only made him available to me when ever I was stuck with a research problem but also allowed me to express my thoughts without hesitation.

I am also extremely grateful to Prof. John Cooper who has been like my co-advisor. I cannot thank him enough for the countless discussion hours and invaluable advice.

I would like to thank my colleagues, Josh Milstein, Jochen Wachter, Servaas Kokkelmans, and Reinhold Walser for the incredible amount of help I received during the course of this thesis.

Apart from those who have been directly connected with my thesis work, I would like to mention a few people without whose support and encouragement I would not be here writing this thesis. Firstly my parents to whom this thesis is dedicated. They were a constant source of motivation without which I would not be the person I am today. My father Dr. Gopal Bhongale who inspired me to think of the world. My undergraduate advisor Prof. Bhanu Das who got me interested in the field of AMO physics.

Lastly I would like to thank my best friend Patricia Rettig for all the support and for standing by me in every situation possible.

Contents

Chapter

Tables

Table

Figures

Figure

Chapter 1

Introduction

Dilute atomic gases present an ideal environment for studying various aspects of many-body physics. These systems can be prepared with precise control and extreme purity. Advancement in the techniques of trapping and cooling based on the detailed understanding of atom-light interactions have allowed experimentalists to cool atomic gases to ultra-low temperatures. This has opened new possibilities for the understanding and investigation of many-body phenomena, for example the prediction of Bose-Einstein condensation (BEC). BEC occurs in bosonic systems where the ground state acquires a macroscopic population when cooled below a certain critical temperature T_c. While first predicted by Bose and Einstein in 1924, it wasn't until 1995 when it was confirmed in the form in which it was originally posed by experiments in a trapped dilute atomic vapor of Rb^{87}, Na and Li^{7} [1, 2, 3]. Recently BEC has been achieved in dilute atomic gases of H, He, K^{41},Cs and Yb, and has also been realized in micro-traps on chips [4] and also in two dimensional surface traps [5].

Since 1995, dilute atomic gases have generated tremendous theoretical and experimental interest and have led to the study of phenomena like atom lasers and vortices. More recently with the advent of techniques based on Feshbach resonances, the interactions between atoms can now be dynamically tuned by changing the external magnetic field. While interactions in condensed matter systems could be modified, for example, by doping a semiconductor material, dynamic control is typically limited. In fact, in

some condensed matter systems such as those that give rise to the fractional quantum Hall effect, there is virtually no control over interactions. Feshbach tuning allows the inter-atomic interaction to be dynamically varied from a repulsive to an attractive one. The ability to tune interactions has allowed us to stretch the scope of possibilities to studying BCS superfluidity [6, 7, 8, 9], guiding of matter waves [10] and molecule formation in a Fermi gas [11]. Thus dilute atomic gases have provided us with a new setting to answer some of the questions and test ideas that have previously been inaccessible in the domain of condensed matter physics.

From a theory point of view, dilute atomic gases are extremely challenging since the theoretical framework required to describe them can be very different in different regimes based on the strength of interaction, temperature scale of interest and density of the atomic gas. For example, in a dilute Bose gas with weak repulsive interactions at $T = 0$ (BEC), a description in terms of mean fields given by the Gross-Pitaevskii (GP) equation is sufficient to account for all the observable properties. However for finite temperatures $0 < T < T_c$, a quantum kinetic description that includes the effect of binary collisions may be necessary. In another situation, a dilute Bose gas at $T = 0$ can be configured to be strongly correlated making the mean field description invalid. In this case, as we will see in the later part of this thesis, an effective field theory picture in terms of composite particles is convenient to completely account for the correlations and predict the physical observables.

Given the richness of this area of research, in this thesis we theoretically investigate some particular aspects of the trapped Bose gas system in two different regimes- the weak interaction regime and the strong interaction regime.

(1) Weak interaction regime:

In this regime we focus on the behavior and working of a continuous-wave (cw) atom laser. An atom laser is essentially a device that produces an intense coherent beam of atoms. Since a BEC is a coherent superposition of atoms in the ground state, one could

simply think of an atom laser as a beam of Bose condensed atoms. The working of an atom laser can be described in complete analogy to the optical laser. As in the case of an optical laser, if a threshold condition is satisfied, the atom laser will operate far from equilibrium in a dynamical steady state. In this dynamic state, the macroscopically occupied quantum state is continuously depleted by loss to the output field, and continuously replenished by pumping from an active medium. The threshold condition for an atom laser is analogous to the critical point associated with the phase transition from a normal gas to a BEC. A version of a "pulsed" atom laser was demonstrated [27, 28] soon after the first experimental realization of BEC in dilute alkali gases. Therefore one of the objectives of this thesis is to model a possible pumping scheme that would continuously replenish the reservoir allowing the BEC to be generated in a dynamical steady state and hence a cw- atom laser.

In order to study the coherence and phase diffusion properties of any such device, it is very important to understand the collisional regime of the dilute trapped Bose gas. While binary collisions is the necessary mechanism for the evaporative cooling technique employed in the realization of a BEC, it is also responsible for the loss of coherence of the condensed component due to collisions with the non-condensed atoms. In order to better understand the effect of collisions, we discuss the dilute Bose gas in the quantum kinetic regime ($T > T_c$, absence of a condensed component). Here, we derive a non-Markovian generalization to the quantum kinetic theory described by Walser et al. [13] for temperatures above the BEC temperature. We show that within this framework, finite duration effects like quasiparticle damping arise naturally and lead to a systematic Markov approximation from a non-Markovian Born theory. Using numerical simulation we demonstrate the emergence of different time scales for correlation and relaxation as well as predict damping rates and frequencies of collective modes [14]. This formulation can be extended to the temperature regime, $0 < T < T_c$, by including the condensed component. Such a theory will be an important step towards a complete understanding

of the cw- atom laser.

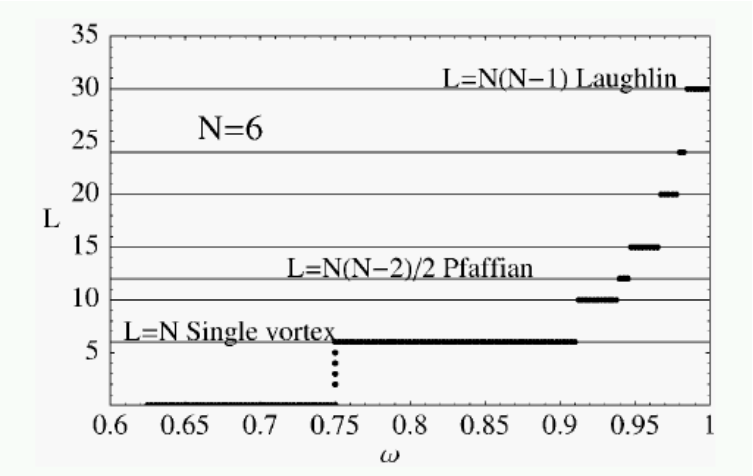

Figure 1.1: The total angular momentum of the stable ground state plotted as a function of the rotational frequency for $N = 6$ atoms with two-body interaction potential in units of harmonic oscillator quanta given by $V = (1/N)\delta(\mathbf{r}_i - \mathbf{r}_j)$. (Figure obtained from N. K. Wilkins and J. M. F. Gunn, Phys. Rev. Lett. **84**, 6 (2000))

(2) Strong interaction regime:

This regime is defined by the situation where the interaction energy is large compared to any other single particle energy scale of the system. A dilute Bose gas can be configured in this regime in various ways. One possibility is to tune the interactions by using Feshbach resonance techniques. Another possibility is to introduce degeneracy in the system, for example by using an optical lattice trapping potential as was used in the experiment involving a superfluid to a Mott transition [89]. In this thesis we consider a two dimensional trapped Bose gas but instead introduce degeneracy by rotating the trap. At a certain critical rotational frequency the system is predicted to enter the strongly correlated regime where the many-body ground state is given by the bosonic variant of the Laughlin wavefunction. This is shown in Fig. 1.1 where the total angular momentum of the stable ground state is plotted as a function of the rotational frequency. The Laughlin state becomes stable only when the rotational frequency is close to the trapping frequency. The Laughlin ground state is precisely the state responsible

for the observation of the fractional quantum Hall effect in two dimensional electron systems. Therefore in this thesis we will refer to this regime of the dilute Bose gas as the fractional quantum Hall regime. Using the tunability of interaction made available by Feshbach resonances, which as mentioned earlier is almost impossible to achieve in an electronic fractional quantum Hall system, we study this regime of the dilute Bose gas in the presence of Feshbach interaction. The importance of employing such resonant interactions in the strongly correlated regime will be apparent from the possibility of creating novel states as well as the opening of new possibilities for answering questions related to the many-body physics of fractional quantum Hall effect.

Overview:

The general flow of topics covered in this thesis is shown in the figure below. In Ch. 2, we discuss a model based on an optical pumping scheme to continuously load the reservoir of a continuous wave atom laser. Here we show that despite loss mechanisms, it is possible to generate BEC in a steady state that is crucial to the working of a continuous wave atom laser. In Ch. 3, we develop a non-Markovian quantum kinetic theory and thereby derive a systematic Markov approximation that includes finite duration effects such as quasiparticle damping. The remainder of the thesis is devoted to the strongly correlated regime of the dilute Bose gas. In Ch. 4, we introduce the electronic fractional quantum Hall effect and show how an analogous many-body state can be generated in a trapped dilute Bose gas system. In Ch. 5, we develop a field theory picture required to describe this regime. Within this picture the strongly correlated regime can be thought of as a Bose condensed phase of composite bosons. The idea of composite particles and its connection to the existence of fractional statistics is also discussed. The importance of such a description will be apparent as it will allow us to theoretically study this regime in the presence of Feshbach interactions. The implications of introducing resonant interactions in this regime are discussed in Ch. 6. The main result of this chapter is the prediction of a novel strongly correlated state unique to the trapped Bose system.

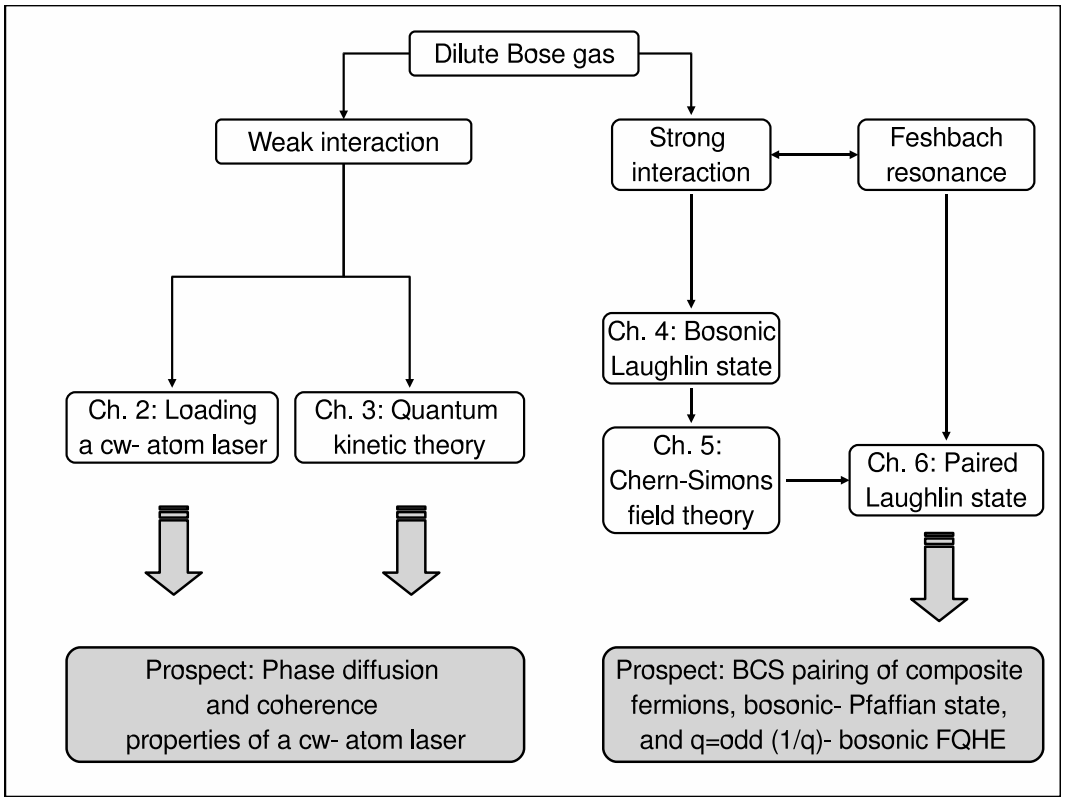

Figure 1.2: Flow chart of the chapters in this thesis. Figure also shows the opening of new possibilities for further study as a result of this work.

Chapter 2

Loading a conitnuous wave atom laser by optical pumping techniques

Published in Physical Review A **62**, *043604 (2000)*

2.1 Introduction

An atom laser is a device which generates an atomic beam which is both intense and coherent [16, 17, 18, 19, 20, 21, 22, 23, 24, 25]. It is typically defined by direct analogy with the optical laser. As in the case of an optical laser, if a threshold condition is satisfied the atom laser will operate far from equilibrium in a dynamical steady state [26]. In this regime, the macroscopically occupied quantum state is continuously depleted by loss to the output field, and continuously replenished by pumping from an active medium. The threshold condition for the atom laser is analogous to the critical point associated with the phase transition from a normal gas to a Bose-Einstein condensate (BEC). A version of the "pulsed" atom laser [27, 28] was demonstrated soon after the first experimental realizations of BEC in dilute alkali gases [1, 2, 3, 29].

The three basic components of an atom laser are: a cavity (or resonator), an active medium (or reservoir), and an output coupler. The cavity is typically a three-dimensional magnetic trap which for containment uses the force on the atomic magnetic dipole via an inhomogeneous potential. The active medium may be composed of a saturated dilute thermal gas formed through evaporative cooling or other techniques. Saturated in this context implies that the energy distribution function of the atoms is such that thermodynamic relaxation of the gas through binary collisions would result in the

stimulated accumulation of atoms into the ground state. The output coupler can be implemented by either applying a short radio-frequency (RF) pulse to the condensate and thereby separating the condensate into a trapped component and an un-trapped component [27, 28, 30, 31], or alternatively by creating a situation in which the atoms tunnel out through a potential barrier [32]. A recent demonstration of a quasi-continuous atom laser used an optical Raman pulse to drive transitions between trapped and un-trapped magnetic sublevels giving the output-coupled BEC fraction a non-zero momentum [33].

To date, no continuous wave (CW) atom laser has been demonstrated in which there is replenishing of the reservoir in direct analogy with CW-optical laser. Replenishing the reservoir is required in steady state to compensate for the loss due to output coupling as well as to compensate for various intrinsic loss mechanisms such as collisions with hot atoms from the background vapor and inelastic two-body and three-body collisions between trapped atoms [16, 25, 34].

In this chapter we propose a scheme for loading the thermal cloud into a magnetic trap by optically pumping atoms from an external cold atomic beam source. Optical pumping is necessary since the magnetic potential is conservative and therefore a dissipative process is required for confinement of the atoms to be achieved. When combined with evaporative cooling, our approach may allow both steady state BEC and the CW atom laser to be demonstrated. The crucial point is that while one is trying to obtain a steady state BEC by injecting atoms into the magnetic trap, the loading mechanism itself should not heat the system or destroy the delicate condensate component.

There have been related proposals to ours using single atom "dark states" for reaching low temperatures by purely optical means—even well below the photon recoil limit [35, 36, 37]. As shown by Castin et al. in Ref. [38], the main hurdle in achieving BEC in all these schemes is that of photon reabsorption. Each reabsorption can remove one atom from the dark state and increment the energy of the cloud on average by one recoil energy. We engineer the analogous effect in our scheme to be negligible by

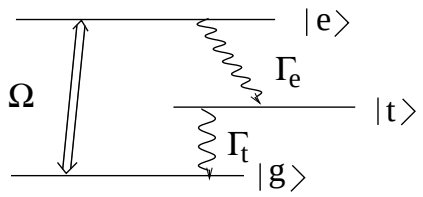

Figure 2.1: Level scheme illustrating: the ground state $|g\rangle$, excited state $|e\rangle$, and trap state $|t\rangle$. A laser is used to couple states $|g\rangle$ and $|e\rangle$ with an intensity characterized by the Rabi frequency Ω. Spontaneous emission of photons occurs with rate Γ_e from $|e\rangle$ to $|t\rangle$ and rate Γ_t from $|t\rangle$ to $|g\rangle$.

configuring the frequency of the emitted photons and adjusting the spatial geometry of the system to reduce the probability of reabsorption by the condensate.

2.2 The Model

We consider atoms whose internal degrees of freedom are described by a three level atomic system as shown in Fig. 2.1. Our description of the loading scheme is motivated by the experimental setup in Ref. [39]. There the atoms were loaded from a background vapor and precooled in a magneto-optical trap (MOT). They were then launched into the second MOT, optically pumped to the desired internal atomic hyperfine state, and transfered to a magnetically confining potential in which evaporative cooling was implemented. Here we study the possibility for loading the thermal cloud into the magnetic trap directly and continuously. This would allow the evaporative cooling to be carried out in steady state, which is the situation considered in Ref. [26].

Our scheme is illustrated in Fig. 2.2. Atoms are injected into the trap in state $|g\rangle$. As the atoms enter the spatial region containing the thermal cloud they pass through a laser field and are coherently pumped to the excited state $|e\rangle$ from which they may spontaneously emit a photon and end up in the trap state $|t\rangle$.

As will be shown later the spontaneously emitted photons may be out of resonance with the bare $|t\rangle \rightarrow |e\rangle$ transition and therefore reabsorption by atoms in the thermal cloud is greatly reduced (the exception to this general statement is the negligible fraction

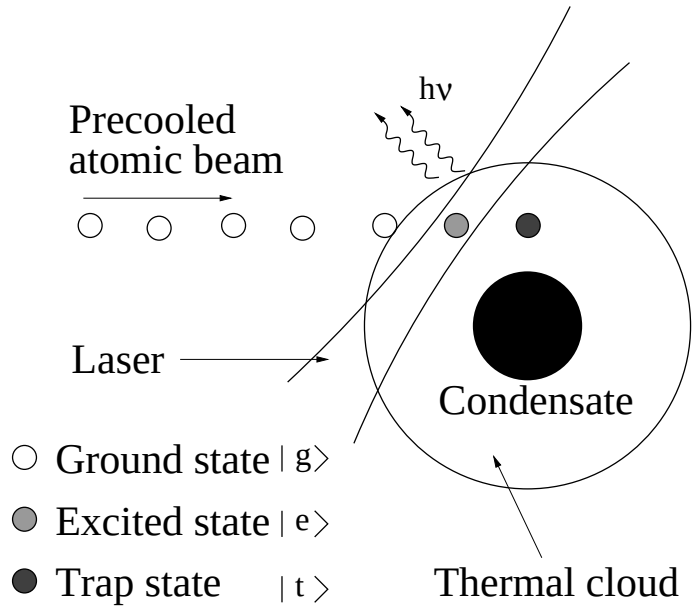

Figure 2.2: Schematic diagram showing the proposed loading scheme for obtaining a steady state BEC and CW atom laser. Atoms entering the laser field are in the ground state. As the atoms pass through the laser field, the population is continuously transferred to the trap state by a sequence of coherent pumping and spontaneous emission.

of thermal atoms in the localized spatial region of the focussed laser beam.) Using this approach atoms may be continuously loaded into the thermal cloud and be confined by the trapping potential without prohibitive reabsorption of the spontaneous photons emitted in the required dissipative process.

We use a master equation [40, 41] to study the evolution of this system. We define the spontaneous emission rates between the excited state and trap state and between the trap state and ground state as Γ_e and Γ_t respectively, and for simplicity neglect spontaneous emission directly from $|e\rangle$ to $|g\rangle$. Assuming that the laser is on resonance with the atomic transition frequency (detuning $\delta = 0$), the coherent interaction can be modeled by the Hamiltonian in the interaction picture

$$H = \frac{\Omega}{2}\hbar(\sigma_+^{ge} + \sigma_-^{ge}) \tag{2.1}$$

where $\sigma_+^{ge}, \sigma_-^{ge}$ are the raising and lowering operators respectively between the ground state $|g\rangle$ and the excited state $|e\rangle$. The master equation for the reduced density op-

erator of the atom includes terms due to both the spontaneous emission and a part corresponding to the coherent driving source. In the interaction picture this takes the form

$$\begin{aligned}\frac{\partial\rho}{\partial t} &= -i\frac{\Omega}{2}[\sigma_+^{ge}+\sigma_-^{ge},\rho]+\frac{\Gamma_e}{2}(2\sigma_-^{et}\rho\sigma_+^{et}-\sigma_+^{et}\sigma_-^{et}\rho-\rho\sigma_+^{et}\sigma_-^{et}) \\ &\quad+\frac{\Gamma_t}{2}(2\sigma_-^{gt}\rho\sigma_+^{gt}-\sigma_+^{gt}\sigma_-^{gt}\rho-\rho\sigma_+^{gt}\sigma_-^{gt}),\end{aligned} \tag{2.2}$$

where $\sigma_+^{et},\sigma_-^{et}$ are the raising and lowering operators respectively between the excited and trap state and $\sigma_+^{gt},\sigma_-^{gt}$ are the raising and lowering operators respectively between the trap state and ground state. From the above master equation we obtain the coupled differential equations for the evolution of matrix elements of ρ with the constraint $\mathrm{Tr}[\rho]=1$. The atomic population in the three levels given by the matrix elements $\rho_{gg}(t),\rho_{ee}(t)$ and $\rho_{tt}(t)$ are obtained for values of $\Gamma_e=1$ and $\Omega=5$ and initial condition given by $\rho_{gg}(0)=1$, $\rho_{ee}(0)=\rho_{tt}(0)=0$. We consider two different values for Γ_t; $\Gamma_t=2$ and $\Gamma_t=0$, which give qualitatively distinct dynamics. The zero value for Γ_t corresponds to optically pumping the atom from the ground to trap state, and leads to complete transfer of population at long times. The non-zero value of Γ_t gives a steady-state solution for the level populations in which the atom cycles indefinitely, which will be useful later for the calculation of the spectrum of the spontaneously emitted photons.

The steady state spectrum of spontaneously emitted photons on the $|e\rangle\rightarrow|t\rangle$ transition is given by the Fourier transform of the two-time correlation function

$$K(t+\tau,t)=\langle\sigma_+^{et}(t+\tau)\sigma_-^{et}(t)\rangle, \tag{2.3}$$

the differential equation for which is obtained by combining the equation for ρ_{tg} and ρ_{te} above along with the quantum regression theorem (QRT) [41].

The QRT states that for a set of operators Y_i, which evolve in steady-state according to

$$\frac{\partial}{\partial\tau}\langle Y_i(\tau)\rangle=\sum_j G_{ij}\langle Y_j(\tau)\rangle, \tag{2.4}$$

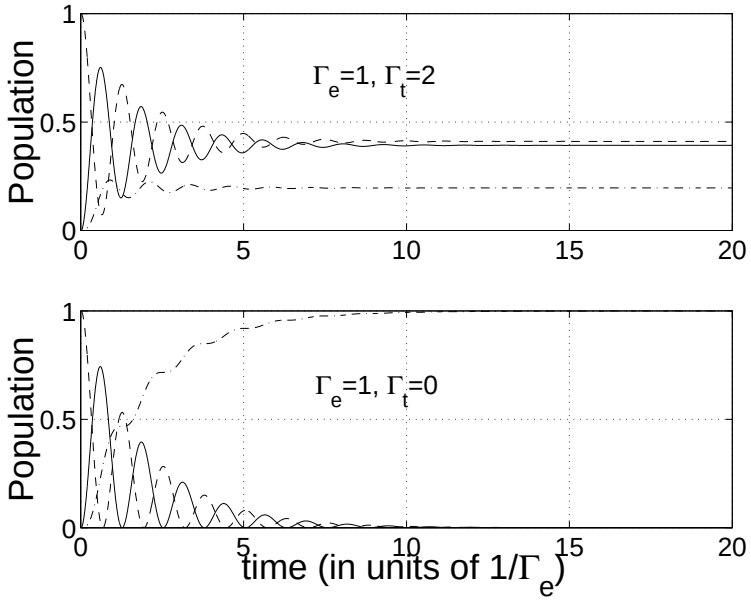

Figure 2.3: Populations as a function of time; ground state $|g\rangle$ shown by a solid line, excited state $|e\rangle$ shown by dashed and trap state $|t\rangle$ shown by dot-dashed line. The parameters used were $\Omega = 5, \Gamma_e = 1$ and (a) $\Gamma_t = 2$, (b) $\Gamma_t = 0$.

then two-time averages can be related to the one-time expectation values by

$$\frac{\partial}{\partial\tau}\langle Y_i(t+\tau)Y_l(t)\rangle = \sum_j G_{ij}\langle Y_j(t+\tau)Y_l(t)\rangle, \tag{2.5}$$

where the G_{ij}'s are the same coefficients in both Eq. (2.4) and Eq. (2.5). For a general non-steady-state problem in which transient dynamics must be considered, application of the QRT is typically more complicated. For simplicity our approach is to take a fictitious non-zero value of Γ_t, and then consider the limit $\Gamma_t \to 0$. The spectrum defined as

$$S(\omega) = \lim_{t\to\infty}\int_{-t}^{t} d\tau K(\tau)e^{-i\omega\tau} \tag{2.6}$$

is then given by

$$S(\omega) = \frac{\rho_{tt}^{ss}}{\pi\Omega_{\text{eff}}}\left[\frac{\left(i\frac{\Gamma_e}{4}+\frac{\Omega_{\text{eff}}}{2}\right)\left(\frac{\Gamma_e}{4}+\frac{\Gamma_t}{2}\right)}{\left(\frac{\Gamma_e}{4}+\frac{\Gamma_t}{2}\right)^2+\left(\omega+\frac{\Omega_{\text{eff}}}{2}\right)^2}\right] + \frac{\rho_{tt}^{ss}}{\pi\Omega_{\text{eff}}}\left[\frac{\left(-i\frac{\Gamma_e}{4}+\frac{\Omega_{\text{eff}}}{2}\right)\left(\frac{\Gamma_e}{4}+\frac{\Gamma_t}{2}\right)}{\left(\frac{\Gamma_e}{4}+\frac{\Gamma_t}{2}\right)^2+\left(\omega-\frac{\Omega_{\text{eff}}}{2}\right)^2}\right] \tag{2.7}$$

where $\Omega_{\text{eff}} = \sqrt{\Omega^2 - \Gamma_e^2/4}$

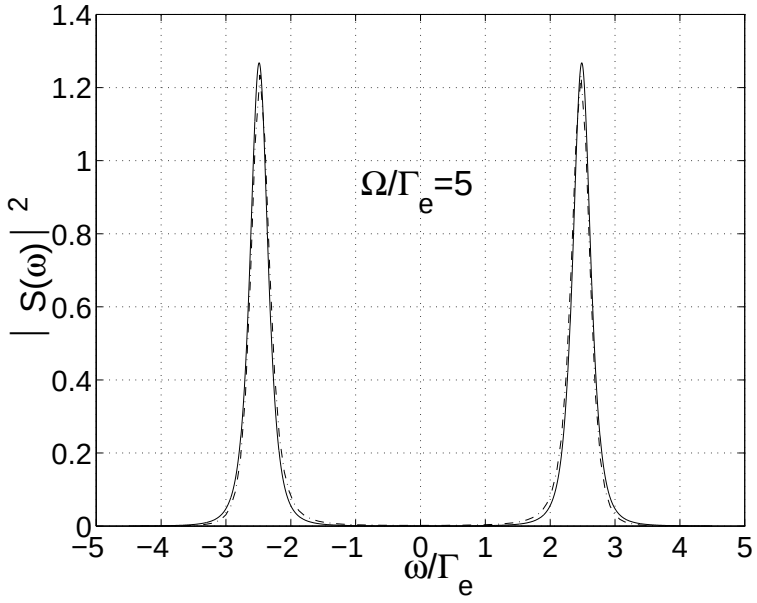

Figure 2.4: Comparison of the $|e\rangle \rightarrow |t\rangle$ transition spectrum using the steady state calculation (solid) and the quantum trajectory method (dash-dot).

In Fig. 2.4 we plot $|S(\omega)|^2$ shown by the solid curve for the limiting case of $\Gamma_t \rightarrow 0$. The spectrum is AC-Stark split into two Lorentzians separated by Ω_{eff}. This spectrum is commonly referred to as the Autler-Townes doublet [43, 44].

For comparison we now use the method described in Ref. [42] to provide an alternative calculation of the fluorescence spectrum, extending our treatment to include the possibility for the time dependence of Ω. This involves the decomposition into "quantum trajectories", where the evolution is conditional on a certain record of dissipative events. In the case of the evolution conditional on the spontaneous emission of no photons, the quantum trajectory $|\psi(t)\rangle$, evolves according to

$$\frac{\partial|\psi(t)\rangle}{\partial t} = \frac{1}{i\hbar} H_{\text{eff}} |\psi(t)\rangle, \tag{2.8}$$

where H_{eff} is the non-Hermitian Hamiltonian defined by

$$H_{\text{eff}} = H - i\frac{\hbar\Gamma_e}{2}\sigma_+^{et}\sigma_-^{et}. \tag{2.9}$$

For the evolution conditional on the spontaneous emission of one photon, each quantum

trajectory $|\psi_{\omega_j}(t)\rangle$ is labelled by the frequency of the photon ω_j. If we consider a time interval $t \in [0, \tau]$, then according to the Fourier sampling theorem a complete description requires choosing each ω_j from a discrete but infinite set of frequencies spaced $(2\pi/\tau)$ apart. The observed spectrum may then be defined as

$$S(\omega) = \langle \psi_\omega(\tau) | \psi_\omega(\tau) \rangle \tag{2.10}$$

with (see Ref. [42])

$$\frac{d}{dt}|\psi_{\omega_j}(t)\rangle = \sqrt{\frac{\Gamma_e}{\tau}}\sigma_-^{et}|\psi(t)\rangle + \frac{1}{i\hbar}(H_{\text{eff}} + \hbar\omega_j)|\psi_{\omega_j}(t)\rangle. \tag{2.11}$$

By solving the coupled Eqns. (2.8) and (2.11) we get

$$|\psi_{\omega_j}(t)\rangle = \begin{pmatrix} 0 \\ 0 \\ f_{\omega_j}(t) \end{pmatrix} \tag{2.12}$$

where

$$\begin{aligned} f_{\omega_j}(t) &= q\mathcal{M}N^{-1}\left((i\omega_j - \Gamma_e/4)^2 + \Omega_{\text{eff}}^2/4\right)^{-1} \\ \mathcal{M} &= \sin\left(\frac{\Omega_{\text{eff}}t}{2}\right)e^{-\Gamma_e t/4}(i\omega_j - \Gamma_e/4) \\ &\quad -\frac{\Omega_{\text{eff}}}{2}\cos\left(\frac{\Omega_{\text{eff}}t}{2}\right)e^{-\Gamma_e t/4} + \frac{\Omega_{\text{eff}}}{2}e^{-i\omega_j t} \\ q &= \frac{4}{\Omega}\sqrt{\frac{\Gamma_e}{\tau}}\left[\frac{\lambda_+\lambda_-}{\lambda_+ - \lambda_-}\right] \end{aligned} \tag{2.13}$$

The single-photon spectrum which is so obtained, $|S(\omega)|^2$, is shown by dot-dashed curve in Fig. 2.4. The normalization constant N is introduced so that $|f_{\omega_j}|^2 \to 1$ as $t \to \infty$. We see a close agreement between the spectra calculated by the two methods, the quantum regression theorem and the quantum trajectory approach of solving conditional dynamics. The crucial observation is the absence of a significant contribution in the zero-frequency region of the fluorescence spectrum where there would be strong photon reabsorption by the thermal cloud. Virtually all of the spontaneous photons are off resonance with the bare $|t\rangle \to |e\rangle$ transition which is the resonant frequency for all thermal atoms out of the laser field focus.

2.3 Effect of time dependent Ω and finite detuning on the transient spectrum

The assumed time independent nature of the interaction picture Hamiltonian (2.1) may not be a realistic situation. In an actual experiment, as the atoms pass through the laser beam they would see a continuously changing intensity and hence a changing Ω. At the same time, existence of finite detuning δ (assumed previously to be zero for simplicity), may result in the time dependence of the operators σ_+^{ge} and σ_-^{ge} given by

$$\sigma_\pm^{ge}(t) = \sigma_\pm^{ge} e^{\pm i\delta t} \tag{2.14}$$

Thus, in a more realistic situation the interaction picture Hamiltonian of Eq.(2.1) should be replaced by the time dependent form

$$H(t) = \frac{\Omega(t)}{2}\hbar(\sigma_+^{ge} e^{i\delta t} + \sigma_-^{ge} e^{-i\delta t}) \tag{2.15}$$

Using this interaction Hamiltonian we now recalculate the AC-Stark split spectrum. Firstly we consider the $\delta = 0$ case with the time dependence solely due to $\Omega(t)$. Since the problem is a transient one in which population is completely transferred to the trap state over a certain time scale, the variation of Ω over this time scale is crucial. Also, from the calculations in the previous section it is clear that a large value of Ω is favorable for our scheme. We therefore consider various time scales over which Ω reaches its maximum value compared to the optical pumping time as shown in Fig. 2.5. The corresponding spectrum shown in Fig. 2.6 is calculated using the method of conditional dynamics discussed in the previous section. The calculation shows that the crucial requirement for our model i.e. that the emitted photons cannot be resonantly absorbed by the thermal cloud outside the laser focus,is only satisfied if the atom sees a field increasing in intensity on a time scale which is short compared to the time it takes to optically pump the population from $|g\rangle$ to $|t\rangle$. For a particular average velocity of the atoms in the atom beam source, this gives the requirement for the spatial variation of

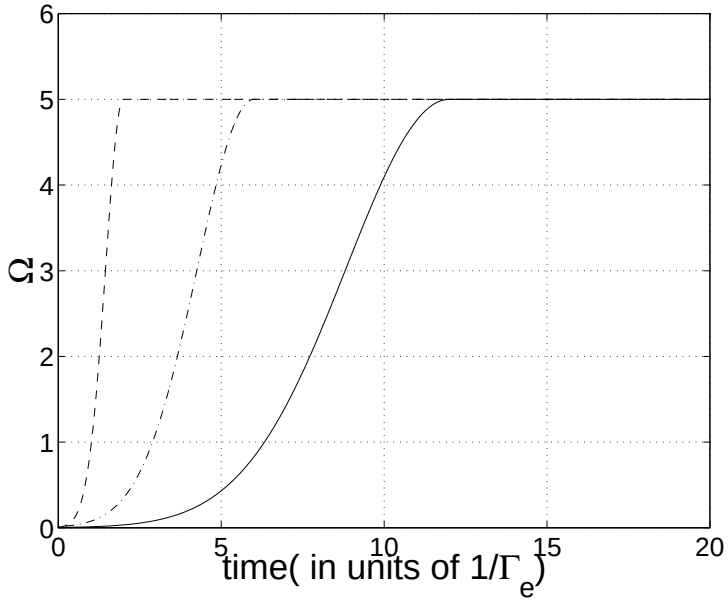

Figure 2.5: Ω as a function of time, t. The three different curves correspond to different time scales over which Ω reaches its maximum value.

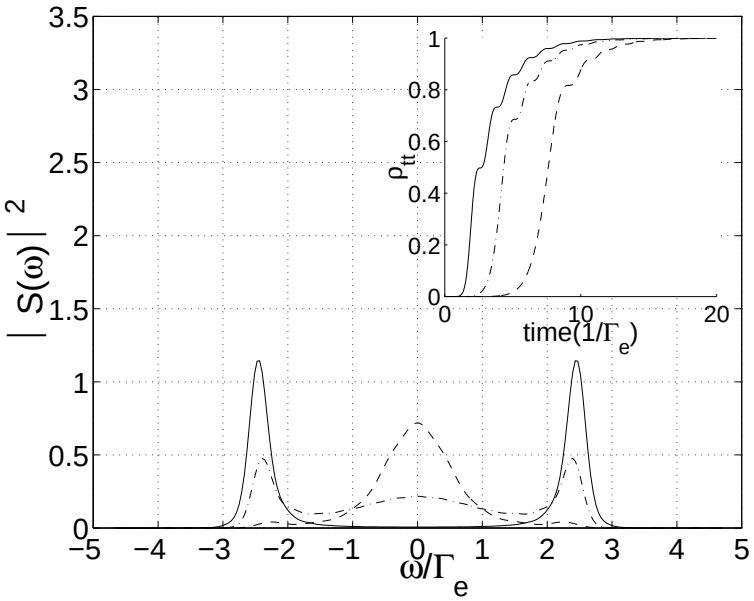

Figure 2.6: Transient spectrum for $|e\rangle \rightarrow |t\rangle$ transition for the different scenarios for $\Omega(t)$ shown in Fig.2.5.

the laser intensity associated with the beam waist. Alternatively, the laser field could be pulsed on and off to achieve a sufficiently rapid rise time.

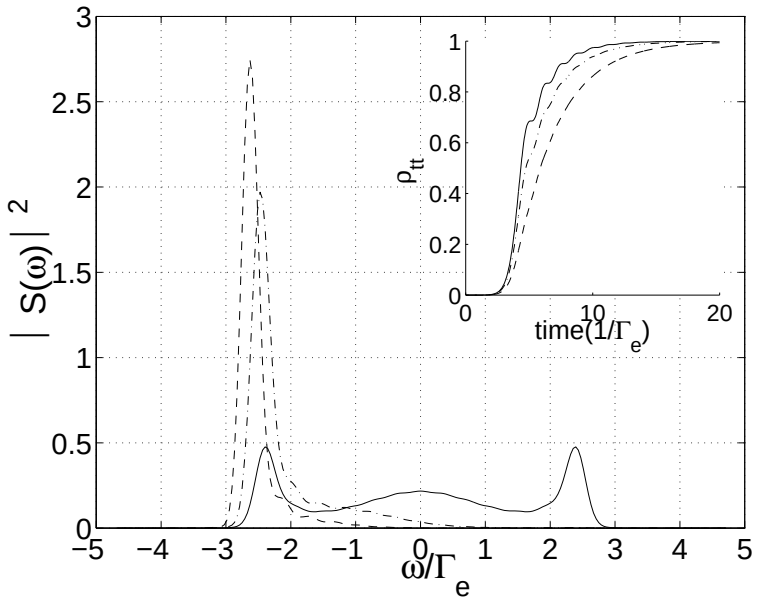

Figure 2.7: Figure shows the effect of detuning on the transient spectrum for $|e\rangle \rightarrow |t\rangle$ transition. Dashed for $\delta = 0$, solid for $\delta = 1$ and dot-dashed for $\delta = 2$.

Now we consider the effect of finite detuning, δ, in addition to the time dependence of Ω. For the case of constant Ω, a finite δ has the effect of transforming Ω to $\sqrt{\Omega^2 + \delta^2}$ [44]. Therefore, even if Ω depends on time, it is intuitive to expect a similar effect resulting in an increased AC-Stark splitting. This is illustrated in Fig. 2.7 where the spectrum is calculated for the case of $\Omega(t)$ shown by dot-dashed curve of Fig. 2.5 for various values of δ. Thus a large detuning may seem to be favorable for our purpose since the spontaneous photons are emitted further away from resonance. On the other hand, large detuning means slower optical pumping rate and hence a wider laser focus will be required for the same $\Omega(t)$ as illustrated in the inset of Fig. 2.7. Therefore, it is important to achieve an optimum set of parameters that would allow a maximum possible splitting depending on the average atomic speed and line width of the atomic levels under consideration.

2.4 Conclusion

The AC-Stark splitting of the spectrum indicates that this scheme may potentially be used to provide a method for continuous loading of the thermal cloud in an atom laser. In the case of constant Ω the spectrum of the spontaneously emitted photons consists of two peaks separated by Ω_{eff}. Even for the realistic case of time varying Ω, large splitting between the two peaks can be achieved provided that the rise time of the laser field intensity is sufficiently small. The splitting can be further enhanced by introducing a finite detuning.

Large splitting of the spectrum is essential to avoid heating due to inelastic multiple scattering of photons. Usually heating in an optical pumping scheme is caused by photon reabsorption and re-emission. Each reabsorption can remove one atom from the tr ap state and increment the energy of the cloud on average by one recoil energy. This effect is significantly reduced in our model since the spontaneously emitted photons are off-resonance with the $|t\rangle \rightarrow |e\rangle$ transition and cannot be reabsorbed by atoms outside the laser focus. Therefore the heating of the thermal component due to photon reabsorption may be suppressed. One can also reduce the cross section for photon reabsorption by designing the shape of the trap, for example a cigar shape or disc shape, such that there is a limited solid angle for photon reabsorption. Another possibility is to align the optical pumping laser and the geometry of the trap to use the intrinsic dipole radiation pattern to reduce spontaneous emission into unfavorable directions.

Our model requires that the atoms be in the trap state before they are out of the laser field, which may place a limit on the maximum speed of atoms in the atomic beam source. However, the faster the incoming atoms, the smaller the rise time of Ω which as previously discussed is required to avoid the emission of photons at zero-frequency. The optimum speed of incoming atoms is therefore a balance between these two requirements. Since our goal is to obtain BEC in a steady state and not just BEC, one possibility to

obtain sufficiently slow speeds is to use a condensate prepared in another trap as a source instead of just laser precooled atoms formed from a magneto-optical-trap.

For a typical alkali atom, the Zeeman level diagram is composed of many hyperfine levels. Even though our three level system is a simplification of a real situation, most of the omitted processes, such as imperfect optical pumping to the trapping state, will lead to additional loss of atoms and modify the effective incident flux. This will impact the possibility for achieving a sufficiently high pumping rate of cold atoms to allow the CW atom laser and steady state BEC to be achieved, as discussed in Ref. [26].

Chapter 3

Memory effects and conservation laws in the quantum kinetic evolution of a dilute Bose gas

Published in Physical Review A **66**, *043618 (2002)*

3.1 Introduction

In the mean-field approximation, a Bose-condensed phase is well described by the Gross-Pitaevskii (GP) equation [45]. Examples of collective phenomena that arise at the mean-field level include the formation of vortex states [46, 47, 48, 49, 50] and collective excitations [51, 52, 53]. In this context, the GP equation is often sufficient to describe the dynamics at $T = 0$. However, at finite temperatures, $0 < T < T_c$, it is important to include effects due to the presence of a thermal component. These thermal, non-condensed atoms interact mutually and with the condensed atoms via binary collisions. In fact, the collisional dynamics is the microscopic mechanism for evaporative cooling and it leads to BEC. Finite temperature effects are also responsible for phenomena such as phase diffusion and damping of collective excitations. In order to describe these effects, the inclusion of collisions due to the thermal component becomes essential. A generalized GP equation, for example the Hartree-Fock-Bogoliubov approach, includes the effects of collisions only indirectly through their energy shifts and hence is valid only at very low temperature (collisionless regime).

In the other limit, $T > T_c$, the condensate component is absent and the thermal component completely determines the dynamics. This limit is well described by the

quantum-Boltzmann (QB) equation. Thus, a non-equilibrium kinetic theory, which interpolates between the GP and the QB limits corresponding to $T = 0$ and $T > T_c$, respectively, is necessary to provide a such a complete description.

Currently, there exist a number of kinetic theories including those based on quantum stochastics [54, 55], the Fokker-Planck equation [56], generalized single-time master equations [57, 58, 59], a semiclassical hydrodynamic approach [60, 61] and a Green's function approach [62, 63, 64]. However, obtaining explicit solutions for the nonequilibrium dynamics has remained a challenge. In particular, the condensate growth dynamics is still a very active area of research [65, 66]. More recently, Monte Carlo simulations have provided an alternative approach to the solution of non-equilibrium master equations [67, 68, 69, 70]. In particular, Jackson and Zaremba [70] have shown good agreement with experimental observations of decay rates and frequencies. However Monte Carlo approaches suffer from the simulation noise which can lead to a spread in the value of quantities that should be exactly conserved. Also the theory as formulated can only be applied to situations in which the anomalous pair correlations are not important (Popov approximation). Under certain conditions, typically when the interactions are strong, anomalous densities can play a significant role. This was the case for example in the recent observation of Ramsey type oscillations [71] and their subsequent theoretical explanation [72].

Energy conservation in theories with Boltzmann type collision integrals is typically enforced by requiring exact energy conservation in each individual collision event. From a fundamental perspective this is unsatisfactory as it would be preferable if energy conservation would arise intrinsically from the theoretical formulation. The essential point is that such an approach would allow off the energy shell collision events so long as energy is conserved overall. In practice this requires including effects arising from the finite duration of a collision and quasiparticle damping.

Another issue for consideration is the question of Markovian vs. non-Markovian

dynamics in a inhomogeneous system. Even though, for a dilute Bose gas, memory effects can be neglected under the principle of rapid attenuation of correlations, non-Markovian behavior is intricately related to the conservation properties [73, 74, 75, 76, 77]. For example, the Markovian-Boltzmann type kinetic equations derived by Walser *et. al.* [13] conserves energy only to first order [78]. Previous attempts to address this issue have been limited to the discussion of systems with translational symmetry [79, 80].

In this chapter, we generalize the kinetic theory derived in [13] in order to address the problems discussed above. Presently, we limit our goal to the derivation of a systematic Markov approximation from the non-Markovian Born theory by including finite duration effects and quasiparticle damping. Using the short and long time behavior of the two time Green's function, we obtain a damping function that gives improved energy conservation to second order in the perturbation parameter.

We apply this theory to a simple model of an inhomogeneous Bose gas confined in a spherical box above T_c with discrete basis states. The usual Born-Markov theory gives a δ-function energy conservation which for any interacting system will result in only exchange collisions. Therefore introducing finite duration effects facilitates the calculation by relaxing the energy conservation condition. The simplicity of this model allows us to study the real time evolution of the system from some initial state to a final state of equilibrium. We perform a linear response calculation to study the stability and damping rates for the steady-state solution. A calculation on similar lines with a more realistic model of a harmonic trapping potential and non-vanishing condensate (α) and pair-correlation ($\tilde{m}$) components will ultimately make comparison with experimental observations of the frequency and damping rates of collective excitations possible.

This chapter is organized as follows. In Sec. 3.2 we derive a non-Markovian generalization to the kinetic theory of Ref. [13] using the prescription of a nonequilibrium statistical operator method [81]. Both quasiparticle damping and damping arising from

the finite time of collision events are discussed in Sec. 3.3. This has implications for the underlying symmetries of the theory and their associated conserved quantities. In Sec. 3.4, we apply this generalized kinetic theory to a simple model of an inhomogeneous dilute Bose gas confined in a spherical box and obtain a self consistent steady-state solution to the second-order kinetic theory. Finally in Sec. 3.5, we study the response of the system to a small perturbation. This allows us to determine the frequencies and damping rates of collective modes.

3.2 Kinetic equations

We start with the many-body Hamiltonian for a weakly interacting Bose gas given by

$$\hat{H} = \hat{H}^{(0)} + \hat{H}^{(1)}, \tag{3.1}$$

where $\hat{H}^{(0)}$ is the single particle Hamiltonian that is defined as

$$\hat{H}^{(0)} = \varepsilon^{12}\, \hat{a}_1^\dagger \hat{a}_2 \tag{3.2}$$

using the implicit summation convention for repeated indices. The two-body energy $\hat{H}^{(1)}$ is given by

$$\hat{H}^{(1)} = \phi^{1234}\, \hat{a}_1^\dagger \hat{a}_2^\dagger \hat{a}_3 \hat{a}_4. \tag{3.3}$$

The bosonic operators $\hat{a}_1$ and $\hat{a}_1^\dagger$ annihilate and create a particle in a single particle state $|1\rangle$, respectively. The abbreviated notation $|1\rangle$ represents a state specified by a complete set of quantum numbers for both the motional and electronic degrees of freedom.

We assume that the particles are confined by an external trapping potential V_{ext}. Thus, the matrix elements of the single particle Hamiltonian are given by

$$\varepsilon^{12} \;=\; \langle 1|\frac{\hat{\mathbf{p}}^2}{2m} + V_{\text{ext}}(\hat{\mathbf{x}})|2\rangle, \tag{3.4}$$

where m is the mass. The binary interaction is mediated by a short range repulsive

potential $V_{\rm bin}$. This gives the symmetrized ($\mathcal{S}$) matrix elements

$$\phi^{1234} \;=\; (\mathcal{S})\langle 1|\otimes\langle 2|V_{\rm bin}(\hat{\mathbf{x}}\otimes\mathbf{I}-\mathbf{I}\otimes\hat{\mathbf{x}})|3\rangle\otimes|4\rangle. \tag{3.5}$$

In the low energy limit $V_{\rm bin}$ can be approximated by a contact potential with the matrix elements given by

$$\phi^{1234} \;\approx\; \frac{V_0}{2}\int_{-\infty}^{\infty}\langle 1|\mathbf{x}\rangle\langle 2|\mathbf{x}\rangle\langle\mathbf{x}|3\rangle\langle\mathbf{x}|4\rangle\, d^3x. \tag{3.6}$$

The interaction strength V_0, is related to the scattering length $a_{\rm s}$ by $V_0 = 4\pi\hbar^2 a_{\rm s}/m$.

Here, we use the well-known nonequilibrium statistical operator method [81, 82] to obtain an explicitly non-Markovian version of the kinetic theory [13]. In this approach, the nonequilibrium state of a weakly interacting quantum gas is specified by a set of single time master variables. For our system the most important master variable is the single particle density matrix $f(t)$,

$$f_{12}(t) = \langle\hat{a}_2^\dagger\hat{a}_1\rangle = {\rm Tr}\left\{\hat{a}_2^\dagger\hat{a}_1\,\sigma(t)\right\}, \tag{3.7}$$

where $\langle\ldots\rangle = {\rm Tr}\{\ldots\sigma({\rm t})\}$ and $\sigma(t)$ is the statistical many-body density operator. We focus our studies on the temperature regime above and in close proximity to the critical temperature for BEC. For this reason, we do not consider either symmetry breaking fields, $\langle\hat{a}_1\rangle$, or the anomalous fluctuations, $\langle\hat{a}_1\hat{a}_2\rangle$. We therefore define $\{\hat{\gamma}_0 = I, \hat{\gamma}_k = \hat{a}_2^\dagger\hat{a}_1 | k\in\{(1,2)\}\}$ as our complete set of relevant operators. The expectation values of these operators, $\gamma_k(t) = \langle\hat{\gamma}_k\rangle$, are the only quantities that will appear in the final kinetic equations.

The time evolution of the nonequilibrium statistical operator $\sigma(t)$ is described by the Liouville equation with an extra source term on the right hand side:

$$\frac{d}{dt}\sigma(t) + \frac{i}{\hbar}[\hat{H},\sigma(t)] = -\eta\left(\sigma(t)-\sigma^{(0)}(t)\right). \tag{3.8}$$

Such a source term breaks the time reversal symmetry of the Liouville equation and represents a convenient way to incorporate the irreversible character of macroscopic

processes. We will see later that this procedure leads to finite duration of collision effects and quasiparticle damping. The relevant distribution $\sigma^{(0)}(t)$ given by

$$\sigma^{(0)}(t) = \sigma^{(0)}_{\{\gamma(t)\}} = \exp\Big\{\hat{\gamma}_k \Upsilon^k(t)\Big\}, \tag{3.9}$$

where $\Upsilon^k(t)$ are the Lagrange multipliers, represents a special solution that maximizes the information entropy $S' = -\mathrm{Tr}\{\sigma' \log(\sigma')\}$ for the given averages $\gamma_k(t)$. Furthermore, at some initial instance $t = t_0$ in the remote past, we can assume that $\sigma(t_0)$ corresponds to its noninteracting value and therefore

$$\sigma(t_0) = \sigma^{(0)}(t_0). \tag{3.10}$$

The Lagrange multipliers $\Upsilon^k(t)$ are calculated from the self-consistency condition

$$\gamma_k(t) \;\; = \;\; \mathrm{Tr}\{\hat{\gamma}_\mathrm{k}\, \sigma^{(0)}(\mathrm{t})\} = \mathrm{Tr}\{\hat{\gamma}_\mathrm{k}\, \sigma(\mathrm{t})\}. \tag{3.11}$$

This essentially enforces the Chapman-Enskog condition [83] for the restricted set of relevant operators at all times.

From the Liouville equation (3.8) one can easily establish the basic equations of motion for the average values,

$$\frac{d}{dt}\gamma_k(t) = \frac{i}{\hbar}\mathrm{Tr}\Big\{[\hat{H}^{(0)}, \hat{\gamma}_k]\, \sigma(t)\Big\} + \frac{i}{\hbar}\mathrm{Tr}\Big\{[\hat{H}^{(1)}, \hat{\gamma}_k]\, \sigma(t)\Big\}. \tag{3.12}$$

The form of $\hat{H}^{(0)}$ enables us to express the first trace on the right hand side of the above equation in terms of the averages $\gamma_k(t)$. The second trace plays the role of the "collision" term, the evaluation of which requires us to seek an integral solution of the Liouville equation. But, before we proceed, it is instructive to repartition the total Hamiltonian Eq. (3.1) into single particle and two-particle contributions,

$$\begin{aligned} \hat{H} \;\; &= \;\; \hat{\tilde{H}}^{(0)}(t) + \hat{\tilde{H}}^{(1)}(t) \\ &= \;\; \Big[\hat{H}^{(0)} + \hat{Q}(t)\Big] + \Big[\hat{H}^{(1)} - \hat{Q}(t)\Big]. \end{aligned} \tag{3.13}$$

This modification anticipates self-energy shifts

$$\hat{Q}(t) = Q^{12}(t)\hat{a}_1^\dagger \hat{a}_2, \tag{3.14}$$

which will inevitably arise in the course of the calculation.

An integral solution for $\sigma(t)$ can then be obtained easily from the Liouville equation (3.8), by using the single particle time evolution operator $\hat{U}^{(0)}(t,t_1)$, the boundary condition Eq. (3.9), and an additional partial integration. Thus, one finds

$$\begin{aligned}\sigma(t) &= \sigma^{(0)}(t) - \int_{t_0}^{t} dt_1\, e^{-\eta(t-t_1)}\hat{U}^{(0)}(t,t_1) \times \Big[\frac{d}{dt_1}\sigma^{(0)}(t_1) + \frac{i}{\hbar}[\hat{\bar{H}}^{(0)}(t_1), \sigma^{(0)}(t_1)] \\ &+ \frac{i}{\hbar}[\hat{\bar{H}}^{(1)}(t_1), \sigma(t_1)]\Big]\hat{U}^{(0)\dagger}(t,t_1). \end{aligned} \tag{3.15}$$

Since the Hamiltonian $\hat{\bar{H}}^{(0)}(t)$ depends on time through the $\hat{Q}(t)$, the time evolution operator $\hat{U}^{(0)}$ is in general a time-ordered exponent

$$\hat{U}^{(0)}(t,t_0) = \hat{T}\exp\left[-\frac{i}{\hbar}\int_{t_0}^{t} dt_1\, \hat{\bar{H}}^{(0)}(t_1)\right]. \tag{3.16}$$

To establish the time derivative $d\sigma^{(0)}(t_1)/dt_1$ in Eq. (3.15), we recall from Eq. (3.9) that the relevant operator depends only implicitly on time through the averages $\gamma_k(t_1)$. Moreover by exploiting the transformation properties of a quantum Gaussian (see Appendix A), one finds that

$$\begin{aligned}\frac{d}{dt}\sigma^{(0)}(t) &= \frac{d}{dt}\gamma_k(t)\,\partial_{\gamma_k}\sigma^{(0)}(t) \\ &= -\frac{i}{\hbar}[\hat{\bar{H}}^{(0)}(t), \sigma^{(0)}(t)] + \frac{i}{\hbar}\mathrm{Tr}\left\{[\hat{\bar{H}}^{(1)}(t), \hat{\gamma}_k]\,\sigma(t)\right\}\,\partial_{\gamma_k}\sigma^{(0)}(t). \end{aligned} \tag{3.17}$$

Using these relations we eliminate the time derivative of $\sigma^{(0)}(t_1)$ in Eq. (3.15), to obtain the integral form of the statistical operator

$$\begin{aligned}\sigma(t) &= \sigma^{(0)}(t) - \frac{i}{\hbar}\int_{t_0}^{t} dt_1 e^{-\eta(t-t_1)}\hat{U}^{(0)}(t,t_1) \times \Big[\mathrm{Tr}\left\{[\hat{\bar{\mathrm{H}}}^{(1)}(\mathrm{t}_1), \hat{\gamma}_\mathrm{k}]\,\sigma(\mathrm{t}_1)\right\}\partial_{\gamma_\mathrm{k}}\sigma^{(0)}(\mathrm{t}_1) \\ &+ [\hat{\bar{H}}^{(1)}(t_1), \sigma(t_1)]\Big]\hat{U}^{(0)\dagger}(t,t_1). \end{aligned} \tag{3.18}$$

Since we are only interested in a weakly interacting gas, we seek a power series expansion in the interaction strength

$$\sigma(t) = \sigma^{(0)}(t) + \sigma^{(1)}(t) + ... \tag{3.19}$$

$$\sigma^{(1)}(t) = -\frac{i}{\hbar}\int_{t_0}^{t} dt_1 e^{-\eta(t-t_1)}\hat{U}^{(0)}(t,t_1) \times \Big[\mathrm{Tr}\left\{[\hat{\hat{\mathrm{H}}}^{(1)}(\mathrm{t}_1), \hat{\gamma}_{\mathrm{k}}]\,\sigma^{(0)}(\mathrm{t}_1)\right\}\partial_{\gamma_{\mathrm{k}}}\sigma^{(0)}(\mathrm{t}_1) + [\hat{\hat{H}}^{(1)}(t_1), \sigma^{(0)}(t_1)]\Big]\hat{U}^{(0)\dagger}(t,t_1). \tag{3.20}$$

With this explicit expression for the statistical operator, the evaluation of the equation of motion (3.12) is straight forward and one obtains the quantum-Boltzmann equation

$$\frac{d}{dt}f(t) = \mathcal{L}[f] + \mathcal{L}[f]^{\dagger}. \tag{3.21}$$

Here, Wick's theorem has been used to express the higher order averages in terms of the single particle ones. The kinetic operator $\mathcal{L}$ consists of a reversible Hartree-Fock (HF) part $\mathcal{L}_{\mathrm{HF}}$ and a collisional quantum-Boltzmann contribution $\mathcal{L}_{\mathrm{QB}}$,

$$\begin{aligned}\mathcal{L}[f] &= \mathcal{L}_{\mathrm{HF}}[f] + \mathcal{L}_{\mathrm{QB}}[f],\\ \mathcal{L}_{\mathrm{HF}}[f] &= -\frac{i}{\hbar}H_{\mathrm{HF}}(t)f(t),\\ \mathcal{L}_{\mathrm{QB}}[f] &= \Gamma_{ff(1+f)(1+f)} - \Gamma_{(1+f)(1+f)ff}.\end{aligned}$$

$H_{\mathrm{HF}} = \varepsilon + 2\,U_f$ is the Hartree-Fock Hamiltonian, with $U_f^{14} = 2\,\phi^{1234}f_{32}$ the self energy, while Γ's are the collision integrals given by

$$\begin{aligned}\Gamma^{15}_{ABCD} &= \frac{1}{\hbar}\int_{t_0}^{t} dt_1 \Big[e^{-\eta(t-t_1)}\phi^{1234}\phi^{1''2''3''4''}\\ &\times \mathcal{K}_{1''1'}(t,t_1)\mathcal{K}_{2''2'}(t,t_1)\mathcal{K}^{\dagger}_{3''3'}(t,t_1)\mathcal{K}^{\dagger}_{4''4'}(t,t_1)\\ &\times A_{31'}(t_1)B_{42'}(t_1)C_{4'2}(t_1)D_{3'5}(t_1)\Big].\end{aligned} \tag{3.22}$$

The propagators $\mathcal{K}(t,t_0)$ are given by

$$\mathcal{K}(t,t_0) = T\exp\left[-\frac{i}{\hbar}\int_{t_0}^{t} dt_1\, H_{\mathrm{HF}}(t_1)\right]. \tag{3.23}$$

Therefore, unlike the collision terms of Ref. [13], the Γ's defined above depend on the past history of the system. Thus Eq. (3.21) represents a non-Markovian generalization of the kinetic equation previously derived in Ref. [13].

3.3 Conservation laws and Quasi-particle damping

The conserved quantities for a closed isolated system are the total energy E and the total number N. These quantities then represent the constants of motion for the full kinetic equation. The total number operator can be represented as a linear combination of the relevant operators,

$$\hat{N} = \hat{a}_1^\dagger \hat{a}_1, \tag{3.24}$$

and therefore the functional $N(f)$, representing the total number is given by

$$N(f) = \mathrm{Tr}\{f\}. \tag{3.25}$$

The kinetic equation for $N(f)$ can then be written as

$$\begin{aligned} \frac{d}{dt}N(f) &= \mathrm{Tr}\left\{\mathcal{L}[f] + \mathcal{L}[f]^\dagger\right\} \\ &= \mathrm{Tr}\left\{\mathcal{L}_{HF}[f] + \mathcal{L}_{HF}[f]^\dagger\right\} + \mathrm{Tr}\left\{\mathcal{L}_{QB}[f] + \mathcal{L}_{QB}[f]^\dagger\right\}. \end{aligned} \tag{3.26}$$

The first order term on the right-hand side involves the trace of a commutator and is trivially equal to zero. The Γ's associated with the second order terms have the following property due to the symmetries of ϕ,

$$\mathrm{Tr}\left\{\Gamma_{ff(1+f)(1+f)}\right\} = \mathrm{Tr}\left\{\Gamma_{(1+f)(1+f)ff}\right\}^*. \tag{3.27}$$

As a result, the second order contribution in Eq. (3.26) can also be shown to be zero. Hence the total number N is a constant of motion. The important point here is that the total number conservation is a result of the symmetries of ϕ and does not dependent on the non-Markovian nature of the collision integral. Therefore a Markov approximation would leave this conservation law unchanged.

While the number conservation is a natural consequence of the self-consistency condition, the total energy conservation is not obvious as the Hamiltonian $\hat{H}$ cannot be represented as a linear combination of the relevant operators. We start with writing

the total energy functional $E(f)$ as a perturbative expansion in ϕ,

$$\begin{aligned} E(f) &= \mathrm{Tr}\{\hat{H}^{(0)}\sigma^{(0)}\} \\ &+ \left[\mathrm{Tr}\{\hat{H}^{(1)}\sigma^{(0)}\} + \mathrm{Tr}\{\hat{H}^{(0)}\sigma^{(1)}\}\right] \\ &+ \left[\mathrm{Tr}\{\hat{H}^{(1)}\sigma^{(1)}\} + \mathrm{Tr}\{\hat{H}^{(0)}\sigma^{(2)}\}\right] + ... \qquad (3.28) \\ &= \mathrm{Tr}\left\{(\varepsilon + U_f)f\right\} + \frac{i}{2}\mathrm{Tr}\left\{\left[\Gamma_{ff(1+f)(1+f)} - \Gamma_{(1+f)(1+f)ff}\right]\right\} + .. \qquad (3.29) \end{aligned}$$

Using the self-consistency condition Eq. (3.11) for the relevant operators, one can show that the third and the fifth trace terms in the right-hand side of the above expression drop out. The kinetic equation for the energy functional $E(f)$ can then be written as

$$\begin{aligned} \frac{d}{dt}E(f) &= \mathrm{Tr}\left\{\varepsilon\dot{f} + U_f\dot{f} + U_{\dot{f}}f\right\} \qquad (3.30) \\ &+ \frac{i}{2}\mathrm{Tr}\left\{\frac{\partial}{\partial t}\left[\Gamma_{ff(1+f)(1+f)} - \Gamma_{(1+f)(1+f)ff}\right]\right\}. \end{aligned}$$

Again, we use the symmetry properties of ϕ, to write the simplified equation

$$\frac{d}{dt}E(f) = -i\frac{\eta}{2}\mathrm{Tr}\left\{\Gamma_{ff(1+f)(1+f)} - \Gamma_{(1+f)(1+f)ff}\right\}. \qquad (3.31)$$

One can now see that the energy is conserved only in the $\eta \to 0$ limit. In this limit the kinetic equation (3.21) represents the Born approximation. A finite value of η could then be thought of as resulting in additional terms that are beyond the Born approximation. Such terms model the duration of collision effects and quasi-particle damping. In principle if this effect is treated self-consistently, η will be a time dependent function at least of order ϕ. This means that the rate of change of E given by Eq. (3.31) is of the order ϕ^3.

Also, if one is only interested in times grater than the correlation time τ_{cor}, the finiteness of η allows us to extend the lower limit of the collision integral to $-\infty$. Now we can approximate the $f(t')$ in the non-Markovian expression of Γ by its instantaneous

value $f(t)$ to obtain the Markov form

$$\begin{aligned}\Gamma^{(m)^{15}}_{ABCD} &= \frac{1}{\hbar}\int_{-\infty}^{t} dt_1 \Big[e^{-\eta(t-t_1)}\phi^{1234}\phi^{1''2''3''4''} \\ &\times \mathcal{K}_{1''1'}(t,t_1)\mathcal{K}_{2''2'}(t,t_1)\mathcal{K}^{\dagger}_{3''3'}(t,t_1)\mathcal{K}^{\dagger}_{4''4'}(t,t_1) \\ &\times A_{31'}(t)B_{42'}(t)C_{4'2}(t)D_{3'5}(t)\Big] \end{aligned} \tag{3.32}$$

One can verify that the above Markov form results in an energy conservation, up to the most significant order given by

$$\frac{d}{dt}E(f) = \mathrm{Tr}\left\{H_{\mathrm{HF}}\left(\mathcal{L}^{(m)}_{\mathrm{QB}}[f] + \mathcal{L}^{(m)}_{\mathrm{QB}}[f]^{\dagger}\right)\right\}. \tag{3.33}$$

If we compare this with the expression for the correlation energy E_{cor} in Refs. [73, 74], the right hand side of Eq. (3.33) is exactly $-\partial E_{\mathrm{cor}}/\partial t$. This is not surprising and can be understood more intuitively by writing the collision integral as a sum of two contributions: correlation and collision

$$\Gamma = \Gamma_{\mathrm{cor}} + \Gamma_{\mathrm{col}} = \int_{-\infty}^{0} ...dt' + \int_{0}^{t} ...dt'. \tag{3.34}$$

For a finite η, the Γ_{cor} contribution decays to zero as $e^{-\eta t}$. Therefore the decaying correlation energy E_{cor} associated with this part shows up in the rate of change of the total energy E. In the Born approximation Γ_{cor} is constant because $\eta \to 0$.

The exponential damping results in a widened delta function and therefore the rate of change of $E(f)$ Eq. (3.33) can be shown to be of order $\eta\Gamma^{(m)}$. Thus, by including terms beyond the Born approximation, we have obtained a collision integral that is Markovian and still conserves energy up to ϕ^2 order. Now if we assume that the equilibration time is of the order $1/\Gamma^{(m)}$, the total change in energy ΔE is therefore

$$\begin{aligned}\Delta E &= E(f^{\mathrm{eq}}) - E(f^{\mathrm{in}}) \\ &\sim \eta\,\Gamma^{(m)} \times \left(\frac{1}{\Gamma^{(m)}}\right) = \eta, \end{aligned} \tag{3.35}$$

where f^{in} and f^{eq} are the initial and equilibrium distributions, respectively.

The importance of the damping term becomes more obvious when one attempts to solve the kinetic equation numerically. One no longer has to worry about the $\eta \to 0$ limit in the Born-Markov approximation, which for a finite system with discrete levels can result in the nonphysical situation of only exchange collisions and hence no equilibration.

3.4 Application to a dilute Bose gas in a spherical box trap

In the previous section, we introduced the general methods and concepts to describe a weakly interacting Bose gas under nonequilibrium conditions. We will now apply these to a simple model of a typical ^{87}Rb experiment, as realized by many laboratories around the world, for example Refs. [1, 51, 84]. The physical parameters are usually quoted in the natural units for a harmonic oscillator trapping potential, i. e., the angular frequency $\omega = 2\pi\,200\,\mathrm{Hz}$, the atomic mass $m_{87} = 86.9092\,\mathrm{amu}$, the ground state size $a_\mathrm{H} = [\hbar/(\omega\, m_{87})]^{1/2} = 763\,\mathrm{nm}$, and the s-wave scattering length $a_\mathrm{s} = 5.82\,\mathrm{nm}$.

However, in the present chapter, we do not pursue the usual harmonic confinement, but rather explore the properties of a radial box as a particle trap. This choice is motivated by previous studies of the self-consistent Hartree-Fock single-particle states [78]. As soon as repulsive mean-field potentials are added to the bare harmonic trapping potentials, the corresponding eigenstates widen in size and look remarkably close to the eigenstates of a box, provided the spatial extensions of the box is chosen appropriately. In particular, we pick a box of radius $R = 1000\,a_\mathrm{S} = 5.82\,\mu\mathrm{m}$.

Thus, our model is represented by a spherical trap with box potential given by

$$V_\mathrm{ext}(r) = \begin{cases} 0, & r < R \\ \infty, & r \geq R, \end{cases} \tag{3.36}$$

The eigenfunctions are a product of spherical Bessel functions $j_{(l)}$ and spherical harmonics $Y_{(lm)}$:

$$\psi_{(nlm)}(r,\theta,\phi) = \begin{cases} \mathcal{N}_{(nl)}\, j_{(l)}(r\, k_{(nl)})\, Y_{(lm)}(\theta,\phi), & r < R \\ 0, & r \geq R. \end{cases} \tag{3.37}$$

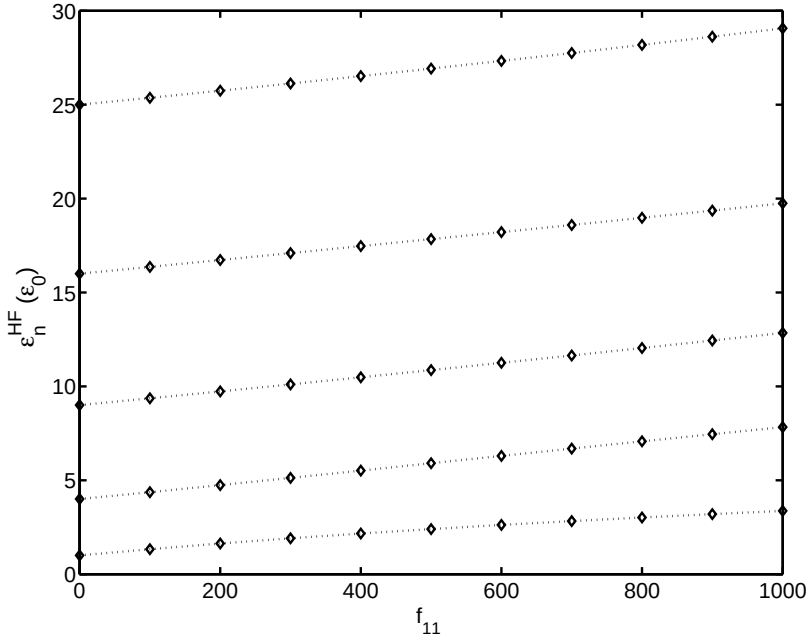

Figure 3.1: Hartree-Fock energies as a function of particles number in the box ground state, f_{11} with all other f_{ij}'s equal to zero.

A normalization constant is represented by $\mathcal{N}_{(nl)}$. The eigenenergies are given in terms of the wave-vectors $k_{(nl)}$, which can be obtained from the n-th nodes of the spherical Bessel-functions of angular momentum l,

$$\varepsilon_{(nl)} \quad = \quad (R\,k_{(nl)}/\pi)^2\,\varepsilon_0. \tag{3.38}$$

Here, ε_0 represents the ground state energy and defines the energy scale of the problem

$$\varepsilon_0 \quad = \quad \frac{\hbar^2\pi^2}{2\,mR^2}. \tag{3.39}$$

All the physical parameters are scaled with respect to this energy unit ε_0 and the radius of the box R.

For simplicity, we assume all the atoms to be in the $l = 0$ state initially. One therefore needs to consider only the $l = 0$ manifold and get for the normalization constant $\mathcal{N}_{(n0)} = n(\pi/(2R^3))^{1/2}$ and radial wave-vector $R\,k_{(n0)} = n\pi$. If the cloud is relatively cold, then most of the population resides in the lowest few energy states. Therefore, we can also limit the number of radial modes $1 \leq n \leq n_{\max}$. For the present

case, we take $n_{\max} = 5$. Obviously, all these simplifications reduce the number of degrees of freedom significantly and thus we are able to study certain aspects of the nonequilibrium dynamics of the trapped Bose gas in great detail.

With the above definitions, the bare single particle box Hamiltonian is given by

$$\varepsilon^{pq} = \delta_{pq}\, q^2 \text{ (noimplicitsumover q)}. \tag{3.40}$$

The interaction part $\hat{H}^{(1)}$ involves the matrix elements of the interaction potential defined by Eq. (3.6)

$$\phi^{pqrs} = \frac{4a_{\rm S}}{\pi}\int_0^\pi \sin(p\,x)\sin(q\,x)\sin(r\,x)\sin(s\,x)\frac{dx}{x^2}, \tag{3.41}$$

which in general have to be computed numerically. Interestingly, in the case of a spherical box this integral can be evaluated analytically and simplified to a finite sum of sine integrals and cosine functions (see Appendix B for details).

The nonequilibrium state of the above system is represented by the single particle distribution function f with time dependence given by Eq. (3.21). Neglecting the second order collision terms, the first order evolution is governed by the Hartree-Fock Hamiltonian $H_{\rm HF}$ and is given by

$$\frac{d}{dt}f = \mathcal{L}_{HF}[f] + \mathcal{L}_{HF}[f]^\dagger. \tag{3.42}$$

The energy eigenstates of the interacting system are therefore shifted from the bare box states due to the self energy effect. These shifts can be significant depending on the total particle number. This is clear from Fig. 3.1 where we plot the eigenenergies as a function of f_{11}, the total particle number in the box ground state (with all other f_{ij}'s equal to zero).

Now note that the time dependent Hartree-Fock equation (3.42) for the density matrix, f, is nonlinear and hence we seek a self consistent solution such that

$$f = \sum_i P(\varepsilon_i)|\varepsilon_i\rangle\langle\varepsilon_i|, \tag{3.43}$$

where $H_{\rm HF}|\varepsilon_i\rangle = \varepsilon_i|\varepsilon_i\rangle$, and for a Bose-Einstein distribution $P(\varepsilon)$ is given by

$$P(\varepsilon) = \frac{1}{\exp((\varepsilon - \mu)/k_B T) - 1}. \tag{3.44}$$

For a given total particle number, N, and temperature, $\beta = 1/k_B T$, a self-consistent chemical potential, $\mu(\beta, N)$, and hence a self-consistent Bose-Einstein distribution is obtained. For example, let us consider three different total particle numbers $N = 10, 100, 500$ at two different temperatures, $\beta = 1/k_B T = 0.01, 0.5$, corresponding to hot and cold clouds, respectively. In Figs. 3.2 and 3.3, we plot the self-consistent solution and the self-energy density in the position space representation. We see that the self-energy density is proportional to the number density only near the center of the trap and drops off faster with increasing radius. This can be attributed to the restricted number of basis states used in our calculation and effectively gives a finite range to the two body potential $V_{\rm bin}$.

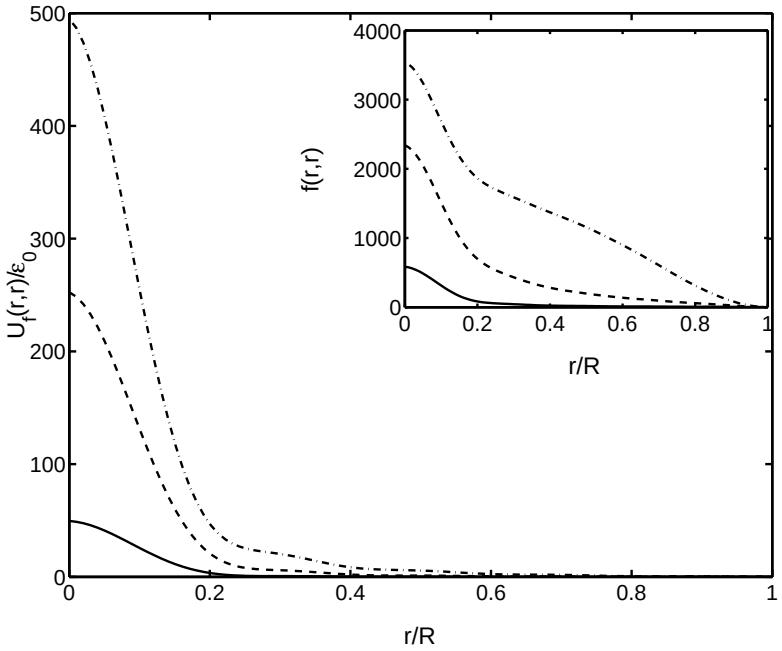

Figure 3.2: The scaled mean-field density, $U_f(r,r)/\varepsilon_0$, as a function of the scaled radial distance, r/R, at a relatively hot temperature, $\beta = 0.01$ is shown for three different values of particle numbers: $N = 10$ (solid curve), $N = 100$ (dashed), and $N = 500$ (dot-dashed). Inset shows the corresponding number density as a function of scaled radial distance.

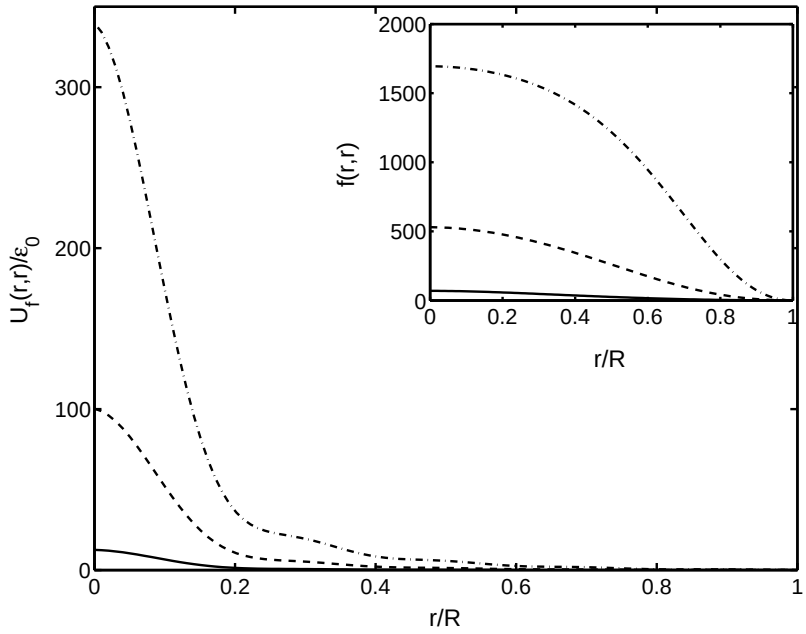

Figure 3.3: The scaled mean-field density, $U_f(r,r)/\varepsilon_0$, as a function of the scaled radial distance, r/R, at a relatively cold temperature, $\beta = 0.5$ is shown for three different values of particle numbers $N = 10$ (solid curve), $N = 100$ (dashed), and $N = 500$ (dot-dashed). Inset shows the corresponding number density as a function of scaled radial distance.

Up to first order, the f equation is totally reversible. The inclusion of the second order terms (collisions) break the reversibility, and therefore represents a relaxation of the system from some initial state to a final equilibrium state. Here we will be using the Markov form (3.32) for the collision integral. We take the Hartree-Fock self-consistent state for the initial condition.

In the previous section, we interpreted the function $\exp(-\eta\tau)$ to account for duration of collision effects and quasi-particle damping. But the exponential form was originally introduced to break the time reversal symmetry and it has the correct long time behavior. However, an exponential damping will result in a Lorenzian line shape for the final equilibrium distribution. Due to the long-reaching wings of the Lorenzian curve, in the Markov limit, off-the-energy shell collisions get weighted strongly. To seek an improved damping function that will have the correct short and long time behavior,

we use the equivalence of kinetic theories based on the Green's function approach [63] and the non-equilibrium statistical operator method [81] as shown in Ref. [85]. The behavior of the retarded Green's function $g(t, t_1)$ for very large and very small time scales is given by

$$g(t,t_1) \sim \begin{cases} e^{-\eta(t-t_1)} & t - t_1 \gg \tau_{\rm cor} \\ e^{-\eta(t-t_1)^2} & t - t_1 \ll \tau_{\rm cor}. \end{cases} \tag{3.45}$$

Therefore, behavior over the intermediate time scale will be best represented by an interpolating function. This is also true for the damping function. From Fig. 3.4 we see that the function

$$\mathcal{F}(t,t_1) = 1/\cosh(\eta(t-t_1)), \tag{3.46}$$

has exactly this behavior and therefore represents a better choice than the exponential form.

With either choice of the damping function, for a particular value of the parameter

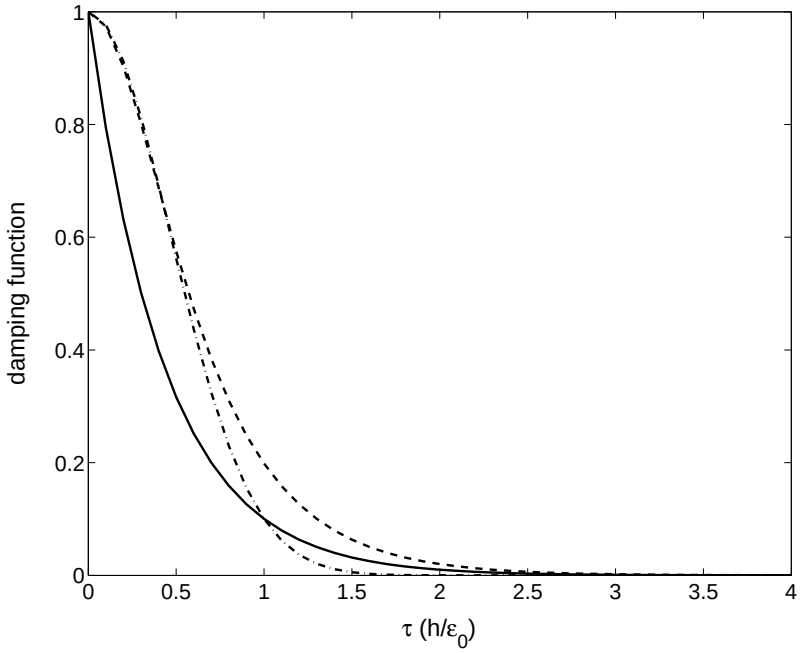

Figure 3.4: Comparison between different damping functions, $\exp(-\eta\tau)$ (solid), $\exp(-\eta\tau^2)$ (dot-dashed), and $1/\cosh(\eta\tau)$ (dashed). Note that the hyperbolic secant function asymptotes to an exponential form for large τ and a Gaussian form for small τ.

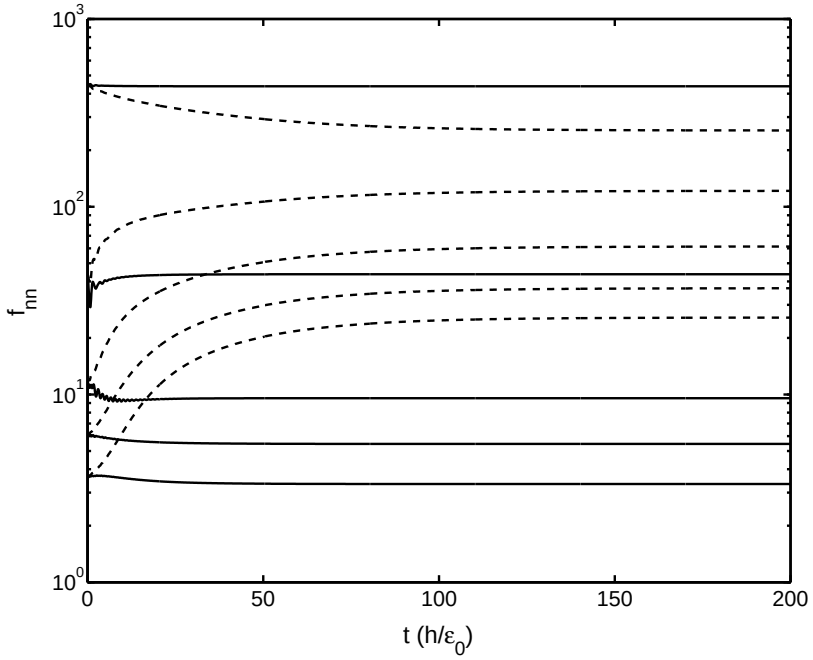

Figure 3.5: Evolution of the diagonal elements $f_{nn}\,(n = 1, 2.., 5)$ (shown with curves from bottom to top) toward a self-consistent steady-state solution starting from an approximate solution. Two different damping functions are used in the evaluation of the Γ's. Dashed and solid curves correspond to exponential and hyperbolic secant respectively.

η, a time propagation results in a self-consistent steady-state solution, $f^{\rm eq}$. Figure 3.5 shows such a time evolution for $N = 500$ particles with an initial temperature corresponding to $\beta = 0.01$. We have chose η to be of the order $\mathrm{Re}[\Gamma] \approx 2.3$. In principle η should be obtained self-consistently at every time step. So long as one considers large enough number of basis states, the final result is reasonable insensitive to the value of η as long as $\eta \geq \mathrm{Re}[\Gamma]$. As mentioned earlier we see that the exponential damping function results in significant transfer of population to the excited states. This effect is less with the hyperbolic secant damping function. We get different steady-state solutions because different damping functions correspond to different initial correlations. Also a plot of $\theta(f_{nn}) \equiv \ln(1/f_{nn} + 1)$ vs the Hartree-Fock energies ε_n^{HF}, shown in Fig. 3.6 shows that the $f^{\rm eq}$ is very close to a Bose-Einstein distribution. The slope, which represents the self-consistent value of β, shows that the change in temperature is far greater for the

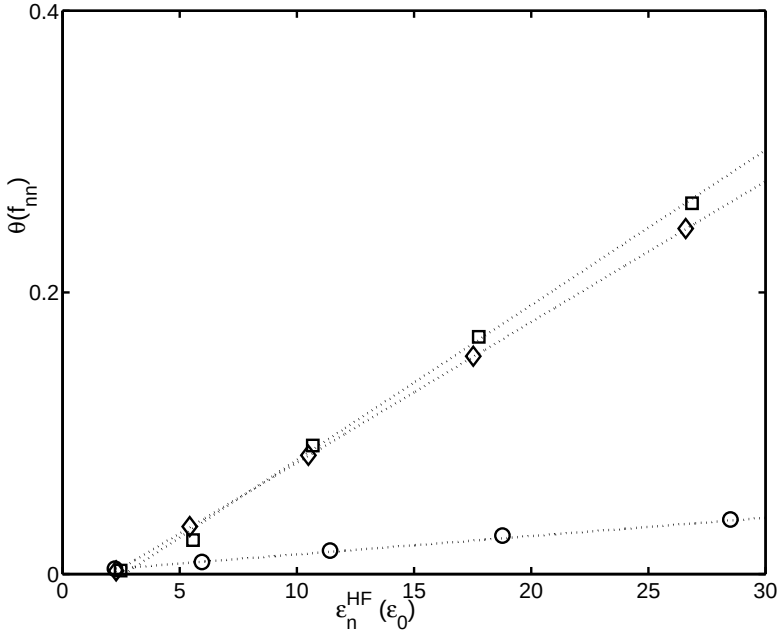

Figure 3.6: Linear behavior of $\theta(f_{nn})$ as a function of ε_n^{HF}. Initial distribution shown with diamonds. Final distribution shown with circles for the case of exponential damping function, and squares for the case of hyperbolic secant damping function.

exponential damping function compared to the hyperbolic secant case, because off-the-energy shell effects are larger as explained previously.

Thus we have obtained a self-consistent steady-state solution to the second order kinetic equation. We emphasize here that the steady-state solution is a result of the real-time non-equilibrium evolution of the system. Deriving such an equilibrium solution, whose absolute value is plotted in Fig. 3.7, is a prerequisite step to the study of collective modes and damping rates of a dilute gas.

3.5 Real time response to perturbation

The properties of the equilibrium solution $f^{\rm eq}$ exhibit the expected characteristics of a Bose-Einstein distribution. In order to verify the stability of this solution and to study the damping rates of the collective excitations, we will now examine the real-time response of the system to a perturbation. First, we will outline the linear response

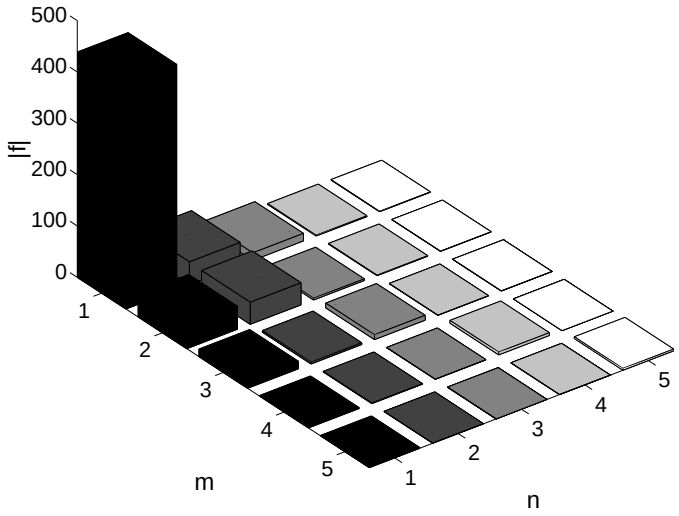

Figure 3.7: Absolute value of $f^{\rm eq}$, the self consistent steady-state solution for the second order kinetic equation. The single particle density matrix is plotted in the Hartree-Fock basis.

theory and discuss the structure of the modes, their frequencies, and the life-time of the excitations. Subsequently, we will use these modes to initially prepare the system and to evolve the full nonlinear quantum kinetic equation towards equilibrium.

One of the fundamental properties of the quantum kinetic equation (3.21)

$$\frac{d}{dt}f(t) \;\; = \;\; \mathcal{L}[f] + \mathcal{L}[f]^\dagger, \tag{3.47}$$

is its Hermitian structure. Thus, if we prepare a physical state initially, it will remain Hermitian with $f(t) = f(t)^\dagger$, indefinitely. We will now consider a weak perturbation of an equilibrium state,

$$f(t) \;\; = \;\; f^{\rm eq} + \delta f(t), \tag{3.48}$$

and calculate the first order response of the system. As usual, we want to assume that we can decompose a general perturbation into fundamental damped and/or oscillatory eigenmodes of the system. Therefore, such a specific perturbation can be parameterized as

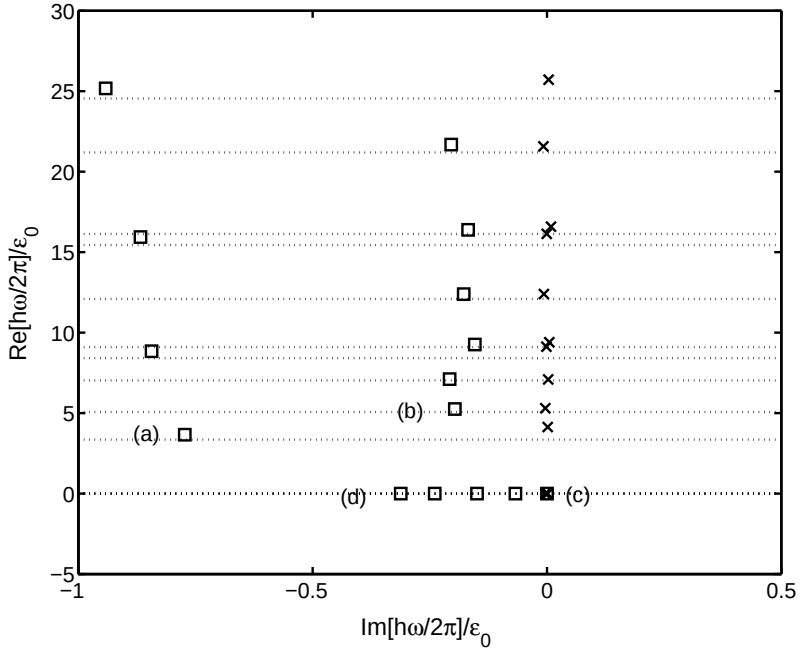

Figure 3.8: Non-negative frequency eigenvalues scaled with respect to ε_0 shown with crosses for the Hartree-Fock equation and squares for the quantum-Boltzmann equation. The dotted lines correspond to difference energies $(\varepsilon_i^{HF} - \varepsilon_j^{HF})/\varepsilon_0$. The modes labelled (a) and (b) – non-zero frequency and damping rate, (c) – zero mode, and (d) – zero frequency and non-zero damping rate will be considered for further discussion.

$$\delta f(t) = e^{-i\,\omega t}\delta f_\omega^{(+)} + \text{h.c.}, \tag{3.49}$$

$$\delta f_\omega^{(+)} = \delta f_\omega^{(c)} + i\,\delta f_\omega^{(s)}, \tag{3.50}$$

where $\delta f_\omega^{(+)}$ denotes a positive frequency amplitude. It turns out to be useful to decompose it into quadrature components

$$\delta f_\omega^{(c)} = \frac{1}{2}\left[\delta f_\omega^{(+)\dagger} + \delta f_\omega^{(+)}\right], \tag{3.51}$$

$$\delta f_\omega^{(s)} = \frac{1}{2\,i}\left[\delta f_\omega^{(+)\dagger} - \delta f_\omega^{(+)}\right], \tag{3.52}$$

and evaluate the kinetic operator $\mathcal{L}[f]$ only for such Hermitian arguments. From a Taylor series expansion of the kinetic operator around the equilibrium distribution, one obtains finally the linear response equations for the fundamental modes

$$(-i\omega)\,\delta f_\omega^{(+)} = \mathcal{L}^{(1)}[\delta f_\omega^{(c)}] + i\,\mathcal{L}^{(1)}[\delta f_\omega^{(s)}] + \mathcal{L}^{(1)}[\delta f_\omega^{(c)}]^\dagger + i\,\mathcal{L}^{(1)}[\delta f_\omega^{(s)}]^\dagger, \tag{3.53}$$

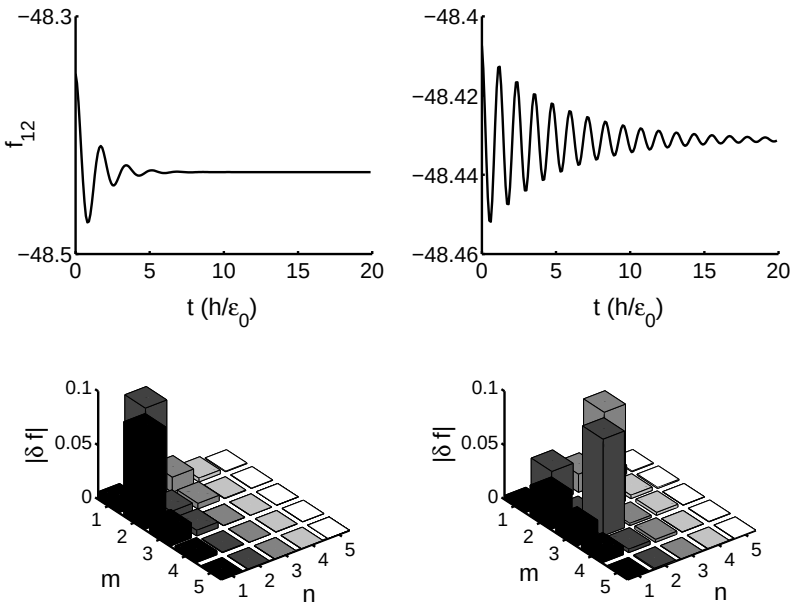

Figure 3.9: The perturbation $\lambda\delta f^s_\omega$ (bottom) is shown in a rotated frame such that $f^{\rm eq}$ is diagonal; the resulting oscillatory and damped behavior (top) of the element f_{12} of f in the box basis is due to the perturbation. The left and right figures correspond to the points marked (a) and (b) in Fig. 3.8 respectively.

where we have defined a linear response operator through an appropriate centered difference limit

$$\mathcal{L}^{(1)}[\delta f] \;=\; \lim_{\lambda\to 0}\frac{\mathcal{L}[f^{\rm eq}+\lambda\delta f]-\mathcal{L}[f^{\rm eq}-\lambda\delta f]}{2\lambda}. \tag{3.54}$$

We solve Eq. (3.53) as an eigenvalue problem. In general, the eigenvalues are complex, with frequency and damping rate given by the real and the imaginary parts respectively. The eigenvalues appear as complex conjugate pairs. The eigenmodes corresponding to non-zero eigenvalues are Hermitian conjugates of each other and are traceless with normalization given by

$$\mathrm{Tr}\{\delta f^{(+)}_\omega \delta f^{(+)\dagger}_\omega\} = 1. \tag{3.55}$$

The physical linear response mode is given by the quadrature components δf^s_ω and δf^c_ω. There also exists a zero mode that has non vanishing trace. The damping rates are all

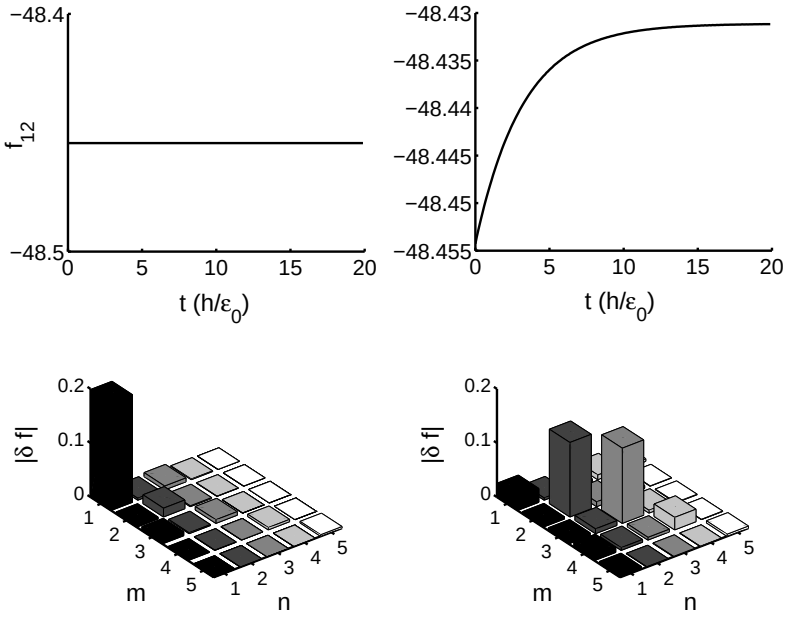

Figure 3.10: The perturbation $\lambda\delta f^s_\omega$ (bottom) is shown in a rotated frame such that $f^{\rm eq}$ is diagonal; the resulting damped behavior (top) of the element f_{12} of f in the box basis is due to the perturbation. The left and right figures correspond to the points marked (c) and (d) in Fig. 3.8, respectively.

negative, thus confirming the stability of the collective modes. In Fig. 3.8, we plot the positive frequency eigenvalues. The dotted lines correspond to the difference frequencies of the Hamiltonian H_{HF}.

It is interesting to see how these different modes evolve in real time. For this we use the equilibrium distribution obtained in the previous section and perturb it with one of the quadrature components

$$f \to f^{\rm eq} + \lambda\delta f^{(s)}_\omega, \tag{3.56}$$

where $\lambda = 0.2$ determines the smallness of the perturbation. In particular we will consider the modes labeled by (a), (b), (c) and (d) in Fig. 3.8.

The real-time response is shown by plotting the off-diagonal matrix element f_{12} of the single particle density matrix in the box basis as shown in Figs. 3.9 and 3.10. In Fig. 3.11, we plot the change in the total energy $\Delta E = E(f) - E(f^{\rm eq})$ as a function

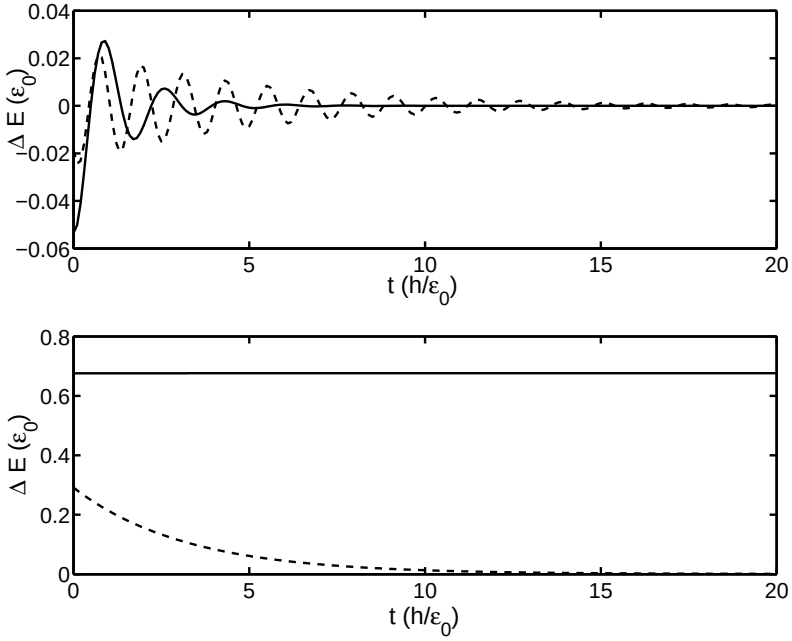

Figure 3.11: The change in the total energy $\Delta E = E(f) - E(f^{\rm eq})$ as the system relaxes to its new equilibrium. In the top figure, the solid and dashed lines correspond to cases (a) and (b), respectively. Similarly in the bottom figure, the solid and dashed lines correspond to cases (c) and (d), respectively.

of time. In cases (a) and (b) we see that the ΔE oscillates about zero and eventually goes to zero. This is expected because such a perturbation tends to create coherences, resulting in an energy change by the amount of $E_{\rm coh}$ (coherence energy) that would eventually decay down to zero. Similar damped behavior is observed for case (d). Such an oscillatory damped behavior of the total energy could be attributed to the Markov approximation in the collision integral Eq. (3.32). On the other hand, perturbations of the kind (c) increase the total particle number by the amount $\delta N = {\rm Tr}\{\lambda \delta f_\omega^{(s)}\}$ and hence result in a finite change in total energy.

3.6 Conclusion

A non-Markovian version of the quantum kinetic theory is derived using the prescription of a nonequilibrium statistical operator method as outlined in Ref. [81]. This theory is shown to conserve energy in the $\eta \to 0$ limit. Inclusion of quasi-particle

damping and duration of collision effects results in a description beyond the Born approximation with energy conservation to ϕ^2 order even in the Markov limit. To obtain collision integrals that involve quasi-particle damping and duration of collision effects and conserves energy precisely, one will have to calculate the T-matrix in the full collision operator keeping terms of all orders in the interaction.

We applied the generalized second order kinetic theory to the nonhomogeneous dilute Bose gas confined in a spherical box to numerically study the full non-equilibrium evolution of the system towards equilibrium. The self-consistent distribution $f^{\rm eq}$ thus obtained is very close to the Bose-Einstein distribution as shown in Fig. 3.6. We also observe a significant Hartree-Fock self energy shift which depends on the single particle distribution function f. The form of the damping function is important in determining the line shape. Particularly, the function with a $1/\cosh$ type of behavior is found to be appropriate and gives improved energy conservation due to smaller initial correlation effect.

The importance of such a real-time calculation is apparent from the full real-time response calculation, where we have calculated the damping rates and frequencies. These damping rates correspond to a shorter time scale compared to the equilibration time scale, which depend on rates in and out of the various levels.

This simple model of a spherical trap can be easily extended to a more realistic situation of a harmonic trap. As in Refs. [13, 86, 87], the condensed component can be easily included by introducing a symmetry broken mean-field, $\alpha_i = \langle \hat{a}_i \rangle$, as one of the relevant observables and Hartree-Fock-Bogoliubov quasi-particle excitations. Even though this extension of the kinetic theory discussed in this chapter may seem simple, the actual calculations are complicated and involved due to the presence of anomalous fluctuations. Also the theory will need to be renormalized in order to ensure a gapless spectrum. Such a calculation will allow us to make experimentally verifiable predictions of damping rates of collective excitations. One can also explore the possibility of in-

cluding a time dependent potential or an external force term to selectively excite one or more of the collective modes.

Chapter 4

Bosonic fractional quantum Hall effect

4.1 Introduction

With the advancements in methods of trapping and cooling atomic gases, a whole new frontier has opened up for the study of many body physics. Due to the extreme control, purity and detailed theoretical understanding of interactions of dilute atomic systems, these systems provide a perfect scenario to test many of the ideas previously limited to condensed matter systems. Since the achievement of Bose-Einstein condensation in weakly interacting atomic gases [1, 2, 3], innumerable papers have been published on the equilibrium properties and dynamical behavior of dilute Bose gases at temperatures above and below the Bose-Einstein condensation temperature, T_c. While many new phenomena have been studied in the regime of weak interactions, the other limit in which the atoms can be strongly correlated has remained unexplored. Strong correlations between particles have shown to produce fascinating effects like the fractional quantum Hall effect (FQHE) in condensed matter systems.

The regime of strong correlations in dilute atomic gases can be achieved by two ways. One possibility is to tune the interactions such that the interaction energy is greater that any other (single particle) energy scale of the problem, for example by using Feshbach resonance [88]. The other possibility is to make the interactions dominate by creating degeneracies. This could be achieved for example by using a periodic trapping potential. Under the conditions that the tunneling amplitude between wells is small

compared to the typical interaction energy, the system has been predicted to undergo a transition from a superfluid to a strongly correlated Mott state [89]. Another way of achieving degeneracies is to rotate the harmonic trap that confines the dilute Bose gas. At rotational frequencies close to the trapping frequency, the system is predicted to enter the fractional quantum Hall regime where the ground state is given by the variational Laughlin wavefunction [90]. This is precisely what we will focus in the remaining of this thesis.

In this chapter, we will discuss the fractional quantum Hall effect (FQHE) in brief. Then we will see how a dilute Bose gas can be prepared under conditions identical to those required for observing the electronic FQHE. Having met the requirements, with simple quantum mechanical arguments we will show that this bosonic system exhibits single and many-particle states identical to that of the electronic FQHE system.

4.2 Fractional quantum Hall effect

The quantization of the Hall effect discovered by von Klitzing, Dorda, and Pepper [91] in 1980 is a remarkable macroscopic quantum phenomenon which occurs in two-dimensional electron systems at low temperature and strong perpendicular magnetic field. Under these conditions the Hall-conductivity exhibits plateaus at integral multiples of a fundamental constant of nature e^2/h. This is the integer quantum Hall effect (IQHE). The striking result is the accuracy of the quantization irrespective of the impurities or the geometric details of the two-dimensional system. Each plateau is associated with a deep minimum in the diagonal resistivity indicating a dissipationless flow of current. This was followed by the discovery of fractional quantum Hall effect (FQHE) by Tsui, Stormer, and Gossard [92] in higher mobility samples where the plateaus occur at fractional multiples of e^2/h as shown in Fig. 4.1. Despite the apparent similarity of experimental results, the physical mechanism responsible for the IQHE and the FQHE are quite different. In the former the random impurity potential plays an important role

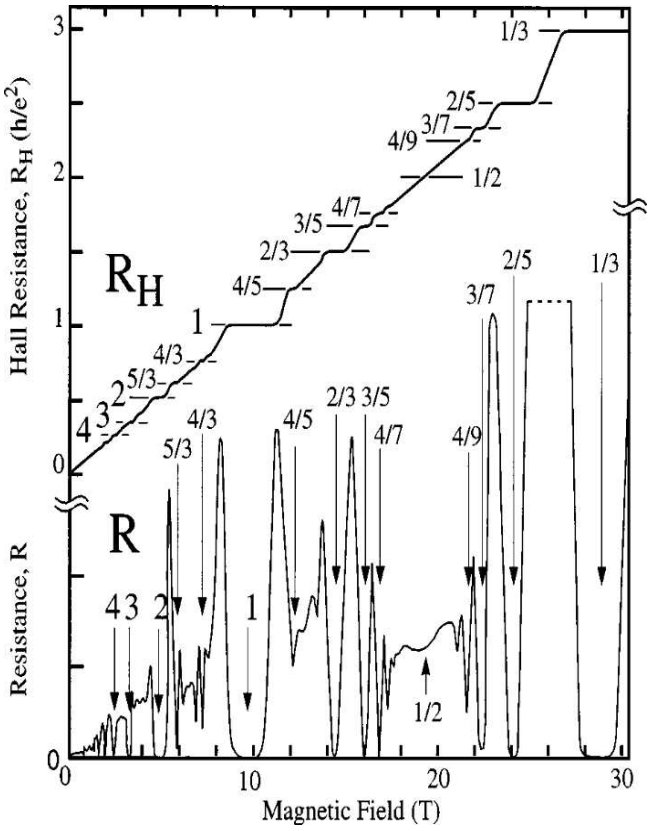

Figure 4.1: The FQHE in ultra high-mobility modulation-doped GaAs/AlGaAs. Many fractions are visible.

while in the latter it is the collective effect arising from the coulombic electron-electron repulsion. Also note that the fractional values originally observed as shown in Fig. 4.1 were all odd denominator fractions. While this is in fact related to the fermionic nature of electrons, more recently [93, 94] even fractions like $\frac{5}{2}$ have also been observed. Occurance of such even fractions is rare, and their existence can be attributed to a Cooper instability [95]; nevertheless, it is again a collective phenomenon due to the interaction between electrons.

Regardless of the nature of the fractions, the many body physics that is important

to the current discussion is that the fractional quantum Hall state is a liquid state exhibiting a gap in the excitation spectrum. This has been very well understood by methods based on exact diagonalization and trial wavefunctions. The variational ground state proposed by Laughlin [90] has been very successful in explaining the FQHE and predicts the existence of quasi-particles with fractional charge. In the forthcoming sections we show that identical many body effect can be predicted for a rotating Bose gas. In fact a bosonic variant of the many body Laughlin wavefunction can be written down to describe the ground state of the system in this strongly correlated regime.

4.3 Electron system versus dilute Bose gas

While at first glance a rotating Bose gas may seem very different from the fractional quantum Hall system, there exists an interesting symmetry with respect to the measurable physical quantities between these systems. This is summarized in the table below where we list the necessary conditions and physical quantities for a rotating Bose gas corresponding to those which define the electronic fractional quantum Hall system.

	Electronic FQHE system	**Rotating Bose gas**
1	2-dimensional at interface between semiconductors	effective 2-dimensional due to strong confinement along the z direction compared to the x and y directions
2	Repulsive coulombic interaction	Repulsive two body potential
3	Vector potential $\mathbf{A}$	Velocity field $\mathbf{u}$
4	Magnetic field $\mathbf{B}$ and magnetic flux ϕ, $\mathbf{B} = \nabla \times \mathbf{A}$; $\phi = \int \mathbf{B} \cdot \hat{n} dS$	Vorticity $\mathbf{\Omega}$ and circulation Θ, $\mathbf{\Omega} = \nabla \times \mathbf{u}$; $\Theta = \int \mathbf{\Omega} \cdot \hat{n} dS$
5	Landau levels fermionic-Laughlin state	Landau levels bosonic-Laughlin state

Table 4.1: Comparison between the electronic fractional quantum Hall system and the rotating Bose gas.

As mentioned previously, the FQHE occurs in a two-dimensional electron system in the presence of a strong perpendicular magnetic field. Identical conditions can be achieved for a dilute Bose gas by having the confinement in the z direction strong compared to the x and y directions while the vorticity $\mathbf{\Omega}$ of the rotating Bose gas plays the role of the $\mathbf{B}$ field. The many body effects are generated by the repulsive two-body inter-atomic potential which replaces the coulombic repulsion for electrons. Thus, apart from the intrinsic statistics and charge of the particles, it is theoretically possible to configure a dilute Bose gas to meet the requirements necessary for observing a FQHE. Therefore in principle one could predict a strongly correlated ground state for the rotating Bose gas.

To begin with we will first address the last row of the above table by showing that the Landau levels describe the single particle spectrum of a rotating Bose gas in complete analogy to the electronic case. By including inter-atomic repulsive interactions we will also show that a bosonic variant of the Laughlin wavefunction can be written down as the variational many body ground state of the rotating Bose gas.

4.4 Landau levels and the many-body Laughlin wavefunction

We start with writing the Hamiltonian for N interacting bosonic atoms confined to a harmonic potential in the rotating frame. Also, we assume the confinement along the axis of rotation to be strong enough that we can neglect the excitations in that direction and consider the system to be essentially two dimensional:

$$H = \sum_{j=1}^{N} \left\{ \frac{p_{jx}^2}{2m} + \frac{p_{jy}^2}{2m} + \frac{m\omega^2 x_j^2}{2} + \frac{m\omega^2 y_j^2}{2} - \Omega L_{jz} \right\} + \sum_{i<j} V(\mathbf{r}_i - \mathbf{r}_j). \qquad (4.1)$$

Here, m is the mass of the atoms, the angular momentum operator is given by $L_z = xp_y - p_x y$, and Ω is the rotating frequency. The repulsive two body potential V depends only on the relative coordinate of the individual atoms. Now if we make the following

identification

$$A_{jx} = \frac{m\omega}{e} y_j; \quad A_{jy} = -\frac{m\omega}{e} x_j, \tag{4.2}$$

the above Hamiltonian can be cast in a form very similar to the fractional quantum Hall Hamiltonian

$$H = \sum_{j=1}^{N} \left\{ \frac{1}{2m}(p_{jx} + eA_{jx})^2 + \frac{1}{2m}(p_{jy} + eA_{jy})^2 \right\} + (\omega - \Omega) \sum_{j=1}^{N} L_{jz} + \sum_{i<j} V(\mathbf{r}_i - \mathbf{r}_j). \tag{4.3}$$

To obtain the single particle spectrum we will first consider the non-interacting case, i.e. $V = 0$. The Hamiltonian can then be rewritten in a more convenient form

$$H = \sum_{j=1}^{N} \left(a_j^\dagger a_j + \frac{1}{2} \right) 2\hbar\omega + \hbar(\omega - \Omega) \sum_{j=1}^{N} (b_j^\dagger b_j - a_j^\dagger a_j), \tag{4.4}$$

where the operators a and b are defined in terms of the covariant momentum $(P_x, P_y) = (p_x + eA_x, p_y + eA_y)$ and the guiding center coordinate $(X, Y) = (x + \frac{1}{2m\omega} P_y, y - \frac{1}{2m\omega} P_x)$

$$a_j = \sqrt{\frac{1}{4\hbar m\omega}} (P_{jx} + iP_{jy}); \quad a_j^\dagger = \sqrt{\frac{1}{4\hbar m\omega}} (P_{jx} - iP_{jy}) \tag{4.5}$$

and

$$b_j = \sqrt{\frac{\hbar}{4m\omega}} (X_j - iY_j); \quad b_j^\dagger = \sqrt{\frac{\hbar}{4m\omega}} (X_j + iY_i) \tag{4.6}$$

obeying the following commutation relations

$$[a_i, a_j^\dagger] = [b_i, b_j^\dagger] = \delta_{ij}; \tag{4.7}$$

$$[a_i, a_j] = [a_i, b_j] = [a_i^\dagger, b_j] = [b_i, b_j] = 0. \tag{4.8}$$

The operators a and $a^\dagger$ annihilate and create a quanta in the Fock space, while the operators b and $b^\dagger$ are the usual angular momentum ladder operators. Now one can easily see that in the absence of interactions, at a certain critical rotational(stirring) frequency $\Omega = \omega$, the Hamiltonian depends only on the a's and $a^\dagger$'s. The corresponding single particle energy states are the Landau levels given by

$$|n_j, l_j\rangle = \sqrt{\frac{1}{n_j!(l_j + n_j)!}} (a_j^\dagger)^{n_j} (b_j^\dagger)^{l_j + n_j} |0\rangle \tag{4.9}$$

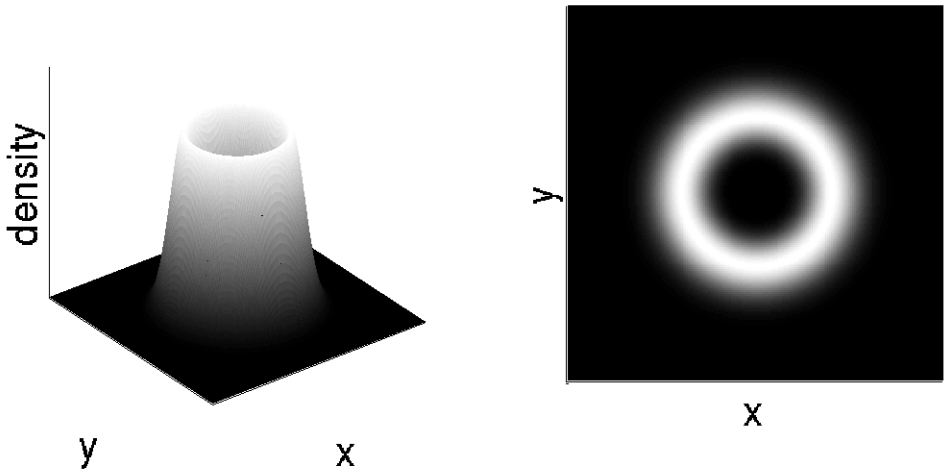

Figure 4.2: Atomic density in the lowest Landau level: left - density in the lowest Landau level with angular momentum quantum number $l = 3$ is sharply peaked at radius $r = \sqrt{l\hbar/m\omega}$, right - density is shown by a concentric ring of thickness $\Delta r = \sqrt{\hbar/4lm\omega}$ in the x-y plane.

with energy eigenvalues $E_{n_j} = (n_j + \frac{1}{2})2\hbar\omega$ and angular momentum $L_j = l_j\hbar$, where $|0\rangle$ is the Fock vacuum. Since the angular momentum operator commutes with the Hamiltonian, each Landau level is degenerate with respect to the angular momentum quantum number l. Now using the action of the operators a and b on the Fock states, the configuration space wavefunction of the zero angular momentum lowest Landau state can be easily shown to be given by

$$\psi_0^0(\mathbf{x}) = \sqrt{\frac{m\omega}{\pi\hbar}} \exp\left(-\frac{m\omega|\mathbf{x}|^2}{2\hbar}\right). \tag{4.10}$$

Therefore using Eq.(4.9), the generic Landau wavefunction can then be written as

$$\psi_l^n(\mathbf{x}) = \langle \mathbf{x}|n,l\rangle = \sqrt{\frac{1}{n!(l+n)!}}(a^\dagger)^n(b^\dagger)^{l+n}\psi_0^0(\mathbf{x}). \tag{4.11}$$

The atomic density in the lowest Landau level given by $|\psi_l^0(\mathbf{x})|^2$ is sharply peaked at radius $r = \sqrt{l\hbar/m\omega}$ as depicted in Fig. 4.2. The lowest Landau states are therefore represented by concentric rings labeled by the angular momentum quantum number l (Fig. 4.2). Thus the single particle spectrum for the rotating Bose gas shows Landau

level structure identical to that of the electrons in a strong perpenticular magnetic field.

Now we include interactions in order to calculate the many-body ground state. We start by writing the Hamiltonian (4.3) as

$$H = H_{\text{Landau}} + H_L + V \tag{4.12}$$

Here H_{Landau} is the quantum Hall single particle Hamiltonian whose single particle states are the Landau levels separated by $2\hbar\omega$. The Hamiltonian $H_L = (\omega - \Omega)L_z$ is proportional to the z component of the total angular momentum $L_z = \sum_{j=1}^{N} L_{jz}$, and V is the interaction term. From now on we would like to consider the limit in which the energy scale characterizing the Hamiltonian H_{Landau} and V is much greater than the one corresponding to H_L. This is possible when the stirring frequency is very close to the harmonic trapping frequency. Also we will consider only contact interaction so that V can be written as

$$V = \eta \sum_{i<j}^{N} \delta(\mathbf{x}_i - \mathbf{x}_j). \tag{4.13}$$

In this limit, the ground states and elementary excitations of the system will lie in the subspace of common zero energy eigenstates of H_{Landau} and V. Thus the many body wavefunction $\Psi(z)$ must lie within the subspace generated by the tensor product of the lowest Landau level single particle states

$$\Psi(\{z\}) = \mathcal{P}(z_1, ..., z_N) \prod_k \exp\left(-\frac{|z_k|^2}{2}\right), \tag{4.14}$$

where $\mathcal{P}(z)$ is a polynomial in each of the scaled complex atomic coordinates

$$z_j = \sqrt{\frac{m\omega}{\hbar}}(x_j + iy_j). \tag{4.15}$$

Now if $\Psi(z)$ is also an eigenstate of V, then due to the delta function nature of V, the polynomial $\mathcal{P}(z)$ has to satisfy the form

$$\mathcal{P}(\{z\}) = \mathcal{Q}(\{z\}) \prod_{i<j} (z_i - z_j)^2 \tag{4.16}$$

Here, the "2" in the exponent, is due to the even symmetry of bosons under exchange. We can now diagonalize H_L within the truncated Hilbert space of wavefunctions of the form specified by (4.14) and (4.16). At the same time when $\mathcal{P}(z)$ is a homogeneous polynomial in z, the state (4.14) is an eigenstate of H_L with eigenvalue $E_M = \hbar(\omega - \Omega)M$, where M is the homogeneous degree of $\mathcal{P}(z)$. Now since the ground state is the state with the lowest angular momentum, we conclude that $\mathcal{Q}(z) = 1$ and the ground state wavefunction can be written as

$$\Psi(\{z\}) = \prod_{i<j}(z_i - z_j)^2 \prod_k \exp\left(-\frac{|z_k|^2}{2}\right). \tag{4.17}$$

This is the essentially the bosonic variant of the Laughlin wave function [96, 97] originally proposed for fractional quantum Hall electrons. The most generic Laughlin wavefunction is represented by

$$\Psi_q(\{z\}) = \prod_{i<j}(z_i - z_j)^q \prod_k \exp\left(-\frac{|z_k|^2}{2}\right) \tag{4.18}$$

where $\frac{1}{q}$ represents the fraction in the FQHE. Therefore as one can immediately notice that, q has to be odd(even) for the case of electrons(bosons) to satisfy the Fermi(Bose) symmetry. Physically the fraction $\frac{1}{q}$, represents the number of electrons(bosons) per flux-quanta(vortex) and is called the filling fraction. Thus the Laughlin wave function (4.17) for the rotating Bose gas represents a $\frac{1}{2}$ bosonic FQHE. The atomic density profile in the $\frac{1}{2}$-Laughlin wavefunction is shown in Fig. 4.3.

4.5 Exact diagonalization

To confirm the validity of the arguments presented in the previous section we numerically diagonalize the Hamiltonian (4.3) for a small system of five bosonic atoms. As before we assume hard core interaction potential represented by a delta function. Also in order to limit the basis states to the lowest Landau levels, the interaction parameter η is chosen such that the interaction energy is small compared to the Landau level spacing, $2\hbar\omega$. We choose the stirring frequency to be smaller than but very close to

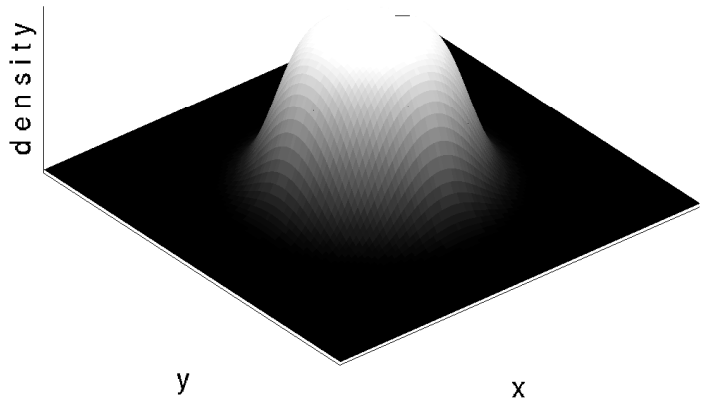

Figure 4.3: The atomic density in the $\frac{1}{2}$- Laughlin state for $N = 5$ atoms.

the trapping frequency, $1 - \Omega/\omega = 0.01$. Such a choice allows us to see the effect of the H_L piece of the Hamiltonian while satisfying the assumptions of the previous section. In Fig. 4.4 we plot the eigenenergies as a function of the total angular momentum L_{tot}. We notice that there is a branch of states well separated from the rest of the spectrum. These states are polynomial states of the form given by (4.14) and (4.16). The ground state is the state with angular momentum $L_{\text{tot}} = N(N-1) = 20$ and is the Laughlin state corresponding to the bosonic $\frac{1}{2}$ FQHE.

4.6 Quasiparticles

The Laughlin wavefunction (4.17) describes a bound state of atoms with even number of zeros or vortices. Now if the area of the system is slightly increased, the number of vortices increases, resulting in a change of the filling fraction from $\frac{1}{2}$. Now consider the case where we introduce one extra vortex. The new wavefunction can then be written as

$$\Psi_{2+\varepsilon}(z) = \prod_i z_j \Psi_2(z) \tag{4.19}$$

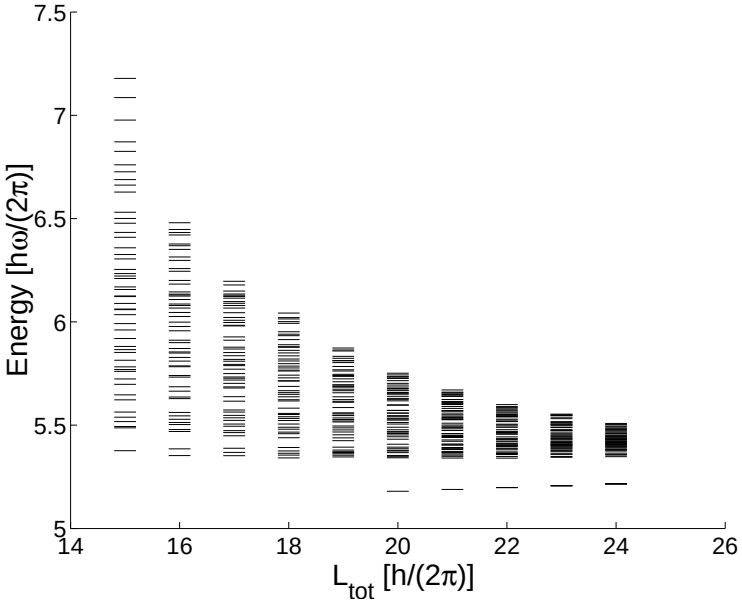

Figure 4.4: Results of exact diagonalization for a small system of $N = 5$ bosonic atoms in a rotating 2-dimensional harmonic trap. The stirring frequency is chosen to be smaller than but very close to the trapping frequency, $1 - \Omega/\omega = 0.01$. The parameter η is chosen such that the interaction energy is very small compared to the Landau level spacing, $2\hbar\omega$. Such a choice allows us to use a truncated Hilbert space of lowest Landau levels.

and possesses a zero at the origin. Physically, the above operation shifts the atomic distribution corresponding to $(l_1, l_2, ..l_N)$ to the one corresponding to $(l_1+1, l_2+1, ..l_N+1)$. This can be verified trivially by expanding the above wavefunction and will be left to the reader. From the experimental point of view, such a situation can be realized by shining a laser at $z = 0$ as proposed by Paredes et al. in [97]. More generally we could shine the laser at some point z_0 (localized within an area $\sim \hbar/(m\omega)$) in which case the Laughlin wavefunction will be multiplied by $\prod_j (z_j - z_0)$ and hence reducing the atomic density at that point to zero. Such an isolated zero acts like a quasi-hole excitation with fractional statistics. This is very easy to see: consider a hypothetical situation in which we introduce two zeros at the same point z_0, and then pin an extra atom to that point. Such an operation would return the ground state to the $\frac{1}{2}$ Laughlin wavefunction of the previous section except now for $(N + 1)$ bosons. Thus two quasi-

holes are annihilated by an atom and hence the quasi-hole corresponds to a particle with $\frac{1}{2}$ statistics. The rotating Bose gas can also be predicted to be incompressible. This is because compressing or expanding the state would require removal or injection of an atom requiring a finite amount of energy. In essence, it is not possible to induce an infinitesimal change in the system by an infinitesimal change in the pressure.

4.7 Conclusion

In this chapter we showed that the rotating Bose gas under certain conditions represents a strongly correlated system in complete analogy to the electronic FQHE system. Here the ground state is given by the bosonic variational $\frac{1}{2}$- Laughlin wavefunction. The $\frac{1}{2}$- quasi-hole excitations can be created by shining a laser at some specific point.

While theoretical understanding of the occurence of such a strongly correlated state is quite clear, experimental realization seems difficult. The main difficulty is due to the extreme low temperature required to access this state. Typically the temperature required is such that [97]

$$\frac{kT}{\hbar\omega} \ll \frac{1}{N}, \frac{\eta}{N}. \tag{4.20}$$

The remainder of this thesis will be devoted to precisely address this issue. We will be considering an alternative approach, where along with creating degeneracies by rotating the trap, we increase the interaction energy by applying Feshbach resonance. The motivation for this approach can be understood from the numerical results of Fig. 4.4 and the nature of the Laughlin wavefunction. The strongly correlated Laughlin state corresponds to the lowest energy state in the separated branch of states. This is because, the Laughlin wavefunction is annihilated by the delta function interaction potential. Therefore, except for the states in this branch, eigenenergies of all the other states have a contribution corresponding to the interaction energy. Therefore, naively, increasing

the interaction energy would increase the gap between the separated branch and the continuum resulting in an increased temperature for observing the ground state.

However, in implementing such an approach, an alternative formulation of the rotating Bose gas is required. This is because, while the physics of such resonances is well formulated in a mean field picture, mean field theories fail to describe the strongly correlated regime. The order parameter describing for example the Laughlin state is no longer given by the expectation value of the atomic field operator. This difficulty can be resolved in a gauge transformed Chern-Simons approach [98, 99]. Here the problem can be formulated in terms of mean fields of composite particles. In the next chapter, we discuss the basic ideas behind this effective field theory picture. Then continuing along the same lines, in Ch. 6 we predict novel strongly correlated states in the presence of Feshbach resonance.

Chapter 5

Chern-Simons theory for a strongly correlated rotating Bose gas

5.1 Introduction

The quasi-hole excitations in the bosonic Laughlin state are $\frac{1}{2}$ bosons as argued in the last chapter. Therefore a field theory model appropriate for the Bose gas in the strongly correlated Laughlin regime should exhibit vortex solutions corresponding to such quasi-holes. Initial ideas of a field theory appropriate to describe such a strongly correlated state were put forth by Girvin and MacDonald [100] in relation to the electronic FQHE. A related model was developed by Zhang, Hansson, and Kivelson (ZHK) [98] directly from the microscopic Hamiltonian. While the starting points were different, both these theories involved coupling of a scalar field to a gauge potential $(a_0, \mathbf{a})$ with a Chern-Simons action (or topological mass term). To understand the necessity of such a gauge term and its relevance to the strongly correlated Bose system that we wish to study, we first need to understand the origin of fractional statistics in a two-dimensional space.

We begin by discussing the origin of anyons, particles with statistics intermediate between Fermi and Bose statistics in two-dimensional space. In fact it is possible to change the statistics of particles in two-dimensional space, for example by attaching fictitious magnetic flux in the case of electrons. The ZHK theory uses precisely this transformation property associated with the gauge term of the Chern-Simons theory to describe the strongly correlated fractional quantum Hall state as a Bose condensed

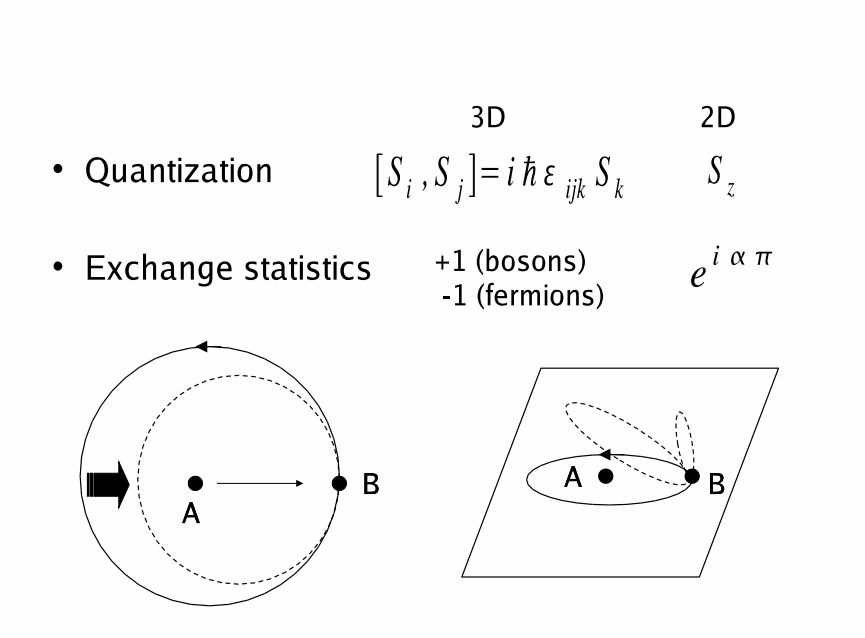

Figure 5.1: Statistics associated with the exchange of two identical particles. The net effect of making the interchange twice is to take one particle around another in a closed loop. In 3-dimensions the loop can be deformed without crossing the other particle which is not possible in two dimensions.

state of bosonized electrons (composite bosons). Within this view point, we show that the atomic Laughlin state of previous chapter can be described as a Bose condensed state of composite bosons.

5.2 Statistics in 2-dimensions

In 3-dimensional space there are only two types of particles, bosons and fermions. They are distinguished by the following properties: (a) intrinsic spin of bosons is $s\hbar$; $s = 0, 1, 2..$ while that of fermions is $s\hbar$; $s = \frac{1}{2}, \frac{3}{2}, ...$, (b) when two identical particles are exchanged, the wavefunction changes its overall sign for fermions but not for bosons, and (c) any number of bosons can occupy a single quantum state, but a single state cannot be occupied by more than one fermion. The non-Abelian algebra,

$$[S_i, S_j] = i\hbar\varepsilon_{ijk} S_k \text{ for } i, j, k = x, y, z \tag{5.1}$$

is responsible for the quantization of spin in 3-dimensions. To the contrary, fractional spin is possible in a 2-dimensional space because there is only one way of rotation, which is around the z axis by embedding the 2-dimensional space into the 3-dimensional space and identifying it with the xy plane. Here the spin operator is S_z with an arbitrary eigenvalue since the rotational group is Abelian. Now for the exchange statistics, as shown in Fig. 5.1, if we move one particle around the other in a closed loop, in 3-dimensions, the loop can be continuously deformed to a point which in 2-dimensional space is not possible without crossing the second particle. Hence in 2-dimensional space, the exchange statistics depends on the loop contrary to 3-dimensional space, where it is an intrinsic property of the particles. Thus particles in 2-dimensions can act like fermions or bosons under exchange depending on the geometry of exchange. Lastly, the Pauli exclusion principle can be interpolated from fermions to anyons (particles in two dimensions with fractional spin) by introducing a statistical interaction g [101] defined by

$$g = \frac{d_N - d_{N+\Delta N}}{\Delta N}, \tag{5.2}$$

where N is the number of particles and d_N is the dimension of the one-particle Hilbert space obtained by holding the coordinates of $N-1$ particles fixed. We have $g = 0$ for bosons, $g = 1$ for fermions and $g = m$ for the composite particles in the $\frac{1}{m}$ fractional quantum Hall state.

5.3 Berry phase

Consider a system in which the Hamiltonian depends on some external parameter represented by a vector $\mathbf{R}$. Also assume that the Hamiltonian has a non-degenerate eigenstate $\Psi_{\mathbf{R}}$

$$H(\mathbf{R})\Psi_{\mathbf{R}} = E_{\mathbf{R}}\Psi_{\mathbf{R}} \tag{5.3}$$

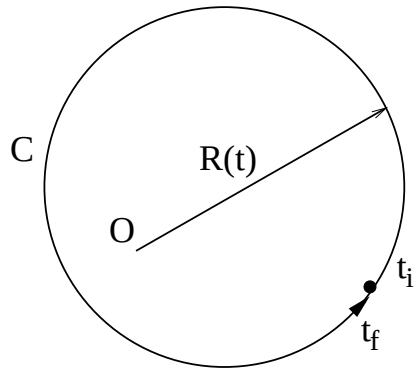

Figure 5.2: Trajectory of the vector $\mathbf{R}(t)$ in the parameter space. The vector $\mathbf{R}(t)$ represents a set of parameters that define the Hamiltonian at some time t. The parameters are changed adiabatically from their initial value at time t_i such that the vector moves in a closed loop and comes back to its original position at some final time t_f

.

Now we start at some initial time t_i and change the parameters such that the vector $\mathbf{R}$ moves in a closed loop C in the parameter space as shown in Fig. 5.2 and returns to its initial value at some final time t_f, $\mathbf{R}(t_f) = \mathbf{R}(t_i)$. If the change is sufficiently slow the state changes continuously and remains an eigenstate at all times. Since we have assumed the state to be non-degenerate, the state at time t_f should be the same as that at t_i except for a multiplicative phase factor. In fact, the states are related by

$$\Psi_{\mathbf{R}(t_f)}(t_f) = \exp\left(-\frac{i}{\hbar}\int_{t_i}^{t_f} dt' E(\mathbf{R}(t')) + i\gamma(C)\right)\Psi_{\mathbf{R}(t_i)}(t_i). \tag{5.4}$$

The first part of the phase factor is the dynamical phase and is due to the eigenenergy of the state. The second part depends on the contour C and is independent of $t_f - t_i$ and is referred to as the geometric phase. This phase can be expressed as

$$\gamma(C) = i\oint_C \langle\Psi_{\mathbf{R}(t)}|\nabla_{\mathbf{R}(t)}\Psi_{\mathbf{R}(t)}\rangle \cdot d\mathbf{R}(t) \tag{5.5}$$

and is called the Berry phase [102]. A typical example is the Aharonov-Bohm (AB) phase [103], which appears when an electron moves in a magnetic field. The AB phase is given by $\gamma(C) = eBS/\hbar$, where BS is the flux passing through the contour C. In the next section we will see how this extra geometric phase is associated with the idea of

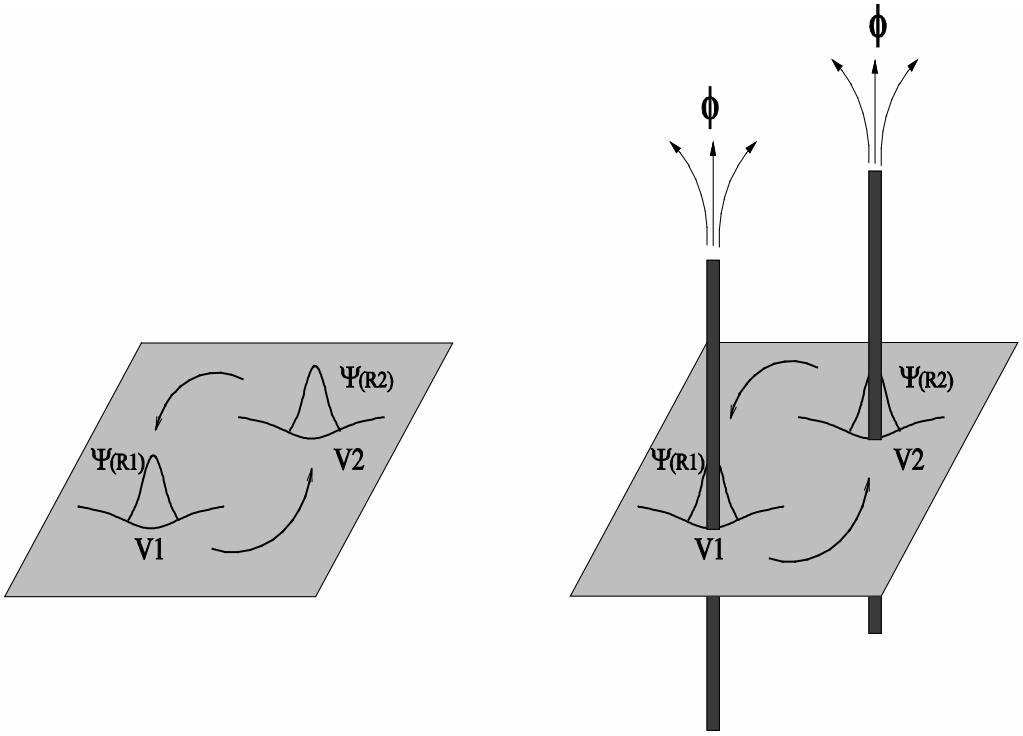

Figure 5.3: Left figure: two-dimensional two-electron system. The electron is localized separately potential valleys $V1$ and $V2$. The valleys are separated such that there is negligible overlap between the electronic wavefunctions. Right figure: the same situation as on the left except now the electrons are independently attached to magnetic flux ϕ and the flux moves along with the electrons.

anyons, the particles with statistics intermediate between Fermi and Bose statistics.

5.4 Anyons

One can change the statistics of the particles in a two-dimensional system based on the fact that the AB phase arises in the presence of magnetic flux. For example, consider a two-electron system, in which each of the electrons are localized in separate potential valleys at $\mathbf{R}_1$ and $\mathbf{R}_2$ as shown in Fig. 5.3. We assume that the valleys are separated so that the overlap of the wavefunctions is negligible. The two electron wave

function can then be written in terms of their bound state wavefunctions $\Psi_{\mathbf{R}}(\mathbf{r})$

$$\Psi_{\mathbf{R}_1,\mathbf{R}_2}(\mathbf{r}_1,\mathbf{r}_2) = \frac{1}{\sqrt{2}}\left[\Psi_{\mathbf{R}_1}(\mathbf{r}_1)\Psi_{\mathbf{R}_2}(\mathbf{r}_2) - \Psi_{\mathbf{R}_2}(\mathbf{r}_1)\Psi_{\mathbf{R}_1}(\mathbf{r}_2)\right] \tag{5.6}$$

Now if we exchange the position of the potential wells adiabatically, the Hamiltonian returns to its original form, but due to the Fermi statistics of the electrons, the total wave function acquires an extra minus sign. Next we consider the situation in which each of the electrons is attached to an infinitesimally thin magnetic flux ϕ as shown in the right figure of Fig. 5.3 and also assume that the flux moves along with the electrons. Again we exchange the position of the potential wells as before, but now there is an extra contribution $e\phi/(2\hbar)$ to the phase due to the flux attachment. We can choose the flux to be such that the additional phase cancels the minus sign due to Fermi statistics. Thus the electrons behave like bosons when a certain amount of flux is attached to them. Since the choice of ϕ is arbitrary, it is possible to make particles with statistics intermediate between that of Fermi and Bose or anyons.

5.5 Composite particle mean field theory

Having introduced the key concepts behind exchange statistics in two-dimensions, we now show how these ideas can be combined into building a field theory applicable in the strongly correlated regime of the rotating Bose gas described by the bosonic-Laughlin wavefunction. We start by defining a unit quantum of flux by $\phi_0 = h/|e|$. Then bosons and fermions can be transformed into fermions and bosons respectively by attaching an odd number of flux quanta to each particle. On the other hand the statistics remains unchanged by attaching an even number of flux quanta. This is shown in Fig. 5.4. Thus electrons in a $\frac{1}{q}$; $q =$ odd FQHE, can be considered as composite bosons with extra $q\phi_0$ fictitious flux in the opposite direction. The mean field of the fictitious flux cancels with the real flux, and the system can be considered as a system of interacting composite bosons in a zero magnetic field. Thus in the mean field picture, the

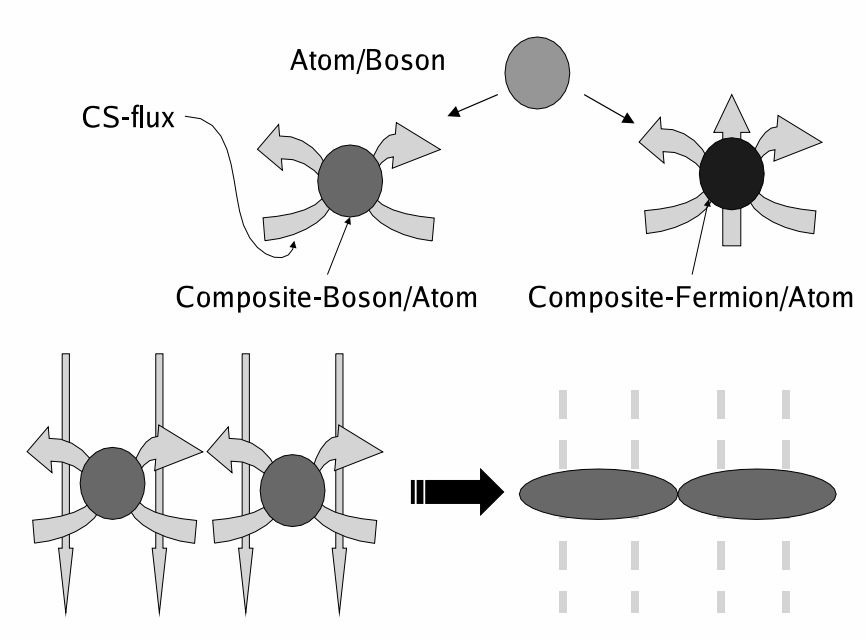

Figure 5.4: Composite particle picture. A boson is transformed to a composite boson(fermion) by attaching an even(odd) number of magnetic flux quanta. The extra fictitious flux cancels the real flux in the mean field approximation resulting in free composite bosons/fermions.

interaction experienced by the composite bosons is just the repulsive coulomb interaction. At the same time we know that a repulsive bosonic system in two dimensions undergoes Bose condensation at zero temperature. Hence in this picture, an odd fractional quantum Hall state can be thought of as a Bose condensed phase of composite bosons.

The same argument holds for our case of bosonic $\frac{1}{2}$ FQHE in rotating Bose gases. Since $q = 2 =$ even, the rotating Bose system can be reduced to a system of interacting composite bosons with zero rotational frequency. The composite bosons still experience the repulsive two-body potential; therefore, the strongly correlated bosonic Laughlin state can be considered as a Bose condensed state of composite bosons.

5.6 Chern-Simons Ginzburg-Landau theory

The starting point of this theory is the second quantized Hamiltonian for atoms(bosons) in the rotating frame. Since we have already made the mapping between the vorticity and magnetic field, we write the second quantized Hamiltonian in terms of the vector potential $\mathbf{A}$ instead of rotating frequency Ω. Also here we specialize to the case of $\Omega = \omega$, so that $H_L = 0$ in (4.3). Thus

$$\hat{H} = \int \hat{\psi}^\dagger(\mathbf{r}) \left[\frac{1}{2m}(-i\mathbf{D})^2\right] \hat{\psi}(\mathbf{r}) d^2r + \frac{1}{2}\int\int \hat{\psi}^\dagger(\mathbf{r})\hat{\psi}^\dagger(\mathbf{r}')V(\mathbf{r}-\mathbf{r}')\hat{\psi}(\mathbf{r})\hat{\psi}(\mathbf{r}')d^2r d^2r' \tag{5.7}$$

where $D_\mu = \partial_\mu + ieA_\mu$ and $\hat{\psi}(\mathbf{r}) = \sum_{l=0}^{\infty} a_l \psi_l^{LL}(\mathbf{r})$ where a_l is the annihilation operator for a particle in the lth single particle lowest landau state. As discussed in the previous section, we would like to work in a composite boson picture. The composite boson field operator $\hat{\varphi}$ is defined by (see App. C)

$$\hat{\varphi}(\mathbf{r}) = e^{-J(\mathbf{r})}\hat{\psi}(\mathbf{r}) \tag{5.8}$$

where the operator J is given by

$$J(\mathbf{r}) = iq \int d^2r' \rho_a(\mathbf{r}')\theta(z - z') \tag{5.9}$$

In the composite picture the second quantized Hamiltonian retains the same form as given above with the operators $\hat{\psi}$ and $\hat{\psi}^\dagger$ replaced by the corresponding composite boson operators $\hat{\varphi}$ and $\hat{\varphi}^\dagger$ and D replaced by $\mathcal{D}$,

$$\mathcal{D}_\mu = D_\mu + iea_\mu(\mathbf{r}) \tag{5.10}$$

where a_μ is the fictitious Chern-Simons gauge field. The Chern-Simons field is an auxiliary field subject to certain constraints rather than a dynamical field obeying Maxwell's equation. In order to derive the constraint equation and the stationary solution it is convenient to use the Lagrangian formulation. In the semi-classical approximation,

the Lagrangian density corresponding to the full second quantized Hamiltonian written above is given by

$$\mathcal{L} = \mathcal{L}_a + \mathcal{L}_{cs} \tag{5.11}$$

where

$$\begin{aligned} \mathcal{L}_a &= \varphi^*(\mathbf{r})(i\mathcal{D}_0)\varphi(\mathbf{r}) + \frac{1}{2m}\varphi^*(\mathbf{r})\mathcal{D}^2\varphi(\mathbf{r}) \\ &- \frac{1}{2}\int \varphi^*(\mathbf{r})\varphi^*(\mathbf{r}')V(\mathbf{r}-\mathbf{r}')\varphi(\mathbf{r})\varphi(\mathbf{r}')d^2r' \qquad (5.12) \\ \mathcal{L}_{cs} &= -\frac{e^2}{4q\pi}\varepsilon^{\mu\nu\lambda}a_\mu(\mathbf{r})\partial_\nu a_\lambda(\mathbf{r}) \qquad (5.13) \end{aligned}$$

This Lagrangian has the usual form except for the last term called the Chern-Simons term. Here μ is the chemical potential and $\varepsilon^{\mu\nu\lambda}$ is the complete antisymmetric tensor with the convention $\varepsilon^{012} = 1$. Therefore the action is given by

$$S = \int \mathcal{L}d^2rdt \tag{5.14}$$

In the rest of the thesis we consider the interaction potentials to be local $V(\mathbf{r}-\mathbf{r}') = V\delta(\mathbf{r}-\mathbf{r}')$. The ground state is the state that minimizes the action S. This implies that the action be invariant under small fluctuations of φ. But first we consider the variation of the action with respect to the zeroth component of the gauge field, $\partial S/\partial a_0 = 0$, which results in the constraint equation

$$\nabla \times \mathbf{a}|_z = -\frac{2q\pi}{e}(\varphi^*\varphi), \tag{5.15}$$

which is essentially the Chern-Simons condition. The extremum condition $\partial S/\partial\varphi^* = 0$ results in the following classical equation of motion for the field φ

$$(i\mathcal{D}_0 + \mu)\varphi(\mathbf{r}) + \frac{1}{2m}\mathcal{D}^2\varphi(\mathbf{r}) - \varphi^*(\mathbf{r})V\varphi(\mathbf{r})\varphi(\mathbf{r}) = 0. \tag{5.16}$$

The most simple solution to the above equation is the one where the Bose field is uniform in space and time $\varphi = \sqrt{\overline{\rho}}$. Also since the system is homogeneous, to avoid infinite mean

field contribution we shift the zero of energy to this mean field energy. Now we see that the uniform solution is possible only if

$$\mathbf{A} + \mathbf{a} = 0 \quad \text{and} \quad \mathrm{a}_0 = 0 \tag{5.17}$$

This implies that $B = (2q\pi/e)\bar{\rho}$ or the filling fraction is $\nu = 1/q$. Thus a uniform solution can exist only when a Laughlin wavefunction can be written down. Thus a bosonic Laughlin state of a rotating Bose gas can be thought of as the Bose condensed phase of composite bosons formed from atoms attached to an even number of vortices.

5.7 Feshbach resonance

From the discussion of the Chern-Simons field theory of the previous section, it is clear that, within this picture, Feshbach interaction can be systematically introduced to tune the inter-atomic interaction. In a typical Feshbach resonance illustrated in Fig. 5.5, the properties of the collision of two atoms are controlled through their resonant coupling to a bound state in a closed channel Born-Oppenheimer potential. By adjusting an external magnetic field, the scattering length can be tuned to have any value. The field dependence of the scattering length is characterized by the detuning ν and obeys a dispersive profile given by

$$a(\nu) = a_{\mathrm{bg}} \left(1 - \frac{\kappa}{2\nu}\right), \tag{5.18}$$

where κ is the resonance width, and a_{bg} is the background scattering length. In fact, all the scattering properties of a Feshbach resonance system are completely characterized by just three parameters

$$U_0 = \frac{4\pi\hbar^2 a_{\mathrm{bg}}}{m}, \quad g = \sqrt{\kappa U_0}, \quad \text{and} \quad \nu. \tag{5.19}$$

Physically, U_0 represents the energy shift per unit density on the single particle eigenvalues due to the background scattering processes, while g, which has dimensions of energy per square-root density, represents the coupling to the Feshbach resonance connecting the open and closed channel potentials.

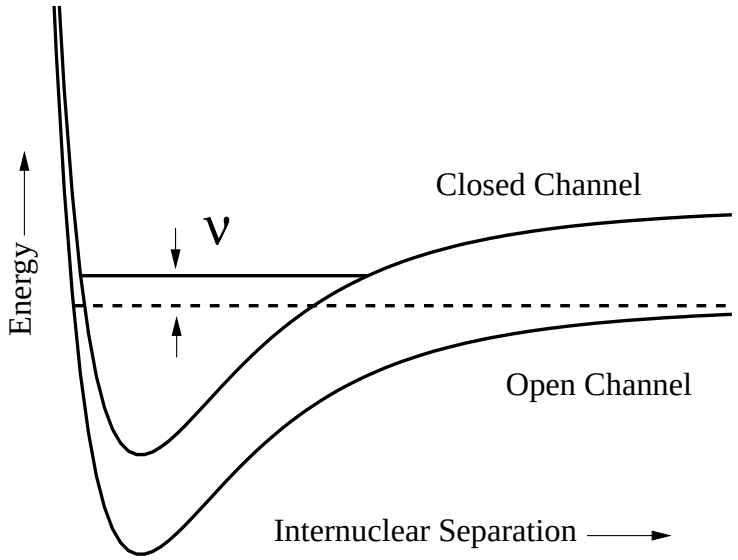

Figure 5.5: A Feshbach resonance results when a closed channel potential possesses a bound state in proximity to the scattering energy in an open channel potential. The detuning of the bound state from the edge of the collision continuum is denoted by ν_0.

The second quantized Hamiltonian for a dilute Bose gas with binary interactions is given by

$$H = \int d^3x\ \psi_a^\dagger(\mathbf{x}) H_a(\mathbf{x}) \psi_a(\mathbf{x}) + \int d^3x d^3x'\ \psi_a^\dagger(\mathbf{x}) \psi_a^\dagger(\mathbf{x}') U(\mathbf{x}, \mathbf{x}') \psi_a(\mathbf{x}') \psi_a(\mathbf{x}) \qquad (5.20)$$

where $H_a(\mathbf{x})$ is the single particle Hamiltonian, $U(\mathbf{x}, \mathbf{x}')$ is the binary interaction potential, and $\psi_a(\mathbf{x})$ is the atomic field operator. In cold quantum gases, where the atoms collide at very low energy, we are only interested in the behavior of the scattering about a small energy range above zero. There exist many potentials which replicate the low energy scattering behavior of the true potential; therefore, it is convenient to carry out the calculation with the simplest one, the most convenient choice being to take the interaction potential as a delta-function pseudo potential when possible.

For a Feshbach resonance this choice of pseudo potential is generally not available since the energy dependence of the scattering implies that a minimal treatment must at least contain a spread of wave-numbers which is equivalent to the requirement of a

nonlocal potential. Since the solution of a nonlocal field theory is inconvenient, we take an alternative but equivalent approach. We include in the theory an auxiliary molecular field operator $\psi_m(\mathbf{x})$ which obeys Bose statistics and describes the collision between atoms in terms of two elementary components: the background collisions between atoms in the absence of the resonance interactions and the conversion of atom pairs into molecular states. This allows us to construct a local field theory with the property that when the auxiliary field is integrated out, an effective Hamiltonian of the form given in Eq. (5.20) is recovered with a potential $U(\mathbf{x},\mathbf{x}') = U(|\mathbf{x}-\mathbf{x}'|)$ which generates the form of the two-body T-matrix predicted by Feshbach resonance theory [104]. The local Hamiltonian which generates this scattering behavior:

$$\begin{aligned} H &= \int d^3x\ \psi_a^\dagger(\mathbf{x})\Big(-\frac{\hbar^2}{2m}\nabla_x^2 + V_a(\mathbf{x}) - \mu_a\Big)\psi_a(\mathbf{x}) \\ &\quad + \int d^3x\ \psi_m^\dagger(\mathbf{x})\Big(-\frac{\hbar^2}{4m}\nabla_x^2 + V_m(\mathbf{x}) - \mu_m\Big)\psi_m(\mathbf{x}) \\ &\quad + \frac{U}{2}\int d^3x\ \psi_a^\dagger(\mathbf{x})\psi_a^\dagger(\mathbf{x})\psi_a(\mathbf{x})\psi_a(\mathbf{x}) \\ &\quad + \frac{g}{2}\int d^3x\ \psi_m^\dagger(\mathbf{x})\psi_a(\mathbf{x})\psi_a(\mathbf{x}) \end{aligned} \tag{5.21}$$

has the intuitive structure of resonant atom-molecule coupling. Here $V_{a,m}$ are the external potentials and $\mu_{a,m}$ are the chemical potentials. The subscripts a, m represent the atomic and molecular contributions, respectively. The Feshbach resonance is controlled by the magnetic field which is incorporated into the theory by the detuning $\nu = \mu_m - 2\mu_a$ between the atomic and molecular fields. The Hamiltonian in equation (5.21) contains the three parameters U_0, g, and ν which account for the complete scattering properties of the Feshbach resonance.

Thus in order to introduce Feshbach interaction within the framework discussed earlier in this chapter, we will have to define composite bosons for the molecules exactly in the same way as we did for the atoms, except that the composite molecular bosons will be attached to twice the number of flux quantaas that for the atoms. All these ideas will be put to work in the next chapter.

Chapter 6

Resonant formation of novel strongly correlated paired states in rotating Bose gases

Published in Physical Review A **69**,*053603 (2004)*

6.1 Introduction

Recently, there has been considerable interest from both the experimental and theoretical perspective in the behavior of rotating Bose gases confined to an effective two-dimensional space [105, 106, 107, 96, 97, 108]. One goal has been to understand and to create strongly correlated states, such as the Laughlin state generated by the fractional quantum Hall effect (FQHE), within ultracold atomic gases. A major challenge to realizing such a state is the need to reach extremely low temperatures in order to resolve the lowest Laughlin state from the first excited state. The size of this energy gap, however, is directly related to the strength of interatomic interactions, so by increasing the interactions it would seem natural that one could increase the gap, making the system more accessible to experiment.

Atomic systems can now be created which allow the microscopic interactions to be dynamically tuned [109, 110]. Feshbach resonances have proven very successful at doing this, allowing one to tune the interactions by adjusting the resonant detuning ν (for example, by varying a magnetic field), and would seem an excellent tool for increasing the gap within a FQHE system. To account for the full effects of the resonance, however, we cannot simply scale the mean-field energy but must incorporate the entire resonant

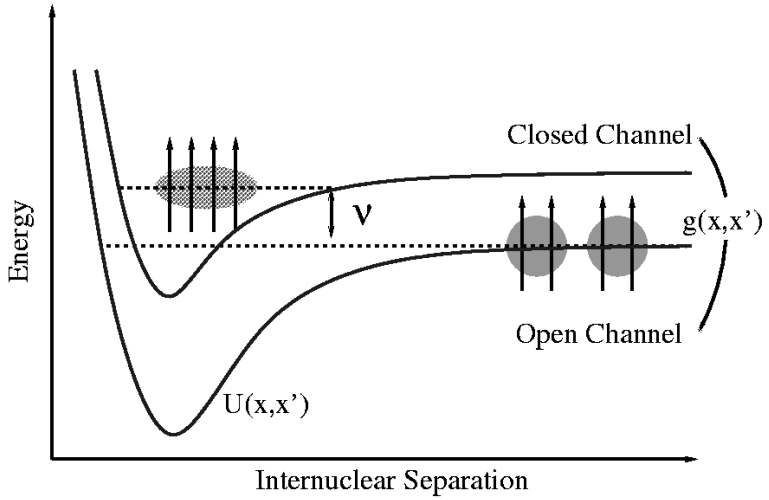

Figure 6.1: The Feshbach resonance pairing mechanism is illustrated by the above Born-Oppenheimer curves. Pairs of composite atoms composed of single atoms and an associated number of quanta of angular momentum (represented by the arrows) approach each other within an open channel potential of background value $U(\mathbf{x}, \mathbf{x}')$. They may form a composite molecule due to the presence of a closed channel bound state, at a detuning ν from the scattering continuum, which is coupled to the open channel with strength $g(\mathbf{x}, \mathbf{x}')$.

structure into our model. This means that we must include the process of molecular formation generated by the introduction of a bound state within the open channel of scattering states [111, 112, 113].

By introducing a bound state, however, we not only modify the relative interaction strength, but we also introduce a physical mechanism for generating pair correlations between particles (see Fig. 6.1). In the context of two-dimensional condensed matter systems, such a mechanism, although arising from a very different source [114], can have a significant effect on the ground state properties. Before we can study the resonant behavior of the gap, we must first understand the effect of resonant interactions on the ground state wavefunction. We will find that as we approach the Feshbach resonance the Laughlin state transforms into a unique, strongly correlated state.

6.2 Inclusion of Feshbach resonance in the Chern-Simons theory

We begin by writing down an effective Hamiltonian, in second quantized form, for a resonant gas of Bosons of mass m rotating in two dimensions with stirring frequency Ω approaching the trapping frequency ω, i.e. $\omega - \Omega \to 0^+$:

$$\begin{aligned}
\hat{H} &= \int d^2x\ \hat{\psi}_a^\dagger(\mathbf{x}) \left[\frac{-1}{2m}(\nabla - i\mathbf{A}(\mathbf{x}))^2\right] \hat{\psi}_a(\mathbf{x}) \\
&+ \frac{1}{2}\int d^2x' \int d^2x\ \hat{\psi}_a^\dagger(\mathbf{x})\hat{\psi}_a^\dagger(\mathbf{x}')U(\mathbf{x},\mathbf{x}')\hat{\psi}_a(\mathbf{x}')\hat{\psi}_a(\mathbf{x}) \\
&+ \int d^2x\ \hat{\psi}_m^\dagger(\mathbf{x}) \left[\frac{-1}{4m}(\nabla - 2i\mathbf{A}(\mathbf{x}))^2 + \nu\right] \hat{\psi}_m(\mathbf{x}) \\
&+ \frac{1}{2}\int d^2x' \int d^2x \Big[\hat{\psi}_m^\dagger(\frac{\mathbf{x}+\mathbf{x}'}{2}) g(\mathbf{x},\mathbf{x}')\hat{\psi}_a(\mathbf{x})\hat{\psi}_a(\mathbf{x}') + \text{H.c.}\Big].
\end{aligned} \tag{6.1}$$

Here $\hat{\psi}_{a,m}^\dagger(\mathbf{x}), \hat{\psi}_{a,m}(\mathbf{x})$ are the creation and destruction operators for atoms and molecules which satisfy the commutation relations $[\hat{\psi}_1(\mathbf{x}), \hat{\psi}_2^\dagger(\mathbf{x}')] = \delta^{(3)}(\mathbf{x},\mathbf{x}')\delta_{1,2}$, where $1,2 \in \{a,m\}$. We define the two-dimensional vector potential $\mathbf{A}(\mathbf{x}) = (m\omega y, -m\omega x)$, $U(\mathbf{x},\mathbf{x}')$ is the two-particle background scattering potential, $g(\mathbf{x},\mathbf{x}')$ is the resonant coupling between the open and closed channel potentials, and ν is the detuning of the open channel continuum from the level of the bound state in the closed channel.

Recently, it has been noted that there is a direct mapping between the Hamiltonian for a rotating two-dimensional gas, the first two terms of Eq. (6.1), and that of the FQHE [96]. The analog of the magnetic field is realized by the angular rotation and the Coulomb interaction is replaced by the two-particle scattering. Therefore, if we were to neglect resonant effects we would expect the many-body ground state to be described by the Laughlin wavefunction [90]

$$\Psi_L(\mathbf{x}_1, \mathbf{x}_2, ...\mathbf{x}_N) = \prod_{i<j}(z_i - z_j)^2 \prod_k \exp\left(-|z_k|^2/2\right), \tag{6.2}$$

where the products run over the indices $i,j,k = (1,2,...N)$ at position $z = x + iy$ for N particles. We will see that the inclusion of the resonant terms in Eq. (6.1) can

significantly modify the form of Eq. (6.2) due to the growth of two-particle correlations.

We approach this problem by an extension of the Chern-Simons theory [115] which allows us to develop a mean-field theory for the rotating system that has removed the complications of the associated rotation. This is done by constructing a composite particle composed of the original particle and an artificially attached number of flux quanta. The composite particle is designed so that the attached flux quanta cancel the total rotation of the original system leaving a system of non-rotating, interacting composite particles. For the resonant system, the composite particles can formally be obtained by the following transformation:

$$\hat{\varphi}_{a,m}(\mathbf{x}) = \exp\Bigg[\; -i \;\; q \int d^2x' \theta(\mathbf{x}-\mathbf{x}') \times \;\; [\rho_a(\mathbf{x}') + 2\rho_m(\mathbf{x}')]\Bigg] \hat{\psi}_{a,m}(\mathbf{x}), \tag{6.3}$$

where $\rho_a(\mathbf{x}')$ and $\rho_m(\mathbf{x}')$ are the atomic and molecular spatial densities, respectively, and $\theta(\mathbf{x}-\mathbf{x}')$ is the topological phase. To guarantee that the resulting composite particle is a Boson, with no loss of generality we set $q = 2$.

In the composite picture, we replace the $\hat{\psi}$ operators in Eq. (6.1) with the corresponding composite operators $\hat{\varphi}$ and introduce the statistical Chern-Simons field $\mathbf{a}(\mathbf{x})$ through the gauge transformation

$$\mathbf{A}(\mathbf{x}) \rightarrow \mathbf{A}(\mathbf{x}) + \mathbf{a}(\mathbf{x}) \tag{6.4}$$

These modifications generate the Hamiltonian formulation of our composite atom/molecule theory. The composite picture can be shown to be equivalent to the single particle picture of Eq. (6.1).

We will now shift to a functional representation of the composite atom/molecule system to clarify the resonant modifications of the Chern-Simons theory and then return

to the Hamiltonian formulation to derive the ground state wavefunction. Defining the action within one temporal and two spatial dimensions

$$S = \int d^3x \sum_{\sigma=a,m} \varphi_\sigma^*(\mathbf{x}) i\partial_0 \varphi_\sigma(\mathbf{x}) - \int dx_0 \hat{H}, \tag{6.5}$$

we generate a Chern-Simons term which couples to the statistical vector field $a_\mu(\mathbf{x})$

$$S_{CS} = -\int d^3x \frac{1}{8\pi} \epsilon^{\mu\nu\lambda} a_\mu(\mathbf{x}) \partial_\nu a_\lambda(\mathbf{x}), \tag{6.6}$$

where the indices of μ, ν, and λ run over the three dimensions $(0, 1, 2)$ and the summation convention over repeated indices is invoked. We have also introduced the antisymmetric tensor $\epsilon^{012} = 1$. To simplify the following calculations we assume contact interactions of the form $U(\mathbf{x}, \mathbf{x}') = U\delta(\mathbf{x}, \mathbf{x}')$ and $g(\mathbf{x}, \mathbf{x}') = g\delta(\mathbf{x}, \mathbf{x}')$. Any complications arising from this replacement of the true potentials with contact potentials should be remedied as explained in Ref. [104]. We next perform the lowest order variation of the action.

Varying with respect to the zeroth component of the gauge field, $\partial S/\partial a_0 = 0$, reproduces the Chern-Simons condition

$$\nabla \times \mathbf{a}(\mathbf{x})|_z = -4\pi \left(|\varphi_a(\mathbf{x})|^2 + 2|\varphi_m(\mathbf{x})|^2 \right). \tag{6.7}$$

Equation (6.7) is a statement of Gauss's law for the statistical gauge field associating an even number of rotational flux quanta with each particle. This relation is simply a restatement of our choice of quasiparticle.

Since we will be interested in the ground state properties of the atom/molecule system, let us assume that the fields $\varphi_a(\mathbf{x})$ and $\varphi_m(\mathbf{x})$ are uniform. By minimizing the action with respect to the atomic and molecular fields, i.e. $\partial S/\partial \varphi_a = 0$, $\partial S/\partial \varphi_m = 0$, we generate the following constraint equation for the molecules:

$$\varphi_m = \frac{g\varphi_a^2}{2[\nu + |\mathbf{A} + \mathbf{a}|^2/m]}. \tag{6.8}$$

Equation (6.8) allows us to eliminate the molecular field from the theory and arrive at a self-consistent relationship for the gauge field

$$|\mathbf{A}+\mathbf{a}|^2 = \left(U + \frac{g^2}{4(\nu + |\mathbf{A}+\mathbf{a}|^2/m)}\right) 2m|\varphi_a|^2. \tag{6.9}$$

Equation (6.9) is the usual result relating the gauge field to the background density only now it is dependent upon the detuning from the resonance.

6.3 Pairing in the strongly correlated ground state

We now switch back to the Hamiltonian form of our theory to derive the ground state wavefunction. After Fourier transforming the composite form of Eq. (6.1) by substitution of the field operators $\hat{\varphi}_a(\mathbf{x}) = \sum_{\mathbf{k}} \hat{a}_{\mathbf{k}} e^{i\mathbf{k}\cdot\mathbf{x}}$ and $\hat{\varphi}_m(\mathbf{x}) = \sum_{\mathbf{k}} \hat{b}_{\mathbf{k}} e^{i\mathbf{k}\cdot\mathbf{x}}$, we follow the usual Hartree-Fock-Bogolubov (HFB) approach to construct a quadratic Hamiltonian which accounts for the lowest order pairing. As before, we assume contact interactions and now make the additional assumption that we may neglect the excited modes of the molecular field keeping only the lowest condensed mode $\hat{b}_{\mathbf{k}} = b_0$. The resulting Hamiltonian for the composite system can be written in the form

$$H = H^0 + \sum_{\mathbf{k}\neq 0} A^\dagger_{\mathbf{k}} M_{\mathbf{k}} A_{\mathbf{k}}. \tag{6.10}$$

H^0 is composed of all terms of less then quadratic order in the operator $\hat{a}_{\mathbf{k}}$, we define a column vector $A_{\mathbf{k}} = (\hat{a}_{\mathbf{k}}, \hat{a}^\dagger_{-\mathbf{k}})$, and $M_{\mathbf{k}}$ is the self-energy matrix. For our purposes we need only concern ourselves with the structure of the second term in Eq. (6.10). Here the self-energy matrix is expressed as

$$M_{\mathbf{k}} = \begin{pmatrix} E_{\mathbf{k}} & \Delta \\ \Delta^* & E_{-\mathbf{k}} \end{pmatrix} \tag{6.11}$$

with the additional definitions for the diagonal and off-diagonal terms

$$E_{\mathbf{k}} = E^0_{\mathbf{k}} + U(|\varphi_a|^2 + n) \tag{6.12}$$

$$\Delta = U(\varphi_a^2 + p) + g\varphi_m. \tag{6.13}$$

Equations (6.12) and (6.13) are expressed in terms of the pairing-field $p = \sum_{\mathbf{k}'} \langle \hat{a}_{\mathbf{k}'} \hat{a}_{-\mathbf{k}'} \rangle$, the normal-field $n = \sum_{\mathbf{k}'} \langle \hat{a}^\dagger_{\mathbf{k}'} \hat{a}_{\mathbf{k}'} \rangle$, and $E^0_{\mathbf{k}}$ is the effective kinetic term which contains the contribution from the gauge field $A(\mathbf{x})$.

Eq. (6.10) can be rewritten in terms of the quasiparticles

$$\hat{\alpha}_{\mathbf{k}} = \frac{1}{\sqrt{(E_{\mathbf{k}} + \omega_{\mathbf{k}})^2 + |\Delta|^2}} \left((E_{\mathbf{k}} + \omega_{\mathbf{k}}) \hat{a}_{\mathbf{k}} + \Delta \hat{a}^\dagger_{-\mathbf{k}} \right) \tag{6.14}$$

$$\hat{\alpha}^\dagger_{-\mathbf{k}} = \frac{1}{\sqrt{(E_{\mathbf{k}} + \omega_{\mathbf{k}})^2 + |\Delta|^2}} \left((E_{\mathbf{k}} + \omega_{\mathbf{k}}) \hat{a}_{-\mathbf{k}} + \Delta^\dagger \hat{a}_{\mathbf{k}} \right) \tag{6.15}$$

which result in the diagonal Hamiltonian

$$\mathcal{H} = \mathcal{H}^0 + \sum_{\mathbf{k} \neq 0} \omega_{\mathbf{k}} \hat{\alpha}^\dagger_{\mathbf{k}} \hat{\alpha}_{\mathbf{k}}, \tag{6.16}$$

where $\mathcal{H}^0$ contains the ground state contribution to the energy and the excitations are given by the spectrum of frequencies $\omega_{\mathbf{k}} = \sqrt{E^2_{\mathbf{k}} - |\Delta|^2}$.

Since there are no quasiparticles present in the ground state $|gs\rangle$, which is what one would expect from an interacting bosonic system at $T = 0$, the ground state must satisfy the condition $\hat{\alpha}_{\mathbf{k}} |gs\rangle = 0$. Substitution of Eqs. (6.14) and (6.15) for the quasiparticle operators result in the relation

$$(E_{\mathbf{k}} + \omega_{\mathbf{k}}) \hat{a}_{\mathbf{k}} |gs\rangle = -\Delta \hat{a}^\dagger_{-\mathbf{k}} |gs\rangle. \tag{6.17}$$

Because $\hat{a}_{\mathbf{k}}$ and $\hat{a}^\dagger_{\mathbf{k}}$ are canonically conjugate variables there is no loss of generality in making the replacement $\hat{a}_{\mathbf{k}} \rightarrow \partial / \partial \hat{a}^\dagger_{\mathbf{k}}$ [116]. This converts Eq. (6.17) into a simple differential equation for the ground state with the solution

$$|gs\rangle = \exp\left[\sum_{\mathbf{k}} \frac{-\Delta}{E_{\mathbf{k}} + \omega_{\mathbf{k}}} \hat{a}^{\dagger}_{-\mathbf{k}} \hat{a}^{\dagger}_{\mathbf{k}}\right] |0\rangle. \tag{6.18}$$

To derive the many-body wavefunction we must now move from second to first quantization. The relationship which links the second quantized ground state $|gs\rangle$ with the first quantized wavefunction Ψ_{CB} can be written for an even number of noncondensed particles $2N$ as

$$\Psi_{CB}(\mathbf{x}_1, \mathbf{x}_2, ...\mathbf{x}_{2N}) = \langle 0|\hat{\varphi}_a(\mathbf{x}_{2N})...\hat{\varphi}_a(\mathbf{x}_2)\hat{\varphi}_a(\mathbf{x}_1)|gs\rangle, \tag{6.19}$$

where it should be noted that Ψ_{CB} is the full-many body wavefunction for the composite Bose particles. If we are able to assume that $E_{\mathbf{k}} + \omega_{\mathbf{k}} \gg \Delta$, an assumption which will remain valid as long as we are not too close to resonance, we may truncate the power expansion of the exponent in Eq. (6.18). This results in the composite boson wavefunction

$$\Psi_{CB}(\mathbf{x}_1, \mathbf{x}_2, ...\mathbf{x}_{2N}) = \mathcal{S}(\psi_{12}\psi_{34}...\psi_{(2N-1)2N}) \tag{6.20}$$

comprised of a symmetrized product $\mathcal{S}$ of paired wavefunctions

$$\psi_{ij} = \sum_{\mathbf{k}} \frac{-\Delta}{E_{\mathbf{k}} + \omega_{\mathbf{k}}} e^{i\mathbf{k}\cdot(\mathbf{x}_i - \mathbf{x}_j)}. \tag{6.21}$$

If we were dealing with a system of fermions, equation (6.20) would be antisymmetrized and would result in a Pfaffian wavefunction [6, 117]. Here, because of the statistics of the particles, we generate a bosonic analogue to this result. The many-body wavefunction for the bare particles can now be extracted from the composite wavefunction [118] resulting in

$$\Psi_{MB} = \Psi_{CB}(\mathbf{x}_1, \mathbf{x}_2..., \mathbf{x}_{2N}) \times \Psi_L(\mathbf{x}_1, \mathbf{x}_2..., \mathbf{x}_{2N}) \tag{6.22}$$

which is a product of the composite particle wavefunction of Eq. (6.20) and the Laughlin wavefunction of Eq. (6.2).

Equation (6.22) is the final result for the ground state wavefunction of the resonant rotating Bose system. This result has important consequences for the generation of the FQHE within a resonant atomic gas. It would imply that an increase of interparticle interactions by a resonant tuning of the interactions simultaneously generates an increase in 2-particle correlations between composite particles resulting in a modification to the ground state wavefunction. As is clear from the form of Eq. (6.20), for large detuning from the resonance, corresponding to small pairing and molecular field, the many-body wavefunction reduces to the Laughlin wavefunction. As one moves nearer to the resonance, however, the off-diagonal part of the self-energy matrix, Δ, grows. This results in an increasing modification of the many-body wavefunction from the Laughlin wavefunction. The ability to tune a Feshbach resonance therefore allows for the direct study of this crossover from a Laughlin wavefunction to a paired wavefunction.

A similar, yet distinct, paired wavefunction as in Eq. (6.22) was found for electronic FQHE systems [114, 117, 119]. This has been used to explain the previously unresolved even denominator filling fractions which result from a pairing instability, such as the observed incompressibility of the 5/2 filling. In this case, a straightforward generalization of the Laughlin wavefunction would result in a symmetric wavefunction, violating the asymmetry of the fermions. However, the generation of an antisymmetric Pfaffian wavefunction which multiplies the generalized Laughlin state allows the overall ground state to be correctly antisymmetrized. For the bosonic system we have treated, the overall wavefunction must remain symmetric, so the corresponding paired wavefunction is symmetric in comparison to the antisymmetric Pfaffian wavefunction.

6.4 Conclusion

In conclusion, because of the extreme diluteness of trapped atomic gases, if strongly correlated effects such as the FQHE are to be observed in these experiments, the interatomic interactions will most likely need to be resonantly enhanced. Feshbach resonances are a convenient method for increasing the interactions, but the molecular processes involved in such a resonant system force one to account for the effects of atomic pairing. The growth of pair correlations among the composite particles leads to a modification of the expected ground state for a rapidly rotating Bose gas. The new ground state wavefunction, which is generated by the Feshbach resonance, exists as a strongly correlated state unique to trapped Bose gases. The tunability of the resonance opens the possibility for the direct study of the crossover transition between the paired state and the Laughlin state.

These results have important implications for the production of the FQHE within atomic gases since the use of a Feshbach resonance results in a state quite different from a rapidly rotating gas where the interactions are quantified by only a large scattering length. For instance, many of the observeable properties of the gas may be modified such as the density profile for both atoms and molecules and the nature of collective excitations. It should also be noted that the crossover transition we have discussed is only a part of a much more general crossover theory made accessible by the tunability of a Feshbach resonance. Although the methods presented here are invalid close to the resonance, one could imagine extending these ideas to describe the resonant system as one passes from a gas of interacting rotating atoms, through the resonance, to a system of tightly bound, rotating molecules.

Chapter 7

Summary

To summarize, in this thesis we have obtained some interesting results for the dilute Bose gas in different regimes.

In the first part, we studied the weak interaction regime. Here we discussed the working of an atom laser and also proposed an all optical method for continuously loading the thermal component (reservoir) of a cw- atom laser. We showed that despite the presence of spontaneously emitted photons, it is possible to configure the trapped system such that the probability of photon re-absorption is small and hence negligible heating of the atomic cloud.

Another essential component is the continuous evaporative cooling mechanism. This would have the effect of pumping thermal atoms into the condensate mode to compensate for the loss due to output coupling as well to compensate for other intrinsic loss mechanisms. Therefore, a proper understanding of a cw- atom laser would require a model satisfying all three basic requirements– loading, evaporative cooling and output coupling. Such a model will then allow us to calculate the phase diffusion properties of the cw- atom laser. Our discussion of the quantum kinetic regime in the second chapter would be very crucial to understanding the collisional contribution to the phase diffusion and hence the line width of the cw- atom laser.

In the second part of this thesis, we showed that under certain conditions a dilute Bose gas can enter the strongly correlated regime. In fact in this regime the Bose sys-

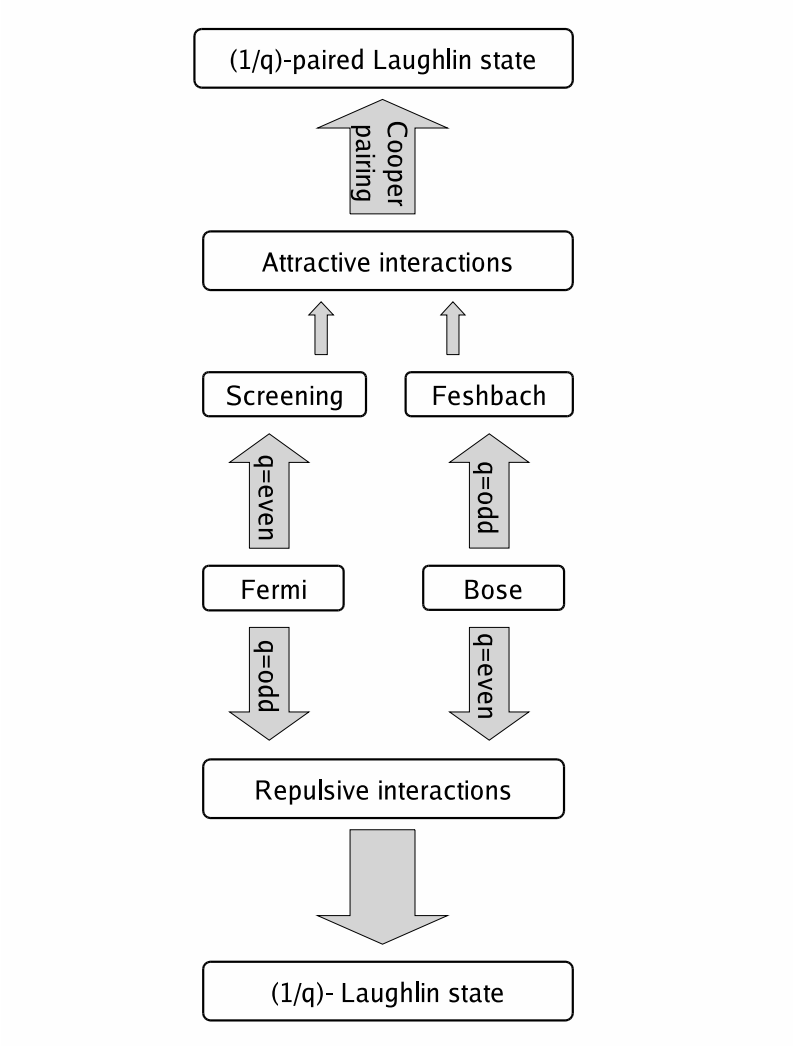

Figure 7.1: Origin of different possible fractions in the fermionic- and bosonic- fractional quantum Hall effect. The tuning of interactions via Feshbach resonance may result in generation of fractions, the underlying mechanism could be compared to that of the even FQHE.

tem showed fractional quantization quite analogous to that in the FQHE. The relevant fraction was found to be $\frac{1}{2}$ with the corresponding ground state given by the bosonic Laughlin wavefunction. Field theory method based on the Chern-Simons gauge was found to be extremely useful in treating the Feshbach mechanism for tuning the interatomic interactions in this regime. While controlling interactions is virtually impossible in the condensed matter fractional quantum Hall systems, our study of the dilute Bose

gas in this regime has opened a whole new set of possibilities for investigating many body effects previously inaccessible in condensed matter systems. The most interesting example would be the existence of even fractions in electronic FQHE. In fact the only observed fraction is $\frac{5}{2}$ and its origin is still an active area of research. From this perspective, a rotating Bose gas with tunable interactions would be very useful. As depicted in the flow chart of Fig. 7.1, an identical mechanism in the Bose case would result in odd bosonic FQHE. Therefore, observing such strongly correlated phases with odd fractional statistics may help enhance our understanding of the even FQHE.

Bibliography

[1] M. H. Anderson, J. R. Ensher, M. R. Matthews, C. E. Wieman, and E. A. Cornell, Science **269**, 198 (1995).

[2] K. B. Davis, M.- O Mewes, M. R. Andrews, N. J. van Druten, D. S. Durfee, D. M. Kurn, and W. Ketterle, Phys. Rev. Lett. **75**, 3969 (1995).

[3] C. C. Bradley, C. A. Sackett, J. J. Tollett, and R. G. Hulet, Phys. Rev. Lett **75**, 1687 (1995).

[4] W. Hänsel, P. Hommelhoff, T. W. Hänsch, and J. Reichel, Nature **413**, 498 (2001).

[5] D. Rychtarik, B. Engeser, H.-C. Nägerl, and R. Grimm; cond-mat/0309536.

[6] J. Bardeen, L. N. Cooper, and J. R. Schrieffer, Phys. Rev. **108**, 1175 (1957); J. R. Schrieffer in *Theory of Superconductivity*, (Perseus Books, Reading, MA 1999).

[7] M. Holland S.J.J.M.F. Kokkelmans, M. L. Chiofalo, and R. Walser, Phys. Rev. Lett. **87**, 120406 (2001).

[8] K. M. O'Hara, S. L. Hemmer, S. R. Granade, M. E. Gehm, and J.E. Thomas, Science **298**, 2127 (2002).

[9] J. N. Milstein, S.J.J.M.F. Kokkelmans, and M. J. Holland, Phys. Rev. A **66**, 043604 (2002).

[10] K. E. Strecker, G. B. Partridge, A. G. Truscott, and R. G Hulet, Nature **417**, 150 (2002).

[11] C. A. Regal, C. Ticknor, J. L. Bohn, and D. S. Jin, Nature (2003); cond-mat/0305028.

[12] S. G. Bhongale and M. J. Holland, Phys. Rev. A **62**, 043604 (2000).

[13] R. Walser, J. Williams, J. Cooper, and M. Holland, Phys. Rev. A **59**, 3878 (1999).

[14] S. G. Bhongale, R. Walser, and M. J. Holland, Phys. Rev. A **66**, 043618 (2002).

[15] S. G. Bhongale, J. N. Milstein, and M. J. Holland, submitted to Phys. Rev. Lett.; cond-mat/0305399.

[16] M. Holland, K. Burnett, C. Gardiner, J. I. Cirac, and P. Zoller, Phys. Rev. A **54**, R1757 (1996).

[17] H. Wiseman, A. Martins, and D. Walls, Quantum. Semiclassic. Opt.**8**, 737 (1996).

[18] R. J. C. Spreeuw, T. Pfau, U. Janicke and M. Wilkens, Europhysics Letters **32**, 469 (1995).

[19] R. J. Ballagh, K. Burnett, and T. F. Scott, Phys. Rev. Lett. **78**, 1607 (1997).

[20] H. Steck, M. Naraschewski, and H. Wallis, Phys. Rev. Lett. **80**, 1 (1998).

[21] A. M. Guzman, M. Moore, and P. Meystre, Phys. Rev. A **53**, 977 (1996).

[22] H. M. Wiseman, Phys Rev. A **56**, 2068 (1997).

[23] G. M. Moy, J. J. Hope and C. M. Savage, Phys Rev. A **55**, 3631 (1997).

[24] H. M. Wiseman and M. J. Collett, Physics Lett. A **202**, 246 (1995).

[25] W. Ketterle and Hans-Joachim Miesner, Phys. Rev. A **56**, 3291 (1997).

[26] J. Williams, R. Walser, C. Wieman, J. Cooper, and M. Holland, Phys. Rev. A **57**, 2030 (1998).

[27] M. -O. Mewes *et al.*, Phys. Rev. Lett. **78**, 582 (1997).

[28] M. R. Andrews, C. G. Townsend, H. -J. Miesner, D. S. Durfee, D. M. Kurn, and W. Ketterle, Science **275**, 637 (1997).

[29] C. C. Bradley, C. A. Sackett, and R. G. Hulet, Phys. Rev. Lett **78**, 985 (1997).

[30] I. Bloch, T. W. Hansch, and T. Esslinger, Phys. Rev. Lett. **82**, 3008 (1999).

[31] G. B. Lubkin, Physics Today, **52**, 17 (1999).

[32] B. P. Anderson and M. A. Kasevich, Science **282**, 1686 (1998).

[33] E. W. Hagley *et al.*, Science **283**, 1706 (1999).

[34] J. J. Hope, Phys. Rev. A **55**, R2531 (1997).

[35] D. Boiron, A. Michaud, P. Lemonde, and C. Salomon, Phys. Rev. A **53**, R3734 (1996).

[36] H. J. Lee, C. S. Adams, M. Kasevich, and S. Chu, Phys. Rev. Lett. **76**, 2658 (1996).

[37] J. Lawall, S. Kulin, B.Saubamea, N. Bigelow, M. Leduc, and C. Cohen-Tannoudji, Phys. Rev. Lett. **75**, 4194 (1995).

[38] Y. Castin, J. Cirac, and M. Lewenstein, Phys. Rev. Lett. **80**, 5305 (1998).

[39] E. A. Cornell, C. Monroe, and C. E. Wieman, Phys. Rev. Lett. **67**, 2439 (1991).

[40] C. W. Gardiner, *Quantum Noise* (Springer, Berlin, 1991).

[41] D. F. Walls and G. J. Milburn, *Quantum Optics*, (Springer, Berlin, 1994).

[42] M. Holland, Phys. Rev. Lett. **33**, 5117 (1998).

[43] S. H. Autler and C. H. Townes, Phys. Rev. **100**, 703 (1955).

[44] Claude Cohen-Tannoudji,Jacques Dupont-Roc, and G. Grynberg, *Atom–Photon Interactions* (John Wiley and Sons, New York, 1992).

[45] F. Dalfovo, S. Giorgini, L. Pitaevskii, and S. Stringari, Rev. Mod. Phys. **71**, 463 (1999).

[46] J. E. Williams and M. J. Holland, Nature **401**, 568 (1999).

[47] B. P. Anderson, P. C. Haljan, C. E. Wieman, and E. A. Cornell, Phys. Rev. Lett. **85**, 2857 (2000).

[48] C. Raman, J. R. Abo-Shaeer, J. M. Vogels, K. Xu, and W. Ketterle, Phys. Rev. Lett. **87**, 210402 (2001).

[49] J. R. Abo-Shaeer, C. Raman, and W. Ketterle, Phys. Rev. Lett. **88**, 070409 (2002).

[50] K. W. Madison, F. Chevy, W. Wohlleben, and J. Dalibard, Phys. Rev. Lett. **84**, 806 (2000).

[51] D. S. Jin, J. R. Ensher, M. R. Matthews, C. E. Wieman, and E. A. Cornell, Phys. Rev. Lett. **77**, 420 (1996).

[52] M. Edwards *et al.*, Phys. Rev. Lett. **77**, 1671 (1996).

[53] S. Stringari, Phys. Rev. Lett. **77**, 2360 (1996).

[54] C. W. Gardiner and P. Zoller, Phys. Rev. A **55**, 2902 (1997); C. W. Gardiner and P. Zoller, Phys. Rev. A **58**, 536 (1998); C. W. Gardiner and P. Zoller, Phys. Rev. A **61**, 033601 (2000).

[55] Y. Castin and R. Dum, Phys. Rev. A **57**, 3008 (1998).

[56] H. T. Stoof, J. Low. Temp. Phys. **114**, 11 (1999).

[57] T. R. Kirkpatrick and J. R. Dorfman, Phys. Rev. A **28**, 2576 (1983); J. Low. Temp. Phys. **58**, 308 (1985); *ibid.*, 399 (1985).

[58] N. P. Proukakis and K.Burnett, J. Res. NIST, **101**, 457 (1996); N. P. Proukakis, K. Burnett, and H. T. C. Stoof, Phys. Rev. A **57**, 1230 (1998).

[59] M. Rusch and K. Burnett, Phys. Rev. A **59**, 3851 (1999).

[60] E. Zaremba, T. Nikuni, and A. Griffin, Phys. Rev. A **57**, 4695 (1998).

[61] E. Zaremba, T. Nikuni, and A. Griffin, J. Low. Temp. Phys. **116**, 69 (1999).

[62] P.O. Fedichev and G. V. Shlyapnikov, Phys. Rev. A **58**, 3146 (1998).

[63] L. Kadanoff and G. Baym, *Quantum Statistical Mechanics* (W. A. Benjamin, Inc., New York, 1962).

[64] M. Imamovic-Tomasovic and A. Griffin, J. Low. Temp. Phys. **122**, 617 (2001).

[65] M. D. Lee and C. W. Gardiner, Phys. Rev. A **62**, 033606 (2000).

[66] M. J. Bijlsma, E. Zaremba, and H. T. C. Stoof, Phys. Rev. A **62**, 063609 (2000).

[67] D. Jaksch, C. W. Gardiner, and P. Zoller, Phys. Rev. A **56**, 575 (1997).

[68] A. Sinatra, C. Lobo, and Y. Castin, Phys. Rev. Lett. **87**, 210404 (2001).

[69] I. Carusotto and Y. Castin, J. Phys. B **34**, 4589 (2001).

[70] B. Jackson and E. Zaremba, cond-mat/0205421.

[71] E. A. Donley, N. R. Claussen, S. T. Thompson, and C. E. Wieman, Nature **417**, 529 (2002).

[72] S.J.J.M.F. Kokkelmans and M. J. Holland, Phys. Rev. Lett. **89**, 180401 (2002).

[73] V. G. Morozov and G. Röpke, Ann. Phys. **278**, 127 (1999).

[74] V. G. Morozov and G. Röpke, J. Stat. Phys. **102**, 285 (2001).

[75] M. Bonitz and D. Kremp, Phys. Lett. A **212**, 83 (1996).

[76] D. Kremp *et al.*, Physica B **228**, 72 (1996).

[77] M. Bonitz, *Quantum Kinetic Theory* (B. G. Teubner Stuttgart, Leipzig, 1998).

[78] R. Walser, J. Cooper, and M. J. Holland, Phys. Rev. A **63**, 013607 (2000).

[79] H. Haug and L. Banyai, Solid State Comm. **100**, 303 (1996).

[80] D. Semkat and M. Bonitz in *Progress in Nonequilibrium Green's Function*, edited by M. Bonitz (World Scientific, Singapore, 2000).

[81] D. Zubarev, V. Morozov, and G. Röpke, *Statistical Mechanics of Nonequilibrium Processes* (Akademie Verlag, Berlin, 1996).

[82] A. I. Akhiezer and S. V. Peletminskii, *Methods of Statistical Physics* (Pergamon Press, Oxford, 1981).

[83] S. Chapman and T. G. Cowling, *The Mathematical Theory of Non-Uniform Gases* (Cambridge University Press, Cambridge, 1970).

[84] D. S. Jin, M. R. Matthews, J. R. Ensher, C. E. Wieman, and E. A. Cornell, Phys. Rev. Lett. **78**, 764 (1997).

[85] J. Wachter, R. Walser, J. Cooper, and M. J. Holland, Phys. Rev. A **64**, 053612 (2001).

[86] J. W. Kane and L. Kadanoff, J. Math. Phys. **6**, 1902 (1965).

[87] P. C. Hohenberg and P. C. Martin, Ann. Phys. (N.Y.) **34**, 291 (1965).

[88] H. Feshbach, Ann. Phys. **5**, 357 (1958), 287 (1962).

[89] Markus Greiner, Olaf Mandel, Tilman Esslinger, Theodor W. Hänsch, and Immanuel Bloch, Nature **415**, 39 (2002).

[90] R. B. Laughlin, Phys. Rev. Lett. **50**, 1395 (1983).

[91] K. von Klitzing, G. Dorda, and M. Pepper, Phys. Rev. Lett. **45**, 494 (1980).

[92] D. C. Tsui, H. L. Stormer, and A. C. Gossard, Phys. Rev. Lett. **48**, 1559 (1982).

[93] R. Willett, J.P. Eisenstein, H. L. Stormer, D. C. Tsui, A. C. Gossard, and J. H. English, Phys. Rev. Lett. **59**, 1776 (1987).

[94] W. Pan, J. -S. Xia, V. Shvarts, D. E. Adams, H. L. Stormer, D. C. Tsui, L. N. Pfeiffer, K. W. Baldwin, and K. W. West, Phys. Rev. Lett. **83**, 3530 (1999).

[95] V. W. Scarola, K. Park, and J. K. Jain, Nature **406**, 863 (2000).

[96] N. K. Wilkin, J. M. F. Gunn, and R. A. Smith Phys. Rev. Lett. **80**, 2265 (1998).

[97] B. Paredes, P. Fedichev, J.I. Cirac, and P. Zoller, Phys. Rev. Lett. **87**, 010402 (2001).

[98] S. C. Zhang, T. H. Hansson, and S. Kivelson, Phys. Rev. Lett. **62**, 82 (1989).

[99] N. Read, Phys. Rev. Lett. **62**, 86 (1989).

[100] S. M. Girvin, and A. H. MacDonald, Phys. Rev. Lett. **58**, 303 (1987).

[101] F. D. M. Haldane, Phys. Rev. Lett. **67**, 937 (1991).

[102] M. V. Berry, Proc. R. Soc. London **392**, 45 (1984).

[103] Y. Aharonov and D. Bohm, Phys. Rev. **115**, 485 (1959).

[104] S. J. J. M. F. Kokkelmans, J. N. Milstein, M. L. Chiofalo, R. Walser, and M. J. Holland, Phys. Rev. A **65**, 053617 (2002).

[105] P. Engels, I. Coddington, P.C. Haljan, and E.A. Cornell, Phys. Rev. Lett. **89**, 100403, (2002).

[106] J. R. Abo-Shaeer, C. Raman, J.M. Vogels, and W. Ketterle, Science **292**, 476 (2001).

[107] T. L. Ho, Phys. Rev. Lett. **87**, 060403 (2001).

[108] U. R. Fischer and G. Baym, Phys. Rev. Lett. **90**, 140402 (2003).

[109] S. L. Cornish, N. R. Claussen, J. L. Roberts, E. A. Cornell, and C. E. Wieman Phys. Rev. Lett. **85**, 1795 (2000).

[110] T. Loftus, C. A. Regal, C. Ticknor, J. L. Bohn, and D. S. Jin Phys. Rev. Lett. **88**, 173201 (2002).

[111] M. Holland, J. Park, and R. Walser, Phys. Rev. Lett. **86**, 1915 (2001).

[112] E. Timmermans, P. Tommasini, R. Cote, M. Hussein, and A. Kerman, Phys. Rev. Lett. **83**, 2691 (1999).

[113] T. Köhler and K. Burnett, Phys. Rev. A **65**, 033601 (2002).

[114] F.D.M. Haldane and E.H. Rezayi, Phys. Rev. Lett. **60**, 956 (1988). .

[115] S.C. Zhang, Int. J. Mod. Phys. B **6**, 25 (1992).

[116] P.A.M. Dirac, *The Principles of Quantum Mechanics*, (Clarendon Press, Oxford, 1958).

[117] G. Moore and N. Read, Nucl. Phys. B **360**, 362 (1991).

[118] T. Morinari, Phys. Rev. B. **62**, 15903 (2000).

[119] M. Greiter, X.G. Wen, and F. Wilczek, Nuc. Phys. B **374**, 567 (1992)

Appendix A

Reference distribution

The reference distribution $\sigma^{(0)}_{\{f\}}$ of Eq. (3.9) is parameterized through its expectation values in Eq. (3.11). From the structure of this quantum Gaussian operator, it follows that

$$\sigma^{(0)}_{\{\mathcal{K}(t,t_0)\, f\, \mathcal{K}^\dagger(t,t_0)\}} = \hat{U}^\dagger(t,t_0)\, \sigma^{(0)}_{\{f\}}\, \hat{U}(t,t_0). \tag{A.1}$$

In the above, $\hat{U}$ represents the single particle propagator of Eq. (3.16) acting in many-particle Fock-space and $\mathcal{K}$ is the corresponding single particle Hilbert-space propagator of Eq. (3.23). This condition implies that

$$\partial_{\gamma_k} \sigma^{(0)} \mathrm{Tr}\{[\hat{\mathrm{H}}^{(0)}, \hat{\gamma}_\mathrm{k}]\} = -[\hat{\mathrm{H}}^{(0)}, \sigma^{(0)}] \tag{A.2}$$

and was used to obtain Eq. (3.17).

Appendix B

Matrix elements

The matrix element of Eq. (3.41) can be evaluated easily by expanding the sin functions into co- and counter-propagating complex exponents and by an additional partial integration. This results in eight separate terms, i.e.,

$$\begin{aligned}
\phi^{ijkl}/a_{\rm S} &= \frac{4}{\pi}\int_0^\pi \sin(i\,x)\sin(j\,x)\sin(k\,x)\sin(l\,x)\,\frac{dx}{x^2}, \\
&= F(i+j+k-l)+F(i+j-k+l) \\
&+ F(i-j+k+l)+F(i-j-k-l) \\
&- F(i+j-k-l)-F(i-j+k-l) \\
&- F(i-j-k+l)-F(i+j+k+l), \qquad \text{(B.1)}
\end{aligned}$$

where

$$\begin{aligned}
F(n) &= \frac{1}{2\pi^2}[\cos(n\pi)+n\pi\,\mathrm{Si(n\pi)}], \qquad \text{(B.2)} \\
\mathrm{Si}(z) &= \int_0^z \frac{\sin(t)}{t}\,dt. \qquad \text{(B.3)}
\end{aligned}$$

An asymptotic expansion of the sine integral leads to the following approximation that is correct at the 1% level, i.e.,

$$\begin{aligned}
F(0) &= \frac{1}{2\pi^2}, \qquad \text{(B.4)} \\
F(n>0) &\approx \frac{1}{2\pi^2}[\frac{\pi}{2}|n\pi| - \frac{\sin(n\pi)}{n\pi} + \frac{2\cos(n\pi)}{(n\pi)^2}].
\end{aligned}$$

Appendix C

Anyon field operator

The anyon field operator $\hat{\phi}_{an}(t, \mathbf{x})$ is represented by

$$\hat{\phi}_{an}(t, \mathbf{x}) = e^{i\alpha\hat{\xi}(t,\mathbf{x})}\hat{\psi}_b(t, \mathbf{x}) \tag{C.1}$$

in terms of the boson operator $\hat{\psi}_b(t, \mathbf{x})$ with the phase field

$$\hat{\xi}(t, \mathbf{x}) = \alpha \int d^2y \theta(\mathbf{x} - \mathbf{y})\rho(t, \mathbf{x}). \tag{C.2}$$

where $\rho(t, \mathbf{x}) = \hat{\psi}_b^\dagger(t, \mathbf{x})\hat{\psi}_b(t, \mathbf{x})$. The Chern-Simons field is expressed as

$$a_k(\mathbf{x}) = \frac{\alpha\hbar}{e} \int d^2y \partial_k\theta(\mathbf{x} - \mathbf{y})\rho(\mathbf{y}). \tag{C.3}$$

We now examine how the exchange phase arises theoretically. We start with the commutation relation

$$[\hat{\xi}(\mathbf{y}), \hat{\psi}_b(\mathbf{x})] = \int d^2z \theta(\mathbf{x} - \mathbf{y})[\rho(\mathbf{z}), \hat{\psi}_b(\mathbf{x})] = -\theta(\mathbf{y} - \mathbf{x})\hat{\psi}_b(\mathbf{x}). \tag{C.4}$$

Now, we use the Hausdorff formula

$$e^A B e^{-A} = B + [A, B] + \frac{1}{2}[A, [A, B]] + ..., \tag{C.5}$$

by setting $A = i\alpha\hat{\xi}(\mathbf{y})$ and $B = \hat{\psi}_b(\mathbf{x})$ we find that

$$e^{-i\alpha\hat{\xi}(\mathbf{y})}\hat{\psi}_b(\mathbf{x})e^{i\alpha\hat{\xi}(\mathbf{y})} = e^{i\alpha\theta(\mathbf{y}-\mathbf{x})}\hat{\psi}_b(\mathbf{x}). \tag{C.6}$$

With this formula we get

$$\hat{\phi}_{an}(\mathbf{x})\hat{\phi}_{an}(\mathbf{y}) = e^{i\alpha\theta(\mathbf{y}-\mathbf{x})}e^{i\alpha\hat{\xi}(\mathbf{x})}e^{i\alpha\hat{\xi}(\mathbf{y})}\hat{\psi}_b(\mathbf{x})\hat{\psi}_b(\mathbf{y}) \tag{C.7}$$

$$\hat{\phi}_{an}(\mathbf{y})\hat{\phi}_{an}(\mathbf{x}) = e^{i\alpha\theta(\mathbf{x}-\mathbf{y})}e^{i\alpha\hat{\xi}(\mathbf{y})}e^{i\alpha\hat{\xi}(\mathbf{x})}\hat{\psi}_b(\mathbf{y})\hat{\psi}_b(\mathbf{x}). \tag{C.8}$$

Now using $\hat{\psi}_b(\mathbf{x})\hat{\psi}_b(\mathbf{y}) = \hat{\psi}_b(\mathbf{y})\hat{\psi}_b(\mathbf{x})$ and $\theta(\mathbf{x}-\mathbf{y}) = \theta(\mathbf{y}-\mathbf{x}) + \pi$, we compare (C.7) and (C.8) to find that

$$\hat{\phi}_{an}(\mathbf{y})\hat{\phi}_{an}(\mathbf{x}) = e^{i\alpha\pi}\hat{\phi}_{an}(\mathbf{x})\hat{\phi}_{an}(\mathbf{y}) \tag{C.9}$$

This is the operator version of the interchange of two anyons.